W A Davis

NATIONAL ACADEMIES OF SCIENCE AND ENGINEERING

NATIONAL RESEARCH COUNCIL

of the

UNITED STATES OF AMERICA

UNITED STATES NATIONAL COMMITTEE

International Union of Radio Science

National Radio Science Meeting

13-15 January 1982

Sponsored by USNC/URSI
in cooperation with
Institute of Electrical and Electronics Engineers

University of Colorado
Boulder, Colorado
U.S.A.

National Radio Science Meeting
13-15 January 1982
Condensed Technical Program

TUESDAY, 12 JANUARY

0900	
CCIR U.S. Study Group 5	OT 8-8
CCIR U.S. Study Group 6	Radio Building
2000-2400	
USNC/URSI Meeting	Broker Inn

WEDNESDAY, 13 JANUARY

0900-1200	
A-1 Time Domain Measurements	CR1-42
B-1 Scattering	CR2-28
B-2 Electromagnetic Theory	CR2-28
C-1 Topics in Information Theory	CR0-30
F-1 Propagation Theory and Models	CR2-26
J-1 Millimeter-Wave Astronomy	UMC Ballroom
1330-1700	
A-2 Microwave/Millimeter Wave Measurements	CR1-42
B-3 Antenna Theory and Practice	CR2-28
B-4 Inverse Scattering	CR2-6
C-2 Digital HF: Equalization and Related Techniques	CR0-30
E-1 EM Noise in the Sea	CR1-40
F-2 Ground-Based Remote Sensing	CR2-26
H-1 VLF-ELF Wave Injection Into the Magnetosphere	CR1-46
J-2 Very Long Baseline Interferometry	UMC 157
1700	
Commission A Business Meeting	CR1-42
Commission C Business Meeting	CR0-30
Commission E Business Meeting	CR1-40
Commission F Business Meeting	CR2-26
Commission H Business Meeting	CR1-46
1800-2000	
Reception	Engineering Center
2000-2200	
IEEE Wave Propagation Standards Committee	CR1-46

THURSDAY, 14 JANUARY

0830-1200	
A-3 Use of Spacecraft and Satellite Links for Scientific Measurements	CR1-42
B-5 Interface and Surface Effects	CR2-28
C-3 Multiple Beam Satellite Antennas for Communication Satellite Systems	CR0-30

United States National Committee

INTERNATIONAL UNION OF RADIO SCIENCE

PROGRAM AND ABSTRACTS

National Radio Science Meeting
13-15 January 1982

Sponsored by USNC/URSI in cooperation
with IEEE groups and societies:

Antennas and Propagation
Circuits and Systems
Communications
Electromagnetic Compatibility
Geoscience Electronics
Information Theory
Instrumentation and Measurement
Microwave Theory and Techniques
Nuclear and Plasma Sciences
Quantum Electronics and Applications

Hosted by:

National Oceanic and Atmospheric Administration
National Bureau of Standards
Institute for Telecommunication Sciences
National Telecommunications and Information Administration
University of Colorado, Boulder
and
The Denver-Boulder Chapter, IEEE/APS

NOTE:

Programs and Abstracts of the USNC/URSI Meetings are available from:

USNC/URSI
National Academy of Sciences
2101 Constitution Avenue, N.W.
Washington, DC 20418

at $2 for meetings prior to 1970, $3 for 1971-75 meetings, and $5 for 1976-81 meetings.

The full papers are not published in any collected format; requests for them should be addressed to the authors who may have them published on their own initiative. Please note that these meetings are national. They are not organized by the International Union, nor are the programs available from the International Secretariat.

MEMBERSHIP

United States National Committee

INTERNATIONAL UNION OF RADIO SCIENCE

Chairman:	Prof. Thomas B.A. Senior*
Vice Chairman:	Prof. Robert K. Crane*
Secretary:	Dr. Thomas E. VanZandt*
Immediate Past Chairman:	Dr. C. Gordon Little*

Members Representing Societies, Groups and Institutes:

American Geophysical Union	Dr. Christopher T. Russell
Bioelectromagnetics Society	Dr. James C. Lin
Institute of Electrical and Electronic Engineering	Dr. Ernst Weber
IEEE Antennas and Propagation Society	Dr. Alan W. Love
IEEE Communications Society	Prof. Raymond Pickholtz
IEEE Electromagnetic Compatibility Society	
IEEE Information Theory Group	
IEEE Microwave Theory and Techniques Society	
IEEE Quantum Electronics Society	Prof. Herman A. Haus
Optical Society of America	

Liaison Representatives from Government Agencies:

National Telecommunications and Information Administration	Dr, Douglass D. Crombie
National Science Foundation	Dr. Vernon Pankonin
Department of Commerce	
National Aeronautics and Space Administration	Dr. Erwin R. Schmerling
Federal Communications Commission	Mr. William A. Daniel
Department of Defense	Dr. George L. Salton
Department of the Army	Lt. Col. Robert Clayton, Jr.
Department of the Navy	Dr. Leo Young
Department of the Air Force	Dr. Allan C. Schell

Members-at-Large:	Dr. Sidney A. Bowhill
	Dr. George W. Swenson, Jr.

* Member of USNC-URSI Executive Committee

Chairmen of the USNC-URSI Commissions are:

Commission A	Dr. Helmut Hellwig
Commission B	Prof. Chalmers M. Butler
Commission C	Dr. Andrew J. Viterbi
Commission D	Dr. Kenneth J. Button
Commission E	Dr. Arthur A. Giordano
Commission F	Dr. Earl E. Gossard
Commission G	Dr. Kenneth Davies
Commission H	Dr. Robert F. Benson
Commission J	Prof. Mark A. Gordon

Officers of URSI resident in the United States:
(including Honorary Presidents)

President	Prof. William E. Gordon*
Honorary President	Prof. Henry G. Booker*

Chairmen and Vice Chairmen of Commissions of URSI resident in the United States:

Chairman of Commission C	Prof. Jack K. Wolf
Vice Chairman of Commission G	Dr. Jules Aarons

Foreign Secretary of the U.S. National Academy of Sciences	Dr. Thomas F. Malone
Chairman, Office of Physical Sciences-NRC	Dr. Ralph O. Simmons
NRC Staff Officer	Mr. Richard Y. Dow
Honorary Members:	Dr. Harold H. Beverage Prof. Arthur H. Waynick

* Member of USNC-URSI Executive Committee

DESCRIPTION OF THE

INTERNATIONAL UNION OF RADIO SCIENCE

The International Union of Radio Science is one of 18 world scientific unions organized under the International Council of Scientific Unions (ICSU). It is commonly designated as URSI (from its French name, Union Radio Scientifique Internationale). Its aims are (1) to promote the scientific study of radio communications, (2) to aid and organize radio research requiring cooperation on an international scale and to encourage the discussion and publication of the results (3) to facilitate agreement upon common methods of measurement and the standardization of measuring instruments, and (4) to stimulate and to coordinate studies of the scientific aspects of telecommunications using electromagnetic waves, guided and unguided. The International Union itself is an organizational framework to aid in promoting these objectives. The actual technical work is largely done by the National Committees in the various countries.

The officers of the International Union are:

President:	W. E. Gordon (USA)
Past President:	W. N. Christiansen (Australia)
Vice Presidents:	A. L. Cullen (U.K.)
	A. P. Mitra (India)
	S. Okamura (Japan)
	A. Smolinski (Poland)
Secretary-General:	J. Van Bladel (Belgium)
Honorary Presidents:	H. G. Booker (USA)
	G. Beynon (U.K.)
	M. B. Decaux (France)
	W. Dieminger (West Germany)
	I. Koga (Japan)
	J. A. Ratcliffe (U.K.)

The Secretary-General's office and the headquarters of the organization are located at Avenue de Lancaster 32, B-1180 Brussels, Belgium. The Union is supported by contributions (dues) from 38 member countries. Additional funds for symposia and other scientific activities of the Union are provided by ICSU from contributions received for this purpose from UNESCO.

The International Union, as of the XXth General Assembly held in Washington, D.C., in August 1981, has nine bodies called Commission for centralizing studies in the principal technical fields. The names of the Commissions and their chairmen follow.

A. Electromagnetic Metrology
V. Kose (FRG)

B. Fields and Waves
H. C. Unger (FRG)

C. Signals and Systems
J. K. Wolf (USA)

D. Electronic and Optical Devices and Applications
J. Le Mezec (France)

E. Electromagnetic Noise and Interference
S. Lundquist (Sweden)

F. Remote Sensing and Wave Propagation
D. Gjessing (Norway)

G. Ionospheric Radio and Propagation
P. Bauer (France)

H. Waves in Plasmas
M. Petit (France)

J. Radio Astronomy
V. Radhakrishnan (India)

Every three years the International Union holds a meeting called the General Assembly; the next is the XXIst, to be held in Florence, Italy, in August/September, 1984. The Secretariat prepares and distributes the Proceedings of these General Assemblies. The International Union arranges international symposia on specific subjects pertaining to the work of one or several Commissions and also cooperates with other Unions in international symposia on subjects of joint interest.

Radio is unique among the fields of scientific work in having a specific adaptability to large-scale international research programs, since many of the phenomena that must be studied are worldwide in extent and yet are in a measure subject to control by experimenters. Exploration of space and the extension of scientific observations to the space environment are dependent on radio for their research. One branch, radio astronomy, involves cosmic phenomena. URSI thus has a distinct field of usefulness in furnishing a meeting ground for the numerous workers in the manifold aspects of radio research; its meetings and committee activities furnish valuable means of promoting research through exchange of ideas.

NATIONAL RADIO SCIENCE MEETING COMMITTEE MEMBERS

Steering Committee

S. W. Maley, Chairman
D. C. Chang
D. Cook
R. Y. Dow
P. L. Jensen
C. G. Little
T. B. A. Senior
T. E. Van Zandt

Technical Program Committee

T. E. Van Zandt, Chairman
R. F. Benson
C. M. Butler
K. Davies
M. A. Gordon
E. Gossard
N. Nahman
H. Nesenbergs
A. D. Spaulding
M. Kindgren, Secretary to the Committee

TIME DOMAIN MEASUREMENTS
Commission A, Session 1, CR1-42
Chairman: E. K. Miller,
Lawrence Livermore National Laboratory,
Livermore, CA 94550

A1-1 0900 EARLY DEVELOPMENTS AND MOTIVATION FOR TIME DOMAIN METROLOGY

Gerald F. Ross, Ph.D., Anro Engineering Consultants, Inc., Sixty The Great Road, Bedford, MA 01730

In this talk, the author will present a historical development and motivation for the use of time domain techniques in metrology. Application areas include microwave network calibration, the measurement of the complex permeability and permittivity of materials, liquid level sensing, microwave antenna diagnostics, and target identification by scattering measurements. The theoretical developments were motivated by seeking solutions to complex problems in a domain where solutions were more transparent. The theoretical work in these areas were significantly enhanced by laboratory support due in part to the development of the hot carrier and tunnel diodes, the avalanche transistor and, in turn, the sampling oscilloscope in the early 1960's. The use of a time domain approach for deriving solutions, in the many problem areas indicated, often provided physical insight that was difficult to obtain; for example, without formally solving Maxwell's equations subject to appropriate boundary conditions. Time domain techniques have also led to the obtaining of measurements at a considerable saving in both time and money over conventional approaches. In the talk, specific examples relating to the fields of materials and liquid level measurement and scattering will be presented to illustrate these savings. Laboratory results obtained in these application areas will be presented to support the utility of the approach. It will be shown how physical insight gleaned from the data has led to new concepts in measurement techniques. The presentation will conclude with some examples of guided wave and free space reflectometry measurement techniques currently being developed.

A1-2
0920

CURRENT STATUS AND FUTURE DIRECTIONS OF TIME DOMAIN MEASUREMENTS

Norris S. Nahman, Senior Scientist
Electromagnetic Technology Division
National Bureau of Standards
Boulder, CO 80303

A review of the state-of-the-art of time domain measurements is presented which includes measurements in the electrical and optical regions of the electromagnetic spectrum. The significance of the IEEE/IEC Pulse Standards 181 and 194 to time domain measurements is briefly discussed. A classification of time domain measurement methods is described which includes the various real time and equivalent time techniques used in electrical and optical transient (pulses, etc.) measurements. The present day capability is summarized in state-of-the-art temporal resolution charts. Also given are some opinions as to the future directions, acceptance, and educational emphasis of time domain view-points and measurements.

A1-3
0940

FAST PULSERS--SMALL AND LARGE: James R. Andrews, Picosecond Pulse Laboratories, 8663 Hollyhock Lane, Lafayette, CO 80026

This is a review paper of the various technologies used to generate fast pulses in the nanosecond and picosecond domain. The technologies involved include: classical electronics with transistors, diodes, and vacuum tubes; cryo-electronics; electrical breakdown phenomena; lasers and photo chemistry; and nuclear phenomena. Generator output powers cover a tremendous range from microwatts to megawatts. Likewise the physical dimensions of the generators range from submicrons to many meters. The concept of trade-offs between pulse energy and switching speeds will be discussed. Several examples will be presented along with tabulated comparisons of various techniques and references.

A1-4 INSTRUMENTATION FOR TIME DOMAIN MEASUREMENTS

1000 J. R. Pressley and G. D. Sower
EG&G WASC
P. O. Box 9100
Albuquerque, NM 87119

The increasing use of integrated circuits in electronic systems has greatly increased the vulnerability of such systems to the very fast transients which can be produced by EMI, EMP, lightning and other phenomena. As a consequence, systems such as communication centers and military hardware, subsystems, boxes and even individual components are being increasingly subjected to threat level vulnerability tests which utilize some form of pulser to drive the system in some electromagnetic or electrical manner, and from which the transient response of the system is measured. The pulses may consist of single shots many minutes apart or repetitive pulses at kilohertz rates. Data recording systems have been developed which can record various electromagnetic field and system response data in a flexible and efficient manner.

Automatic transient data systems are described which require little operator intervention and not only automatically set up instrumentation but also provide sequenced control of pulsers. Wideband data transmission paths, both hard-wired and electrically isolated, are described as are various signal conditioning procedures such as attenuation, impedance transformation, and integration. The transient data system also includes special equipment, such as lossless active signal splitters and programmable trigger delay units to provide recording instrumentation inputs. Software in the data system automatically calibrates the telemetry links and corrects the recorded data for signal path component transfer functions and provides a final time-tied output in engineering units.

A second type of transient data system makes use of sampling techniques when repetitive signals are available. A sampling oscilloscope can usually be utilized whenever the repetitive signals occur at a rate of a few hertz or faster. Signal levels down to a few millivolts may be measured with this technique, with risetimes as fast as a few tens of picoseconds. Special techniques to obtain these fast risetimes, such as the use of compensated delay lines will be explained as will such additional signal processing as integration of derivative data in "sample-time".

A1-5
1020

TIME DOMAIN SENSORS AND RADIATORS

Motohisa Kanda
Electromagnetic Fields Division
National Bureau of Standards
Boulder, Colorado 80303

The purpose of this talk is to review various sensors and radiators commonly used for time domain antenna measurements. The sensors and radiators discussed here are passive and analog devices which convert the electromagnetic quantity of interest to a voltage or current at their terminal ports. Moreover, they are primary standards in the sense that their transfer functions can be calculated from their geometries and are preferably flat (constant) across a wide frequency range. One of the major requirements for these sensors and radiators is that the electromagnetic far fields, transmitted or received, are replicas or high fidelity derivatives of the original pulse. (Note that the transmitting transfer function of an antenna is the time derivative of the receiving transfer function of the same antenna which follows from the Rayleigh-Carson reciprocity theorem).

For electric field strength measurements, linear antennas loaded non-uniformly and continuously with resistance, capacitance or both resistance and capacitance are discussed. Also a conical antenna, an asymptotic conical antenna, and a resistively loaded bowtie antenna are discussed from the standpoint of an improved figure of merit. For an improved directivity, various types of TEM horns are discussed, e.g., a conducting TEM horn, a Calspan antenna, and a resistively loaded TEM horn. For magnetic field strength measurements an impedance-loaded loop antenna is discussed. The proper impedance loading is selected to shift the poles of its transfer function so as to obtain desired impulse response.

A1-6
1050

SCALE MODEL TRANSIENT MEASUREMENTS

H. S. Cabayan, E. J. Bogdan, L. C. Martin,
D. M. Wythe and H. G. Hudson
Lawrence Livermore National Laboratory
P. O. Box 5504
Livermore, CA 94550

Many civilian and military systems are required to meet certain performance criteria when operating in a strong and possibly hostile electromagnetic environment. This requires the evaluation of the coupling of electromagnetic fields to rather complicated systems such as communication facilities, ships, aircraft, missiles, etc. Very often the coupling needs to be evaluated to the exterior metallic envelope (for example, induced currents and fields on the surface of an aircraft) and also interior to the envelope (i.e., cables connected to sensitive components). Because analytical and computational tools presently available are not yet capable of providing accurate and believeable predictions, much effort has been expended at developing transient electromagnetic simulators to test the response of critical systems. These tests, although the most reliable, for generating the necessary data base, can be very expensive. This may limit the amount and range of testing that can be performed.

In order to compliment the full scale testing, efforts have gone into developing a technology base in scale model testing. Compared to full system tests these are relatively inexpensive to perform and can be used more exhaustively. Scale model tests have been performed in small CW and transient simulators. The validation of scale model data that have been performed indicate very good accuracies for determining exterior coupling. For estimating interior coupling the technology base is still in its infancy, however, and much work remains to be done.

In this paper, we present an overview of existing transient simulators and show some comparisons that have been performed between scale model predictions and the full scale test data. Limitations of this technology will be covered. The future needs for data acquisition and signal processing of this technology base will be highlighted.

A1-7
1105

EMP MEASUREMENT TECHNIQUES, J.P. Castillo, Air Force Weapons Laboratory, Kirtland Air Force Base, NM 87117; and L. Marin, The Dikewood Corporation, Santa Monica, CA 90405

EMP tests are performed for the purpose of determining how nuclear generated transient electromagnetic fields can interfere with the appropriate functioning of electronic equipment onboard systems. Three different aspects of EMP testing are covered, namely

- available simulation facilities (the fields produced by the simulators, types of systems that can be tested in them, data acquisition rates that they allow for)
- sensors and probes used to measure system responses to generated fields (B-dot and D-dot sensors used to measure surface current and charge densities and how they are mounted on different surfaces, current and voltage probes and how they are used to measure line currents/voltages)
- recording equipment (advantages/disadvantages of using "simple" systems such as oscilloscopes placed inside shield boxes or advanced ones such as remotely controlled automatic systems)

Examples of different types of data that have been acquired will be presented and the use of them for different purposes will be discussed.

A1-8
1120

TIME-DOMAIN MEASUREMENTS OF DIELECTRIC PROPERTIES OF AGRICULTURAL MATERIALS

B. P. Kwok, Formerly, Department of Electrical Engineering, University of Nebraska, Lincoln, NE
S. O. Nelson, U. S. Department of Agriculture, ARS, Russell Research Center, Athens, GA 30613
E. Bahar, Department of Electrical Engineering, University of Nebraska, Lincoln, NE 68588

Dielectric properties of certain materials and the frequency dependence of those properties have been important in research on controlling stored-grain insects with radiofrequency (RF) energy and in studies of RF treatment of seeds to improve their germination. Dielectric properties of grain and their variation with frequency have also been of interest in applications such as moisture measurement with RF electronic moisture meters. Needed data have been obtained by frequency-domain techniques, but often the accumulation of necessary data over a sufficiently wide frequency range is tedious and time-consuming. Therefore, some effort was directed toward the measurement of the dielectric properties of such materials by time-domain techniques.

Coaxial-line sample holders were constructed for use with a commercial time-domain reflectometer, and an X-Y recorder was used for observation of waveforms reflected from a short-circuit termination and, subsequently, from samples of materials placed in the coaxial line. Desired sections of waveforms were sampled at about 1000 points, and the digital information was processed by a computer which calculated the Fourier transforms, reflection coefficient, and the dielectric constant and loss factor at desired frequencies. Both long-sample (single-reflection) and thin-sample (multiple-reflection) techniques were used.

Satisfactory agreement between dielectric properties of *n*-heptanol from the literature and those provided by the time-domain measurement system was obtained with both single-reflection and multiple-reflection methods over the frequency range from 30 MHz to 1.7 GHz. Single-reflection results were somewhat better than the multiple-reflection results at frequencies below 50 MHz and above 400 MHz (B. P. Kwok, S. O. Nelson, and E. Bahar, *IEEE Trans.* IM-28 109-112, 1979). Measurements on samples of wheat kernels, alfalfa seed, and adult rice weevils gave dielectric properties in reasonably good agreement with those determined by frequency-domain techniques, but in the case of these granular materials, the multiple-reflection technique gave more consistent results than the single-reflection method. With the time-domain system, broad dielectric dispersion and absorption regions similar to those found by frequency-domain measurements were determined with significant reductions in time and effort.

A1-9 SUBSURFACE TRANSIENT-RADAR SENSING APPLICATIONS

1135 J. D. Young and L. Peters, Jr.
The Ohio State University ElectroScience Laboratory
Department of Electrical Engineering
Columbus, Ohio 43212

There are many underground objects and features whose contrasting electromagnetic parameters are amenable to electromagnetic sensing. These include tunnels and subsidence voids, non-metallic man made objects from land mines to plastic pipes and clay drain tiles. Also naturally occurring geological strata and formations have contrasting permittivity and/or conductivity. Transient radar systems have been developed and demonstrated for these sensing applications. The transient approach has the advantages of propagating through widely varying soils, yielding the best resolution which soil propagation characteristics will permit, as well as enabling echo processing techniques such as range gating to remove clutter and transient target indentification algorithms.

At least two unique problem areas in subsurface sensing are worthy of mention: First, the primary undesired signal is not noise, but clutter, the echos from inhomogeneities and objects which are random with respect to position, not time. Second, the sensing antenna problem requires an element which has extremely wide bandwidth and minimum impulse dispersion, while operating on or near the boundary between air and a lossy, inhomogeneous, dispersive half-space (the ground).

Despite the above problems, several types of transient underground radar systems have been used to produce very interesting results. A portable plastic pipe locator has been developed (Transportation Research Record 631, National Academy of Sciences); a detection and indentification system for land mines has been demonstrated (Proc. IEEE, July 1979); a temograph system for locating underground formations between two boreholes has been demonstrated (symposium or Tunnel Detection, Golden, Colo., July 1981) and several mapping systems have been develope Thus application of the technology is occurring in spite of the need for further advances in underground electromagnetic sensing technology. Areas for further research and development include improved analysis techniques for propagation and antenna performance, further research in target signatures and inverse scattering techniques, and further improvement on impulse generator power and jitter and sampling system sensitivity and dynamic range. Finally, a whole frequency regime, the "low frequency window" remains to be explored for deep penetration applications.

A1-10
1150

TRANSIENT ELECTROMAGNETIC SIGNAL PROCESSING: AN OVERVIEW OF TECHNIQUES*, J.E. Zicker, J.V. Candy, and D.B. Harris, Lawrence Libermore National Laboratory, P.O. Box 5504, L-156, Livermore, CA 94550

Instrumentation that can digitize analog signals with frequency components into the Gigahertz range has provided a useful tool for acquiring transient electromagnetic data. Transient electromagnetic experiments are relatively easy to perform compared to continuous wave experiments. The processing of transient measurements is, however, more difficult than processing continuous wave measurements. The digital processing of transient data requires knowledge of signal processing techniques, the acquisition instrumentation and the physics of the experiment.

The result of this combination of knowledge is a collection of processing techniques for transient signals. Unfortunately, since each experiment is different, a global method for handling transient data is not feasible. Each transient measurement must be analyzed taking into consideration the physics of the experiment and the limitations of the measurement system.

We present the practical methods and techniques developed from experience with several transient measurement experiments. Most of the methods are directed towards estimation of frequency spectra and system identification.

---

* Work performed under the auspices of the U.S. Department of Energy by the Lawrence Livermore Laboratory under contract number W-7405-ENG-48.

SCATTERING
Wednesday morning, 13 Jan., CR2-28
Chairman: W.A. Davis, Department of Electrical Engineering, Virginia Polytechnic Institute, Blacksburg, VA 24060

B1-1 0900 ANALYSIS OF INTERNALLY REFLECTED RAYS IN ELECTROMAGNETIC SCATTERING BY DIELECTRIC SPHEROIDS: Sujeet K. Chaudhuri, Department of Electrical Engineering, University of Waterloo, Waterloo, Ontario, Canada, N2L 3G1; Frederick B. Sleator, Cancer Centre, Medical Sciences Campus, University of Puerto Rico, San Juan, Puerto Rico; and Wolfgang-M. Boerner, Communications Laboratory, Information Engineering Department, University of Illinois at Chicago Circle, P.O. Box 4348, Chicago, IL 60680

The solution of electromagnetic scattering by dielectric objects is of considerable importance in bioelectromagnetic and radar meteorological applications. The investigations in the past have mostly been confined to a spherical structure. In this paper, for an arbitrary sized prolate spheroid, various components of the scattering mechanism responsible for the backscattered energy (which is of interest to monostatic radar systems) are analyzed for arbitrary direction of incidence and polarization.

In case of a spherical structure, due to the symmetry, the conditions for existence of glory rays and internal surface rays are straight forward. It will be shown that for the prolate spheroid, with arbitrary direction of incidence, one has to resort to a numerical method of ray tracing. The solution of this numerical method, along with some geometrical arguments, show that for most of the cases of arbitrary scatterers, the single bounce glory ray will not exist and, therefore, will not contribute to the backscattering energy. Similarly, the conditions for the existence of internal surface waves will be presented. Various other internally reflected rays which contribute to the backscatter energy and were not reported by earlier investigators (probably because they do not exist for spherical scatters) will also be presented.

C. Warner (VA Tech)
Watson's Transform [Nussenzveig, 1969 + Inada + Piona 1970]
Glory Rays ⇒ Ring sources for Prot Sph. (2 halos possible)
Internal S, Waves with critical ∠.

B1-2 0930 SCATTERING BY A RESISTIVE PLATE; Thomas B.A. Senior, Electrical and Computer Engineering Department, University of Michigan, Ann Arbor, MI 48109

A program has been developed to compute the scattering by an infinitesimally thin resistive (planar) plate. The formulation is based on the Stratton-Chu equations (equivalent to the use of vector and scalar potentials) which, in contrast to the Franz representation, imposes lower continuity requirements on the unknowns. The resulting coupled integral equations for the components of the current are then expressed in matrix form using an interwoven mesh (A.W. Glisson and D.R. Wilton, Trans. IEEE Antennas Propagat. 28, 593-603, 1980) of rectangular elements, and solved by the moment method. The program is valid for any incident field, any prescribed (possibly variable) resistivity over the plate, and any plate geometry consistent with rectangular elements, but is in practice limited to plates not more than about a square wavelength in area.

Results have been obtained for plane wave incidence on perfectly conducting and resistive plates, and these show the dramatic reduction in the edge currents that even a small amount of resistivity provides. For a rectangular plate, the results are in excellent agreement with measured data, and comparisons are shown.

$$(\nabla_t^2 + k^2)\int \bar{J} G \, ds' \simeq \hat{z} \times \frac{\partial \bar{H}^{inc}}{\partial z}$$

$$- i \frac{R}{k Z_0} \left\{ k^2 + \hat{z} \times \nabla (\hat{z} \cdot \nabla \times) \right\} \bar{J}$$

Sheet Resistance

use with EFIE + $\nabla \cdot \bar{J} \Rightarrow \rho / \epsilon_0$

$+ \hat{z} \times E = R \hat{z} \times \bar{J}$

B1-3
1000

ELECTROMAGNETIC SCATTERING BY LOADED OPEN CIRCULAR WAVEGUIDES, D.L. Moffatt and C.Y. Lai, ElectroScience Laboratory, Department of Electrical Engineering, Ohio State University, Columbus, OH 43212

The electromagnetic scattering by loaded open circular waveguides is examined in the time domain. Exact (numerical integration) axial backscatter computations for guide diameters less than 0.6 wavelengths are combined with asymptotic calculations at higher frequencies. A Fourier synthesis procedure is used to produce the canonical (impulse, step and ramp) response waveforms of the loaded open circular waveguide.

Loading consists of a planar, multiple bladed fan structure within the guide and 5 guide diameters from the open end. Response waveforms for several static positions of the blades are combined to yield the dynamic response waveforms. For the static configurations, known errors in the asymptotic calculations for guide diameters less than 1.0 wavelength are approximately corrected in the time domain using moment conditions on the waveforms. The diagnostic potential of the real time-dependent canonical response waveforms is demonstrated.

ELECTROMAGNETIC THEORY
Wednesday morning, 13 Jan., CR2-28
Chairman: D. Dudley, Department of Electrical Engineering, University of Arizona, Tucson, AZ 85731

B2-1
1030

ON THE SINGULARITY IN GREEN'S FUNCTION:

J.A. DeSanto, Electro Magnetic Applications, Inc., 1978 S. Garrison Street, Denver, Colorado 80227

We discuss the singularity in the derivative of the free-space Green's function G^0. This occurs, for example, in scalar scattering from surfaces and bodies as well as in electromagnetic and elastic problems where the dyadic Green's function is used. The method is somewhat different from that in Kellogg's book. It is based solely on integral singularities and complex function theory.

We use the two dimensional Fourier transform of G^0. This is differentiated and it is shown that the z-component of the derivative can contain a delta function singularity. This is subtracted off and, using complex integration techniques, the result is written as a principal value part plus this delta function. Different subtraction techniques are possible and these will be discussed. Although the subtraction procedure is not unique (the principal value is the simplest example), it is not arbitrary with respect to symmetry. The two-dimensional representation of G^0 is symmetric with respect to its z-variables. Its derivative is anti-symmetric and the (two-dimensional transverse) delta function is multiplied by a signum function in the z-coordinates.

B2-2 1100 PROPAGATION IN MEDIA WITH TRANSVERSE AND LONGITUDINAL VARIATIONS

N. Marcuvitz
Polytechnic Institute of New York, MRI
Farmingdale, New York 11735

Wave propagation through an inhomogeneous medium, having transverse and longitudinal variability is discussed via a singularity free quasi-particle method[1] that is based on an exact set of first order, coupled mode-type equations. The conventional paraxial or parabolic approximation appears as an uncoupled approximation to these equations. Formally exact coupled quasi-particle kinetic equations are derived for both the forward and reflected mode-tykes and, on the case where fast and slow space-time scales are distinct, can be readily approximated for numerical computation. Coupling of the forward and reflected mode-tykes is described in terms of a frequency dependent, separately calculable reflection coefficient. Comparisons with the usual parabolic equation approximation will be illustrated for a number of medium profiles.

(1) N.Marcuvitz, "Quasi-particle View of Wave Propagation" Proc. IEEE vol 63, No.11, Nov. 1980

This Research supported by Office of Naval Research under contract #ONR N00014-76-C-0176

B2-3
1130

ON THE APPLICATION OF UGTD TO MULTIPLE EDGE DIFFRACTION: Alfonso Malaga, SIGNATRON, Inc., 12 Hartwell Avenue, Lexington, MA 02173

The rigorous solution to the problem of diffraction by a knife-edge can be obtained by applying the well known Fresnel-Kirchoff theory, according to which the knife-edge is treated as a semi-infinite aperture. This theory has also been used to treat diffraction by two or more edges (Millington, et. al., Proc. IEE, V109C, 419-429, 1962). The solution (diffraction loss) is expressed in terms of Fresnel surface integrals. The Fresnel-Kirchoff theory can, in principle, be formally extended to treat diffraction by three or more successive knife-edges by replacing the surface (double) Fresnel integral with volume (triple) or higher order Fresnel integrals. Neither closed form nor tabulated solutions of the surface or volume Fresnel integrals are, however, available. Due to the complexity of the Fresnel-Kirchoff theory for multiple knife-edges many simple geometric methods have been proposed such as those of Epstein-Peterson (Proc. IEEE, V41, 595-611, 1953), the Japanese Atlas (1957), and Deygout (IEEE Trans. Ant. & Prop., VAP-14, 480-489, 1966). None of these methods are very accurate. They tend to overestimate the losses in some situations and underestimate the losses in others. A fourth method which is easy to apply for any number of edges is based on Keller's Geometrical Theory of Diffraction. The loss due to each edge is expressed in terms of an edge diffraction coefficient. This method gives the correct result when the observation point is in the shadow or lit regions but breaks down in the transition region.

In this paper we show that a method based on the Uniform Geometrical Theory of Diffraction recovers the exact Fresnel-Kirchoff solutions which are readily available for the case of one and two edges. The solution is similar to that obtained from the GTD solution. It differs from it in that a renormalized diffraction coefficient, which reduces to the GTD diffraction coefficient in the shadow and lit regions, is used instead. However, unlike GTD, this diffraction coefficient does not break down in the transition region where it recovers the solution obtained from the Fresnel-Kirchoff theory.

TOPICS IN INFORMATION THEORY
Wednesday morning, 13 Jan., CRO-30
Chairman and Organizer: Aaron D. Wyner,
Bell Telephone Laboratories, Murray Hill, NJ 07974

C1-1 0900 NETWORK INFORMATION FLOW: T.M. Cover, Stanford University, Stanford, CA 94305

We know that Kirchoff's laws describe current flows in networks. Gauss's law applies to electromagnetic flux through boundaries, and the max-flow min-cut theorem applies to the flow of water through pipes. We discuss the extent to which these laws apply to the flow of information in noisy communication networks.

C1-2 DISTRIBUTED ALGORITHMS FOR DATA NETWORK CONTROL

0930 R.G. Gallager
Massachusetts Institute of Technology,
Cambridge, Massachusetts 02139

A number of standard combinatoric problems for graphs, such as shortest paths, shortest spanning trees, maximum flow, and connectivity, find frequent applications as building blocks in algorithms for controlling data networks. In situations where the network topology and operating conditions are subject to change, it is desirable to solve these standard problems in a distributed fashion. That is, each node is originally ignorant of the network topology and knows only the status of its adjoining links. The nodes then co-operate, through communication over the network links, in solving the given standard combinatoric problem. Important performance measures for such algorithms are the amount of required communication and the required time. We present several recently developed distributed algorithms for those problems and then discuss an interesting tradeoff between time and communication cost.

C1-3 1030 CONFLICT RESOLVING ALGORITHMS FOR MULTI-USER COMMUNICATION SYSTEMS

Jack Keil Wolf
Department of Electrical and Computer Engineering
University of Massachusetts
Amherst, Massachusetts 01003

If two or more users simultaneously transmit over a common communications channel using nonorthogonal carriers, these signals conflict and need to be retransmitted. This paper is concerned with scheduling algorithms for resolving these conflicts.

Some previously described algorithms are reviewed and compared with new algorithms which are simpler to implement and exhibit improved performance. Several different models are considered, these models differing in how two or more interfering signals are interpreted at the receiver.

C1-4
1100

CAPACITY OF A PEAK-LIMITED OPTICAL CHANNEL

Aaron D. Wyner
Bell Laboratories
Murray Hill, New Jersey 07974

In this talk we consider an optical channel defined as follows. The channel input is a waveform $x(t)$ for which $|x(t)| < P$. The channel output is a Poisson process with intensity parameter equal to $x(t) + c$, where c represents a "dark current". The waveform $x(t)$ is restricted to be piecewise constant over intervals of length T, so that the "bandwidth" is proportional to $1/T$. The channel capacity of this channel is found explicitly in the limit as T approaches infinity (i.e., no bandwidth constraint).

We also study the situation in which the Poisson process is imbedded in Gaussian noise, and show that this does not degrade the channel capacity.

C1-5
1130

THEORY OF PERFORMANCE AND SURVIVABILITY OF LARGE C^3I NETWORKS UNDER ECM AND NUCLEAR-STRESSED CONDITIONS

Ira Kohlberg, GTE Products Corporation
STRATEGIC SYSTEMS DIVISION,
Needham Heights, MA 02193

A theory for predicting the performance and survivability of large redundant path C^3I networks under ECM and nuclear-stressed conditions is developed. These networks possess nearly a thousand nodes (message centers, relay terminals) and propagation links ranging from VLF to SHF. The networks include numerous critical message centers (e.g., command posts), with the required performance between them generally being different. The performance of a network is evaluated in terms of a set of functions $F_\mu(z,t)$ which for the μ^{th} command post pair is defined as the probability that the bit error rate (BER) is less than or equal to z, at time t following the onset of the threat. It is shown that $F_\mu(z,t)$ is of the form:

$$F_\mu(z,t) = \sum_\ell G_\ell(z,t)\bar{P}_\ell(t) + \sum_m \sum_n G_n(z,t)\, G_m(z,t)\bar{P}_m(t) + \sum_q \sum_r \sum_s \ldots$$

where the $\bar{P}$'s are polynomial functions of the individual probabilities of survival, P_i, for the nodes, and the G's are functions of the link parameters. The $\bar{P}$ and G functions depend upon the entire connectivity between the command post pair and hence incorporate a part of the redundancy in the system. Whereas the nodes are modelled as binary random variables, the links have a continuous distribution in BER due to degradation of the propagation medium caused by nuclear detonations. For a large number of links, the calculation of $F_\mu(z,t)$ may involve extensive computer cost. To circumvent this, an approximate method for determining $F_\mu(z,t)$ is developed based on a "Minimization Principle" which selects as the output BER of a relay terminal the smallest BER of the set of BER's entering the node. This approach leads to a sequential reduction of the network and a greatly simplified computation for F_μ.

Using the aforementioned equation for F_μ we find the minimum cost to achieve network survivability by first selecting the required BER's between command post pairs, z_μ, and the time t_o at which minimum performance is to be achieved. We subsequently express the network cost function as: $C_{NT}=\sum_i C_i(P_i)$, where $C_i(P_i)$ is the cost required to harden node i to probability of survival P_i, and N is the number of nodes. Minimizing C_{NT} subject to the set of inequality constraints, $F_\mu(z_\mu, t_o) \geq H_\mu$ = constant = required time availability for each μ gives the minimum cost for network survivability. The relevant mathematical algorithm is discussed. Several realistic examples of the Minimization Principal and cost minimization are presented.

PROPAGATION THEORY AND MODELS
Wednesday morning, 13 Jan., CR2-26
Chairman: James R. Wait, University of Arizona,
Tucson, AZ 85721

F1-1
0900

A THREE-PATH MODEL FOR REFRACTIVE FADING ON BROADBAND LINE-OF-SIGHT LINKS

Steen A. Parl
SIGNATRON, Inc.
12 Hartwell Avenue
Lexington, Massachusetts 02173-3198

A model of refractive layer multipath in the atmosphere is presented. The model characterizes all essential parameters of interest, including amplitude, delay, angle-of-arrival, and the frequency selectivity. Theoretical results are presented which show that the number of rays between two terminals is odd, and that there is always exists a height of the elevated duct for which the number of rays is 1 or 3+4p for some integer p. Multipath conditions in terms of distance, terminal heights, and refractivity gradients are presented. It is shown that modeling the ray angles at the antenna locations is much more important than has been assumed in the past. Even though more than three rays can occur it is suggested that a three-ray model is sufficient in most cases. The characteristics of the new model are discussed and compared to existing multipath models which do not consider the ray angle effects.

F1-2
0920

APPLICATION OF THE PARABOLIC EQUATION METHOD TO PROPAGATION IN INHOMOGENEOUS REFRACTIVE LAYERS:

J. P. Skura, J. W. Sari, and H. W. Ko, all at: The Johns Hopkins University/ Applied Physics Laboratory, Laurel, Maryland 20707

Numerical solutions have been obtained to the parabolic equation approximation for electromagnetic propagation in an inhomogeneous, stratified atmosphere. The solutions have used the split-step Fourier algorithm developed by Hardin and Tappert (SIAM Rev., 15, 423, 1973). The algorithm has been applied previously to acoustic propagation in inhomogeneous media (McDaniel, J. Acous. Soc. Am., 58, 1975). Both infinitely and finitely conducting earth models are assumed, with a point electromagnetic source.

In the models for inhomogeneous propagation, particular attention is paid to cases when a surface and radically curved elevated duct appear simultaneously. Such situations may result during a land/sea breeze cycle near a coastline. The elevated duct contour may vary with altitude due to boundary layer dependence on surface roughness.

For the case of an elevated source, solutions to the parabolic equation indicate enhanced coupling with the surface when the elevated layer varies with altitude. Characteristics of the solutions as a function of source altitude and frequency are compared.

The results suggest energy from the elevated source being coupled to the surface duct via transfer and leakage from the elevated layer.

F1-3
0940 TROPOSPHERIC PROPAGATION OF RADIATION FOR AN INHOMOGENEOUS, STRATIFIED ATMOSPHERE:

J. W. Sari and R. I. Joseph, both at:
The Johns Hopkins University/Applied Physics Laboratory, Laurel, Maryland 20707

Electromagnetic wave equations for propagation over a spherical earth are derived for the case of an atmosphere whose dielectric constant, ε, may vary both radially and horizontally, $\varepsilon = \varepsilon(r,\theta)$. For a dielectric constant varying reasonably slowly in the horizontal direction and relatively oblique wave propagation, the wave equations are shown to satisfy a parabolic approximation comparable to that given by Leontovich and Fock (J. Phys., U.S.S.R., 10, 13, 1946) for a one-dimensionally inhomogeneous atmosphere, $\varepsilon = \varepsilon(r)$. The wave equations may be applied to problems of super-refraction in the case of a vertically- and horizontally-stratified atmosphere. The limits of applicability of the equations are discussed. Two numerical solutions are proposed: a marching type, split-step Fourier algorithm given by Hardin and Tappert (SIAM Rev., 15, 423, 1973), and an iterative technique applied to an equivalent integral equation for a raised point source.

F1-4
1000 FOCUS WAVE MODES IN HOMOGENOUS WAVE EQUATION: James N. Brittingham, Lawrence Livermore National Laboratory, Livermore, CA 94550

To begin the experimental study of three-dimensional, source-free pulses in electromagnetic waves which remain focused for all time, one needs a pulse solution to Maxwell's homogenous equations. These pulse solutions need to move at light velocity in a straight line. The pulse functions must decrease in front, behind, and transversely to the axis of propagation as the pulses move through free space. Since singularities and discontinuities depict sources in classical electromagnetic theory, these solutions must not have either characteristic. Because the fundamental building block of all theoretical electromagnetics is the wave equation, it is natural to begin the study by searching for such solutions in the homogenous wave equation.

This paper will present the mathematical solutions to the homogenous wave equation which represents three-dimensional pulses propagating at light velocity in a straight line. The pulses' shape, which remains fixed for all time, decreases in front, behind, and transverse to the axis of propagation. The pulse functions are continuous with no singularities. Therefore, it is conceivable that these solutions might relate to source-free soliton.

F1-5
1040

FADE DURATION STATISTICS OF A RAYLEIGH-DISTRIBUTED WAVE

W. F. Bodtmann and H. W. Arnold
Bell Laboratories, Crawford Hill Laboratory
Holmdel, NJ 07733

This paper presents measured fade-duration and level-crossing statistics of a hardware-simulated fading channel with a Rayleigh amplitude distribution. This channel simulates radio propagation to a moving vehicle. The measurements agree well with existing analytical results and extend them to show the distribution of fade durations for shallow fades.

The channel is modeled as having a uniform angular distribution of paths arriving at the vehicle. This distribution produces a sharply peaked Doppler spectrum. It is known (S. O. Rice, BSTJ, 581-635, 1958) that the distribution of the duration of deep fades (>10 dB below the median signal level) is a function only of the ratio of the second to the zeroth moments of this Doppler spectrum. Measurements will be presented which confirm this dependence. These measurements show that the distribution of the duration of shallower fades is more influenced by the exact shape of the Doppler spectrum. Preferred durations for shallow fades are caused by the sharp peaks in the Doppler spectrum.

Deep fades are short and infrequent. Only 0.2 fades per wavelength occur whose depths exceed 20 dB. Only 1% of these fades have durations exceeding 0.1 wavelength. These results will be applied to the problem of communication with a moving vehicle.

F1-6
1100

TWO-FREQUENCY RADIATIVE TRANSFER THEORY FOR A RANDOM DISTRIBUTION OF ABSORPTIVE SCATTERERS WITH PAIR CORRELATIONS:

A. I. Tsolakis, I. M. Besieris and W. E. Kohler
Virginia Polytechnic Institute and State University
Blacksburg, Virginia 24061

Multiple scattering by a random distribution of discrete scatterers has been studied extensively over the past thirty five years, primarily because of its relevance to a large number of pressing applied problems that arise in radio physics and engineering. Based on the original work of Foldy, Lax, and Twersky, contributions in this area are confined for the most part to the computation of the coherent field and the incoherent field intensity. The simplifying assumption is also made that pair correlations among scatterers may be neglected, and, in actual applications, highly specialized scatterer distribution characteristics are often chosen. Due to these restrictions, the Foldy-Lax-Twersky theory cannot provide adequate answers for physical situations where large-angle scattering, anisotropies, absorption, and correlation among scatterers must be taken into consideration.

Our goal in this exposition is to present a systematic derivation of a two-frequency radiative transfer equation for scalar waves in the presence of a random distribution of absorptive scatterers with pair correlations. The derivation is based on the Dyson and Bethe-Saltpeter equations at the level of the direct interaction and ladder approximations, respectively. If, in addition to pair correlations, the assumptions are made that the number of scatterers is large and the average distance between any two scatterers is large compared with the wavelength, the Dyson and Bethe-Saltpeter equations are analogous to those associated with a continuous medium with fluctuations of the permittivity which are distributed according to a normal law and with a deterministic refracting profile directly linked to the number of scatterers per unit volume.

The analysis uses a continuous stochastic transport theory that was originally introduced by Barabanenkov et al. [Izv. Vuz. Radiofiz. 15, 1852 (1972)] and subsequently extended to the two-frequency context by Besieris and Kohler [Proc. Symp. on Multiple Scattering and Waves in Random Media, edited by P. L. Chow, W. Kohler and G. Papanicolaou (North-Holland, Amsterdam, 1981)].

F1-7
1120

RESOLUTION OF THE DISCREPANCIES BETWEEN DIFFERENT PHYSICAL OPTICS SOLUTIONS FOR ROUGH SURFACE SCATTERING

Ezekiel Bahar, Electrical Engineering Department
University of Nebraska-Lincoln, Lincoln,
Nebraska 68588-0511

The analysis presented here resolves the discrepancies between the different Physical Optics expressions for the scattered field derived by several researchers in the field. On applying the divergence theorem (in two dimensions) the term associated with the "edge effect" is shown to vanish identically for all scatter directions. Thus it is also shown that the so-called "edge effect" which appears in earlier derivations of the Physical Optics solution for rough surface scattering is a result of premature truncation of the closed surface integral expression for the scattered fields. Therefore this term must be suppressed even when it is not very small compared to the scattered field in the off specular direction. Since the Kirchhoff approximations for the surface fields are used in the Physical Optics approach, it cannot account for wave diffraction by edges. The Physical Optics solution derived here for arbitrary source excitation is shown to satisfy reciprocity and realizability relationships in electromagnetic theory. The integrand in the integral expression for the scattered field is identified with the specific reflectance (per unit area) of the rough surface.

MILLIMETER-WAVE ASTRONOMY-JOINT WITH AAS
Wednesday morning, 13 Jan., UMC Ballroom
Chairman: M.A. Gordon, National Radio Astronomy Observatory, Tucson, AZ 84745

J1-1
0830 AN OVERVIEW OF MILLIMETER-WAVE ASTRONOMY

M. L. Kutner, Department of Physics, Rensselaer Polytechnic Institute, Troy, New York 12181

J1-2
0930

A COMBINED SOUTH-NORTH CO SURVEY OF THE GALACTIC DISK; RADIAL DISTRIBUTION OF MOLECULAR CLOUDS FROM ℓ = 330° TO 70°: D.B. Sanders and P.M. Solomon, SUNY Stony Brook, NY 11794

We have observed ^{12}CO and ^{13}CO emission every 1° in longitude between 330° and 359°. The figure shows the radial distribution to peak at 6kpc in the Southern plane with a half width of 5kpc compared to a peak at 5.7kpc for Northern latitudes and a width of 3kpc. We have observed 1400 observations in the North out to b = $\pm$ 2°. Combining all of the data we find the equivalent face on CO integrated intensity at 6kpc to be 3 K·km/s corresponding to an H_2 surface density of 17$M_\odot$/pc^2. Conversion to mass is based on an empirical analysis of extinction, and CO data in dark clouds. The H_2 mass is 4 times the HI mass at 6kpc. Total H_2 is 2.7 x 10^9 $M_\odot$ inside the solar circle. The difference in the shape of the distributions is due to real features at 4 and 6 kpc in the S. and 5.5kpc in the North.

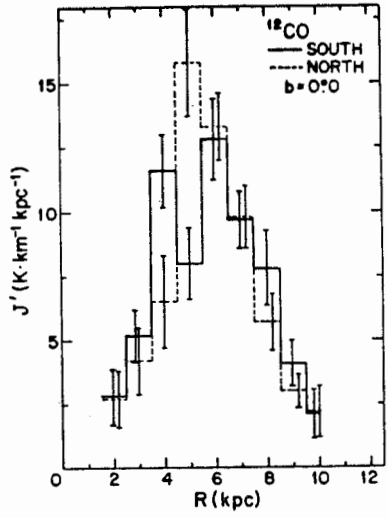

J1-3
0945

CO OBSERVATIONS OF THE EDGE ON SbI GALAXY NGC 891:

P.M. Solomon, J. Barrett, D.B. Sanders and R. Dezafra,
SUNY, Stony Brook, NY 11794

CO observations spaced every 45" at λ = 2.6 mm have been made along the major axis of N891 using the FCRAO 14m millimeter wave antenna (HPBW = 44"). (45" = 3.1 kpc for D = 14 Mpc). The CO integrated intensity as a function of distance from the center is shown below along with similar data for HI and 1412 MHz continuum (Sancisi and Allen, A.&A. 74, 73, 1979). CO emission was found at all positions observed out to $\pm$225"; however, its intensity falls off much more rapidly with distance from the center than does that of the HI. The radial width of the CO emission (and hence of the H_2 density) is closer to that of the radio continuum than to that of the HI. The concentration of molecular clouds towards the inner part of N891 is also apparent on line profiles and spatial-velocity diagrams. The average CO surface brightness is about twice that of our galaxy, although it would be equal for R > 6 kpc if D = 7 Mpc. There is a monotonic decline in CO emissivity with galactocentric distance. CO self-shielding is apparent at the central position.

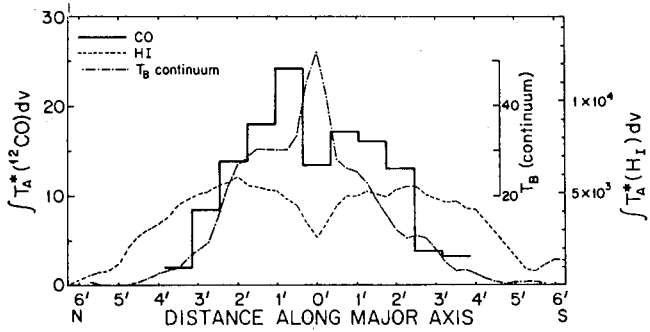

J1-4
1000

CO EMISSION FROM THE GIANT SC I GALAXY M101: P.M. Solomon, D.B. Sanders, J. Barrett and R. Dezafra, SUNY, Stony Brook, NY 11794

CO observations at λ=2.6mm were made at 42 positions in the disk of M101, using the NRAO 11m and FCRAO 14m antenna. The radial distribution shows a continuous rise towards the center in contrast to HI emission. There is no drop in CO inside of 4 kpc as in our galaxy. (Scoville & Solomon, Ap.J. 199, L105, 1975). There is a strong correlation between CO surface brightness and optical surface brightness. The CO has an exponential fall off with a scale length of 4 to 5 kpc. The surface density of molecular clouds and H_2 is linearly related to stellar luminosity; the star formation rate on a galactic scale is therefore proportional to the first power of average H_2 density.

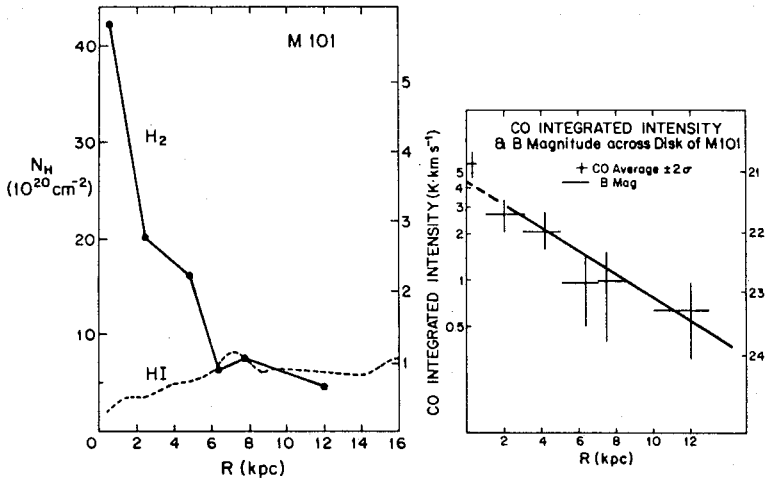

J1-5
1015

HCO^+ SYNTHESIS MAPS OF VELOCITY STRUCTURE IN K3-50

S.N. Vogel and W.J. Welch
Radio Astronomy Laboratory
University of California, Berkelely, CA 94720

We have mapped the molecular cloud surrounding the compact H II region/IR source K3-50 in the 89 GHz (λ3.4 mm) J=1-0 transition of HCO^+. A resolution of 8" x 13" was obtained with the Hat Creek interferometer; spectral resolution was 250 kHz (0.84 km s^{-1}). Visibilities were refered to the compact H II region (size 2") present in the off-line channels.

The HCO^+ maps reveal systematic velocity structure centered on the compact H II region/IR source. The position of peak HCO^+ intensity varies monotonically as a function of velocity, changing by 15" over a velocity range of 20 km s^{-1}. At line center the peak brightness temperature reaches 30 K.

K3-50 exhibits the signposts of early O star formation. Although evidence for high velocity gas exists in other regions of early O star formation (e.g. W51 IRS2), K3-50 is the first such region in which systematic velocity structure has been mapped.

J1-6 MILLIMETER AND OPTICAL DARK CLOUD OBSERVATIONS:

1030 R.M. Crutcher, Astronomy Department,
University of Illinois, Urbana, IL 61801

Interstellar spectral line observations have been performed at millimeter and optical wavelengths toward HD29647, a heavily reddened B8V star which is 20 arcminutes north of the center of Taurus Molecular Cloud 1. The possibility of studying grain properties as well as being able to obtain both radio and optical data for spectral lines gives a more complete picture of the properties of dense clouds than radio studies alone. We find $E(B-V) = 1.0$; since $R = 3.5$ from infrared photometry (Whittet et al., MNRAS, 196, 81P-85P, 1981), $A_V = 3.5$ magnitudes. The ultraviolet extinction is unique in that the 2200 Å absorption feature due to graphite is absent (Snow and Seab, Ap.J., 242, L83-L86, 1980). Whittet et al. (above) also find no 3.07 μm ice band, which suggests that the graphite grains are not coated with thick ice mantles; they suggest that graphite grains have been chemically processed and that molecules containing carbon may be especially abundant.

We have detected millimeter lines of CO, ^{13}CO, $C^{18}O$, HCN, and HCO^+ and have searched for HC_3N and DCN. Optical lines of K I, Na I, Ca II, CH, and CN were detected; others were searched for. (Additional millimeter and optical observations should be available by January 1982.) The ratios of column densities of CH, CN, and CO to A_V are enhanced by factors of 1, 10, and 100, respectively, with respect to values for the prototypical diffuse cloud toward ζ Oph. The $^{13}CO/A_V$ ratio is typical (Dickman, Ap.J. Suppl., 37, 407-427, 1978) for dark clouds. Since less than 20% of the carbon is in the form of CO and since cyanopolyynes do not appear to be tremendously overabundant, there is no evidence for chemical processing of the graphite grains which normally produce the 2200 Å feature.

We find $T_{kin} = 10$ K from CO. The gas density is well determined since the optical CN data provide direct measures of the populations of the N = 0, 1, and 2 states. The excitation temperature $T_{01}(CN) = 3.7$ K requires $n(H_2) \simeq 2 \times 10^4$ cm^{-3} for collisional excitation. This density is consistent with our detection of the J = 1-0 lines of HCN and HCO^+ weakly in emission. HCN/H and HCO^+/H have typical dark cloud values of about 10^{-9}. The fractional ionization has been determined in two independant ways. Determination of the quantity $Z = n(H_2) \cdot x(HCO^+)/x(CO)$ and the application of ion-molecule chemistry (Wootten, Snell, and Glassgold, Ap.J., 234, 876-880, 1979) yielded a fractional ionization of about 10^{-7}. Ionization equilibrium calculations for the observed atomic constituents yielded $n_e \simeq 10^{-3}$ cm^{-3}, in excellent agreement with the ion-molecule chemistry result.

J1-7
1045

LOW MASS STAR FORMATION IN THE DENSE INTERIOR OF BARNARD 18: P.C. Myers, MIT, Research Lab of Electronics, Building 26, Room 349, Cambridge, MA 02139

CO observations, visible obscuration, and near-infrared estimates of extinction in the star-forming cloud Barnard 18 indicate that the relatively dense ($n(H_2) \lesssim 3000$ cm^{-3}), visibly opaque region is associated with a less dense ($n(H_2) \lesssim 700$ cm^{-3}), nearly transparent region of greater spatial extent ($\sim$2 pc x 5 pc). A two-component model of the cloud and measurements of stellar extinction give estimates of the line-of-sight stellar positions with respect to the gas. These indicate that the dense inner gas has 9 known stars, star formation efficiency $\sim$ 2%, and star space density $\sim$ 8 pc^{-3}; the less dense outer gas has 8 known stars, star formation efficiency $\sim$ 1%, and star space density $\sim$ 0.9 pc^{-3}. Therefore these young ($\sim 3 \times 10^5$ yr), low-mass stars are preferentially located in the dense inner gas. Since their birth, the motion of the stars relative to the cloud is small compared to the cloud dimensions. Thus the stars were preferentially born in the dense inner gas. Calculations of escape speed and estimates of stellar speed indicate that most of the stars are probably gravitationally bound by the cloud.

J1-8
1055 INTERSTELLAR TURBULENCE AND THE ORIGIN OF ISOLATED DARK GLOBULES: C.M. Leung, M.L. Kutner, K.N. Mead, Rensselaer Polytechnic Institute, Department of Physics, Troy, NY 12181

Recent high-resolution carbon monoxide observations of over a dozen isolated dark globules indicate that a power-law correlation exists between the internal velocity dispersion (inferred from the line width) and cloud size. This suggests that the internal velocity field is dominated by turbulent motions in which small-scale motions are produced by the turbulent decay of larger-scale ones. The power-law relation implies the presence of supersonic turbulence and is rather similar to that found in other diffuse clouds and molecular cloud complexes (Larson, M.N.R.A.S., 194, 809). Thus the observed motions in globules may be all part of a common hierarchy of interstellar turbulent motions, suggesting that the physical origin, dynamical state and evolutionary stage of dark globules are intimately linked to the characteristics of interstellar turbulence. Most of the globules are found to be gravitationally bound and in virial equilibrium. The average gas density seems to decrease systematically with increasing cloud size, suggesting that gravitational contraction may account for the difference in gas density. The presence of some systematic gas motions, superimposed upon the turbulent motions and possibly due to slow contraction, is also suggested by the observed asymmetries in the line profiles. The effects of gravitational contraction which tends to increase the central gas density, coupled with the more rapid dissipation of turbulent motions in high density regions may account for the observed difference in velocity dispersion in different parts of a globule. The results are thus consistent with the scenario that isolated dark globules represent condensed fragments from nearby filamentary cloud complexes, the formation of which depends strongly on the properties of interstellar turbulence.

J1-9 1105 MESOTURBULENCE IN MOLECULAR CLOUDS: A NUMERICAL APPROACH: R. Dickman and S. Kleiner, University of Massachusetts, Department of Physics and Astronomy, Amherst, MA 01002

Despite the profound evolutionary effects which stochastic internal motions may produce in interstellar clouds, observational evidence for such motions remains ambiguous. As part of an observational and theoretical program to critically assess the utility of spectral line data in elucidating the amplitude and length scale of turbulent cloud motions, a molecular line formation model for stochastic flows has been developed. The model employs discrete velocity field realizations whose correlation lengths may be varied parametrically. We demonstrate its application to the formation of optically thick CO lines in clouds with radially decreasing source functions. By varying the model correlation length, we show explicitly that the endemic self-reversals predicted for such clouds by microturbulent line formation theory become progressively less evident as the correlation length of the flow is increased: The absence of self-reversed CO line profiles in most clouds does not imply the absence of substantial turbulent motions. The presence of self-reversed line profiles for species like HCO^+ or CS in clouds having single-peaked CO lines is shown to constrain the correlation length of any turbulent motions present. The utility of our models for interpreting velocity fluctuations in molecular cloud maps is briefly discussed.

This work was supported by NSF grant AST80 26702 to Five College Radio Astronomy Observatory.

J1-10
1115

HIGH-RESOLUTION MAPS OF IRC +10216 IN THE 89GHZ LINE OF HCN

W. J. Welch, B. Chapman, J. H. Bieging, University of California, Berkeley, CA 94720

J1-11
1130

HIGH-RESOLUTION SYNTHESIS MAPS OF 86 GHZ SO EMISSION TOWARD ORION-KL

R.L. Plambeck, M.C.H. Wright, B. Baud,
J. Bieging, P.T.P. Ho, S.N. Vogel, and W.J. Welch
Radio Astronomy Laboratory,
University of California, Berkeley, CA 94720

The 86 GHz (λ3.4 mm) 2,2-1,1 transition of sulfur monoxide has been mapped to a resolution of 6" x 6" toward the Orion-KL infrared source. Observations were made with the Hat Creek interferometer. The SO line was observed simultaneously with the 86 GHz SiO maser in Orion, which served as a phase and amplitude reference. Spectral resolution was 1.2 MHz or 4.2 km s^{-1}. The SO emission is concentrated in a region which has a FWHM size of 10" x 18" and is extended in a NE-SW direction, perpendicular to the two lobes of vibrationally excited molecular hydrogen emission. Although no single 20 μm source is associated with the SO emission peak, the SO centroid lies closest to IRc2 (which is coincident with the SiO maser). Our maps appear to exclude the BN object as a source of the high-velocity molecular emission.

Since the average H_2 density in the Orion-KL region is $>10^6$ cm^{-3}, the excitation of the SO transition will be dominated by collisions rather than infrared radiation. Therefore, the excitation temperature of the 2,2-1,1 line should be comparable to the gas kinetic temperature of 70-100 K. We observe a peak brightness temperature of about 50 K, which implies that the line has an optical depth of <1.5 and should be a good indicator of H_2 column densities.

The SO maps show a change in structure with velocity in the sense that emission to the NW of IRc2 tends to be redshifted from the peak velocity of +9 km s^{-1}, while emission to the SE is blueshifted. This velocity structure may be interpretable as an anisotropic outflow of material from the core of KL. The outflow probably has higher velocities to the NW and SE because the gas density falls more rapidly in these directions.

MICROWAVE/MILLIMETER WAVE MEASUREMENTS
Commission A, Session 2, CR1-42
Chairman: N.S. Nahman,
National Bureau of Standards, Boulder, CO 80303

A2-1
1330

A REVIEW OF THE SIX-PORT NETWORK ANALYZER DEVELOPMENT AT NBS

Glenn F. Engen
Microwave Metrology Group
National Bureau of Standards
Boulder, Colorado 80303

The impact on digital technology in the field of microwave metrology is perhaps best illustrated by the emergence of the automatic network analyzer. To a very large degree this has made it possible to eliminate the effects of hardware imperfections from the measurement results.

The initial efforts at NBS were based upon prior experience with four-port reflectometer theory. Here the key to accuracy proved to be the performance of the associated complex ratio detector. Accordingly, a sizable effort was invested in developing a high performance unit.

While this effort proved moderately successful, the overall approach lead to a system of substantial complexity with its attendant maintenance problems. More recently, interest has shifted to the so called "six-port" measurement technique, which provides an alternative method for implementing an ANA, while eliminating some of the complexity associated with the earlier NBS approach. In particular, the complex heterodyne ratio detector and associated local oscillators, mixers, etc., are eliminated in favor of simple diode on bolometric type detectors; yet the phase measurement capability has been preserved. Although a larger number of mathematical manipulations are required with the six-port technique, they are still within the scope of a desk-top computer.

An interesting feature of the six-port technique is the ability to trade precision in the detectors for dynamic range in the measured parameter. For example, the dynamic range of a thermister type power meter is typically 20 dB, yet the use of NBS developed instrumentation in conjunction with the six-port technique provides a useful dynamic range for attenuation measurements in excess of 60 dB. Apart from heterodyne detection systems, this is without precedent. Moreover, because the system is overdetermined, a continuous monitor of system performance is possible. Ultimately, it may prove possible to infer the absolute accuracy, for certain types of measurements, from this feature.

A2-2
1355

CORRELATION OF KNOWN SURFACE CURRENT VALUES WITH MEASUREMENTS UTILIZING INFRARED TECHNIQUES:

Ronald M. Sega, Department of Physics, U.S. Air Force Academy, CO 80840
Robert W. Burton, Department of Electrical Engineering and Computer Science, University of Colorado, Colorado Springs, CO 80907

The surface currents induced by electromagnetic radiation incident on conductive bodies produce joule heating measurable by infrared techniques. Qualitative studies have shown that surface current amplitude information can be determined from the surface heating pattern. A quantitative analysis, via infrared techniques, of surface current amplitude distributions on flat plates, cylinders, and spheres is presented. The results on the simple shapes are then compared to amplitudes distributions determined by analytical calculations and electromagnetic computer codes.

In determining the surface temperature distribution of an object by thermographic analysis, the problem of directional emissivity--angular and material dependence of infrared emission from varying surfaces--must be accounted for. An experimental arrangement using a blackbody simulator was developed to measure this geometric dependence such that a digital IR representation of the object could be corrected for geometry on a point by point basis. The corrected digital result was then correlated with the known results.

The IR results obtained with simple shapes, and compared with standard techniques, can now be extended to those objects that are more difficult to mathematically model. By considering the entire object with one IR measurement, the process provides a rapid and cost effective method of determining the relative surface current amplitudes. Electromagnetic energy in the microwave range is used for the simple shapes which should allow the transition to scale modeling of complex shapes to be efficiently accomplished.

A2-3 HORN-TYPE MILLIMETER-WAVE NOISE STANDARDS
1420

W. C. Daywitt
Electromagnetic Fields Division
National Bureau of Standards
Boulder, CO 80303

Increased waveguide loss and engineering difficulties urge the use of horn-type configurations for precise noise standards at millimeter-wave frequencies in place of the waveguide standards common to the microwave bands. Difficulties arise, however, because of the problem of defining and analyzing the aperture-to-waveguide loss in the horn; and because of the need to eliminate thermal "background" radiation. This talk reports on investigations undertaken to solve these problems preliminary to the design and construction of a millimeter-wave noise standard for the WR10 frequency band. Resulting criteria for a pyramidal horn specifically designed for use in such a standard are presented.

A2-4
1505

THERMAL RESPONSE OF THIN CONDUCTIVE COATINGS TO MICROWAVE ABSORPTION

Victor M. Martin, Department of Physics, U.S. Air Force Academy, CO 80840
Robert W. Burton, Department of Electrical Engineering and Computer Science, University of Colorado, Colorado Springs, CO 80907

It has been qualitatively demonstrated that the surface currents induced by incident electromagnetic radiation produce I^2R heating detectable through thermographic techniques. Of fundamental importance to the quantitative measurement of these currents, is the ability to predict resulting surface temperature increases in thin conductive coatings due to incident microwave radiation.

A theoretical analysis will be presented which will begin with a solution of Maxwell's equations. After solving for the electric fields inside the coating, the deposited energy density, σE^2, is then used in the heat equation to arrive at the theoretical thermal profile. The final equations are analyzed numerically on a Hewlett-Packard 9845B mini-computer. The result is a family of curves relating coating thickness to steady state surface temperatures as a function of electrical conductivity and relative permeability.

Selected experimental results will also be presented.

A2-5 95 GHz 6-PORT NETWORK ANALYZER

1530

M. P. Weidman
Electromagnetic Technology Division
National Bureau of Standards
Boulder, CO 80303

A dual and/or single 6-port system has been developed in WR-10 waveguide to operate in the 95 GHz region. The system is capable of measuring power, complex reflection coefficient, attenuation and phase. The system is automated except for the control of the klystron source. This system will be used for calibrations at NBS for the aforementioned parameters. Initial estimates show a system resolution (short term standard deviation) of 0.12 percent for power measurements, 0.001 for reflection coefficient, 0.005 to 0.5 dB for attenuation between 0 and 50 dB, and 0.1 degree for phase. Overall uncertainties will be higher.

A2-6
1555 ELECTROMAGNETIC SURFACE WAVE INVESTIGATION OF A DIELECTRIC LAYER OVER A CONDUCTIVE SUBSTRATE: Stuart A. Long, Weiming Ou, and C. Gerald Gardner, Department of Electrical Engineering, University of Houston, Houston, TX 77004

The thickness and permittivity (or dielectric constant) of a dielectric layer over an electrically conductive substrate can be determined by the propagation characteristics of surface electromagnetic waves traveling along the structure. This work uses the dependence of the propagation constant on frequency, and the cutoff frequency, of selected TE and TM modes to calculate the physical parameters of the dielectric layer.

An experimental investigation was also undertaken in which surface electromagnetic waves were launched using a prism coupling technique. The guiding structure consisted of a layer of polypropylene over an aluminum ground plane. The measured propagation characteristics over the 8-12 GHz range were then used to calculate the thickness and permittivity of the dielectric. These results were then compared with the known thickness and dielectric constant of the material. By scaling the apparatus to higher frequencies, the same method could be used as a nondestructive measurement technique for thin protective coatings on metals.

A2-7
1620

REVIEW OF AN ERROR ANALYSIS FOR USING THE MOON IN BROADBEAM ANTENNA-SYSTEM MEASUREMENTS

W. C. Daywitt
Electromagnetic Fields Division
National Bureau of Standards
Boulder, CO 80303

Using the radio output of extraterrestial noise sources can considerably lessen the difficulty in measuring antenna-system parameters like G/T. For medium-sized antennas the moon provides a convenient standard whose output can be calculated as a function of lunar phase and earth-moon separation distance from a formula with a minimum of pre-measured constants. A number of easy-to-use but precise algorithms for the calculation are presented in this talk, along with the results from a detailed error analysis.

ANTENNA THEORY AND PRACTICE
Wednesday afternoon, 13 Jan., CR2-28
Chairman: J.F. Mink, Army Research Office,
Research Triangle Park, NC 27709

B3-1
1330 A GENERALIZED RUZE'S FORMULATION FOR ANTENNA TOLERANCE THEORY: Y. Rahmat-Samii, Jet Propulsion Laboratory, California Institute of Technology, Pasadena, CA 91109

Both systematic distortions and random irregularities in the reflector antenna surfaces cause the antenna radiation patterns to be markedly changed from those of perfectly smooth reflector surfaces. The amount of changes introduced depends on many factors such as the distribution, magnitude and shape of irregularities, reflector illumination pattern, etc. In the past, the prime concern was on the control of the peak gains in terms of the acceptable level of the rms surface errors and Ruze's classical paper provided a simple solution for determining the gain loss as a function of surface rms error. Recently, application of multiple beam satellite reflector antennas demands that an accurate estimate of the sidelobe levels should also be made in terms of surface errors. These estimates are important in order to evaluate the isolation levels between multiple beams for a non-interfering multiple beam communication system.

The reflector pattern distortions can be approximately determined by studying the effect of its aperture phase errors. For random phase errors a statistical model was originally suggested by Ruze. His model was later advanced by Vu who allowed variable correlation intervals and standard deviations. However, Vu's model also has some limitations as it is only applicable for the uniform amplitude taper. In this work, Ruze's and Vu's models are generalized to study the effects of the random phase errors for most general cases. Both one-dimensional and two-dimensional aperture models are considered and the far-field average patterns are constructed for the non-distorted and statistically distorted phase errors. Results are presented for different sidelobe levels correlation intervals and variable standard deviations. Useful guidelines are suggested to control the sidelobe performances at the acceptable level. The results of this study can be useful for reflector antennas, aperture antennas and near-field measurement techniques.

B3-2
1355 A NOVEL GLOBAL SURFACE INTERPOLATION FOR REFLECTOR ANTENNA APPLICATIONS: Y. Rahmat-Samii and V. Galindo-Israel, Jet Propulsion Laboratory, California Institute of Technology, Pasadena, CA 91109

In many practical situations, reflector surfaces or their associated distortions cannot be described in a closed functional form. Rather, the surface may only be described at some discrete points. For example, one may refer to three cases: the result of a finite element model which only gives the location of the thermally distorted surface at certain discrete points, the dual reflector shaping synthesis which provides both the surface locations and their normals at discrete points, and measured targets which provide the surface locations and the slopes at a limited number of discrete points. In order to study the radiation characteristics of these reflectors, one must evaluate the diffraction integral. The accurate and efficient evaluation of the diffraction integral necessitates that the accurate knowledge of in-between points and their normals be available as the integration process proceeds. This is achieved by using an interpolation technique.

In general, there are two types of interpolation schemes which may be referred to as local and global. In the local interpolation, one employs spline function patches to interpolate between adjacent points with the requirement that both the function and a prescribed order derivative be continuous between adjacent patches. In the global scheme, one typically describes the surface in terms of a two-dimensional polynomial with unknown coefficients and then tries to determine the coefficients using a least squares error algorithm or some other method. Both the local and global interpolations have their advantages and disadvantages. It is the objective of this paper to present a useful new global interpolation scheme which is not only compatible with the local interpolation but is also very efficient and accurate. The scheme uses orthogonal expansions in terms of the Fourier-Jacobi series, which is functionally very attractive for interpolating most antenna surfaces of practical interest. In this scheme the unknown coefficients can be obtained by evaluating integrals for the expansion coefficients. In the process of performing these integrations one can use the description of the surface either as a closed functional form or as a local interpolation representation. It is shown that for a large class of useful reflector systems only a few coefficients are needed to represent the surface and its normals. Once the coefficients are determined, they can be used very simply and efficiently for repeated evaluations of the diffraction integral, and for convenient and simple storage of the reflector shapes. A typical set of representative examples will be presented to demonstrate the range of applicability of this interpolation scheme.

B3-3
1420

THE APPLICATION OF ANTENNA THEORY TO THE CALCULATION OF ELECTRIC SHIELDING DUE TO METALLIC REINFORCEMENT IN A CYLINDRICAL SHELTER:

L. Lewin*, Campus Box 425
Department of Electrical Engineering
University of Colorado, Boulder, CO 80309

This study has application to the protection of equipment in a shelter from the electric flash of a nuclear explosion. The main energy of concern is below about 1 MHz, or a free-space wavelength of 300 m, much larger than the size of most civilian shelters. Hence, quasi-static calculations are made. The reinforcement is modeled by a cylinder of equi-spaced rods, excited as dipoles with mutual interaction. This corresponds to an open cylinder. A second model has connected radial spokes at the two ends corresponding to an electrically closed cylinder.

Currents are assumed on the rods, the Hertzian potentials are calculated, and the resulting fields deduced. The requirement that the total tangential electric field at the rod surfaces be zero determines the current amplitudes, whence the electric fields inside the cylinder can be found.

The field at the cylinder center depends on the rod spacing, the length to diameter ratio of the shelter, and, to a lesser extent, the rod diameter. Typical attenuations for a rod spacing of 30 cm is from 10 to 25 dB if the cylinder is open, and about 22 to 27 dB if the cylinder is closed; the lower figures for a length as little as twice the diameter of the shelter. There is a substantial deterioration for the open cylinder for an axial displacement from the center, but little effect for a radial displacement.

In this latter respect the electric field behaves rather differently from the magnetic field, for which the shielding is known to deteriorate close to the walls.

A more rigorous solution exists for infinitely long cylinders and is closely approached for the field at the center when shelter length to diameter ratios exceed about six.

*This study was performed while the author was on Sabbatical leave at E.N.S.T. (Bretagne), France.

B3-4
1445

BEAM SCANNING IN OFFSET GREGORIAN ANTENNAS*:

V. Krichevsky and D.F. DiFonzo, COMSAT Laboratories, 22300 Comsat Drive, Clarksburg, MD 20871

The analytical solutions of the constant beam direction feed loci (CBDFL) and the optimum feed position locus (OFPL) in offset Gregorian antennas in the case when the symmetry axes of both parent surfaces of the reflectors make an arbitrary angle are described. The intersection of both loci produces the optimum feed position (OFP) with the best focusing for any specific scanned beam direction. In terms of the second-order approximation, the OFPL in canonical form is shown to be represented by an ellipsoidal surface.

The solution is based on the ray optics approximation and the assumption of the small feed displacement from the antenna focus compared with the subreflector focal length. Computer analysis of several specific beam scanning cases has confirmed that (a) CBDFL does represent the feed positions which provide the same beam direction with a good beam pointing accuracy; and (b) the feed located at the intersection of the CBDFL and OFPL does produce the best beam performance in terms of the beam sharpness and symmetry, maximum gain and minimum sidelobes compared with the other feed positions on the CBDFL or on the plane tangential to the OFPL at the focus for the same beam pointing.

The results can be applied to the design of the multi-beam and shaped beam antenna systems.

*This paper is based upon work performed at COMSAT Laboratories under the sponsorship of the International Telecommunications Satellite Organization. (INTELSAT).

B3-5
1530

A NOVEL BEAM-SCANNING TECHNIQUE FOR CIRCULAR RECEIVING ANTENNA ARRAYS

J.A. Leise, B.L. Weber, and P.A. Miller
NOAA, ERL, Wave Propagation Laboratory
Boulder, Colorado 80303

A convolution equation governing circular passive receiving antennas is derived from first principles. Practical implementation is achieved as a steered deconvolution technique. Because the beam pattern is invariant (insensitive) to the steer angle, the method is called angle-invariant deconvolution (AID). A distinguishing feature of the AID method is that the pattern is independent of the radius of the antenna - unlike aperture theory, which requires the beamwidth to be inversely proportional to the radius. Practical design is, nonetheless, consistent with conventional practice. Experimental results are given to verify the theory, design, and practical utility.

B3-6
1555

AN EXPERIMENTAL INVESTIGATION ON THE END-ADMITTANCE OF AN OPEN MICROSTRIP WITH APPLICATION TO MICROSTRIP PATH ANTENNA:

Robert Johnk and David C. Chang,
Electromagnetics Laboratory, Department of Electrical Engineering, University of Colorado, Boulder, CO 80309

The end-susceptance used in conventional theories for a rectangular microstrip patch antenna is usually computed from a quasi-static assumption. The dynamic nature of this susceptance was pointed out only recently by Chang and Kuester (Radio Science, 16, 1, p.1-13, June 1981) in their study of the canonical problem of a TEM plane obliquely incident onto the edge of a semi-infinite microstrip patch. The end admittance, obtained from a Wiener-Hopf formulation is valid, strictly speaking, only when the fringing field at the two corners of a finite width microstrip can be ignored. This of course is not an unreasonable assumption in view of the fact that in practice, the width of a patch antenna is typically between one-half to one free-space wavelength. However, the Wiener-Hopf result is typically a factor of two or greater than the quasi-static result and they have a very different frequency dependence. In order to investigate the validity of the Wiener-Hopf result, we have conducted in this work an experimental investigation in the frequency range of 1-2 gHz. This frequency range is chosen so that the size of the microstrip can be scaled up enough to allow us to measure the electric field standing-wave pattern near the open end from a probe inserted into a long, but narrow slot in the ground plane under the microstrip. Measured end susceptance (normalized to the characteristic impedance of the microstrip) indeed agrees very well with the Wiener-Hopf calculation even when the strip width is only a fraction of the free-space wavelength. As predicted by the theory, the value of this end susceptance is affected by the incidence angle of waves impinged at the open end and therefore, is determined indirectly by the width of microstrip. However, the behavior of the measured end conductance agrees with the Wiener-Hopf result (which has the same form as other wide microstrip theories) only when the strip width is at least one half of the free-space wavelength. For electrically narrow strips, the measured end conductance shows a frequency dependence of ω^{α} with α varying from $\alpha = 1$ for a wide strip to $\alpha = 2$ for a narrow strip.

B3-7
1620

BROADBAND, WIDE-ANGLE, QUASI-OPTICAL POLARIZATION ROTATORS:

N. Amitay and A. A. M. Saleh
Bell Laboratories
Crawford Corner Road
Holmdel, New Jersey 07733

A quasi-optical and wide-angle (of incidence) polarization rotator is described and analyzed. It consists of three or more parallel, equispaced wire-grid polarizers whose wires are oriented in different directions. With the proper choice of the number of grids, their spacings, and their relative orientations, such a polarization rotator is capable of operating over a broad frequency band and a wide range of angles of incidence.

A 7-grid 90° polarization rotator was designed to operate over a 42 percent relative bandwidth for a $\pm 60^{\circ}$ range of angles of incidence with less than 0.1 dB transmission loss. Various designs based upon our analysis are given. The impetus for this work is the specific application of this polarizer in a dually polarized multibeam satellite ground station antenna employing a linear array feed. The design of a 7-grid polarization rotator for the ground station antenna is presented.

INVERSE SCATTERING
Wednesday afternoon, 13 Jan., CR2-6
Chairman: G.P. Tricoles, General Dynamics Corp., San Diego, CA 92101

B4-1
1330 EVALUATION OF EXPERIMENTAL DATA ON THE OPTIMAL POLARIZATION PROPERTIES OF BUOY TARGETS MEASURED IN FREE SPACE AND PARTIALLY SUBMERGED IN WATER: Wolfgang-M. Boerner, Mohammed B. El-Arini, Sasan S. Saatchi, and Marat Davidovitz, Electromagnetic Imaging Division, Communications Laboratory, Information Engineering Department, SEO-1141, University of Illinois at Chicago Circle, P.O. Box 4348, Chicago, IL 60680; Steven Weisbrod and Lee A. Morgan, Radar Division, Teledyne Micronetics, 7155 Mission Gorge Road, San Diego, CA 92170

Basic theories of polarization utilization in radar target classification are summarized for the purpose of analyzing the optimal polarization properties of buoy targets. Experimental data measured by Weisbrod and Morgan are used to analyze the optimal polarization concept. Two specific shapes of buoy targets (four-corner dihedral reflectors and horizontal open-pipe sections) with different sizes measured in free space and submerged in a water range are used. The data were measured for a wide range of aspect angles at one single frequency of 3.150 GHz.

The moduli of the power scattering matrix elements (σ_{HH}, σ_{VV}, and σ_{HV}), the relative phases of the scattering matrix elements ($\alpha_{HH}-\alpha_{HV}$, $\alpha_{VV}-\alpha_{HV}$, $\alpha_{HH}-\alpha_{VV}$), the loci of the COPOL and XPOL null locations on the Huynen polarization map, and the spherical angle between the two COPOL nulls are plotted. A succinct interpretation of the graphical results is presented showing that polarization control applied to radar target classification represents an indispensable tool.

B4-2
1400 A DECOMPOSITION THEOREM FOR THE POWER SCATTERING MATRIX OF RADAR TARGETS: Chung-Yee Chan and Wolfgang-M. Boerner, Electromagnetic Imaging Division, Communications, Laboratory, University of Illinois at Chicago Circle, P.O. Box 4348, Chicago, IL 60680

Various representations of the polarization of an electromagnetic plane wave are presented with special reference to the formulation of useful radar target scattering matrices. The formulation, characteristic properties, and measurement techniques of the monostatic coherent (relative phase) Sinclair's scattering matrix, Graves' power scattering matrix, the symmetric Mueller matrix, and the incoherent symmetric time-averaged Mueller matrix of radar targets are reviewed. It is there shown that the power scattering matrix can be decomposed into two supplementary matrices which are then used to reconstruct the scattering matrix with relative phase and/or the symmetric Mueller matrix.

A method of determining the optimum polarization for the maximum total backscattered power ratio between target and clutter is presented. This method involves straight-forward differentiation of the backscattered power ratio and the solution is expressed in terms of the elements of the two supplementary power scattering matrices. The use of this decomposition theorem for the verification of Kennaugh's co-polarization null concept of optimum polarization in target versus clutter discrimination is demonstrated utilizing real-time experimental data measured by Poelman.

B4-3
1430 RECOVERY OF THE PRINCIPAL CURVATURES OF CLOSED CONDUCTING/DIELECTRIC SHAPES FROM POLARIMETRIC SCATTERING MATRIX DATA USING HF INVERSE SCATTERING THEORY: Sujeet K. Chaudhuri, Department of Electrical Engineering, University of Waterloo, Waterloo, Ontario N2L-3G1, Canada; and Bing-Yuen Foo and Wolfgang-M. Boerner, Communications Laboratory, Information Engineering Department, University of Illinois at Chicago Circle, P.O. Box 4348, Chicago, IL 60680

The information content of the complete scattering matrix at relatively (compared to scatterer dimension) small wavelengths has been analyzed. In particular, based on the time-domain first order correction to the physical optics currents a relationship between the phase factors of the scattering matrix elements and the principal curvature at the specular point is established.

The above phase-curvature relationship is tested by applying it to theoretical as well as experimental backscattering data, obtained from a prolate spheroidal scatterer. The results of these tests not only determine the acceptability of the phase-curvature relationship, it also points out the range of frequency over which the first order correction to the physical optics current is valid.

B4-4
1530 NUMERICAL EXPERIMENTS WITH A ONE-DIMENSIONAL PROFILE RECONSTRUCTION TECHNIQUE IMPLY STABILITY IN THE PRESENCE OF NOISE: W. Ross Stone, IRT Corporation, P.O. Box 80817, San Diego, CA 92111

There exist several approaches, in both the time and frequency domains, for reconstruction of one-dimensional conductivity and/or permittivity profiles from only backscattered data. Most of these suffer from at least two limitations: They magnify errors due to noise in the measurements, and they reconstruct the portion of the profile beyond a maximum with significantly less accuracy (if at all) than the portion between the measurement and the peak. A technique which overcomes these limitations would be of great value for such applications as determining the vertical electron density profile of the ionosphere using only a bottomside sounder. This paper presents evidence that such a technique exists.

Recently, N.N. Bojarski (Wave Motion, 2, 1980, pp. 115-124) presented reasonably efficient "causal space" methods of calculating direct and inverse scattering results in the time domain. He presented an example using a conductivity profile with a sharp discontinuity. The behavior of this example in the presence of errors in the simulated measured data was such that the corresponding errors in the reconstructed profile accumulated and were magnified.

This paper reports on several numerical experiments by the author using the causal space method to simulate the reconstruction of ionospheric electron density profiles using data such as could be obtained with a ground based vertical incidence sounder. The results show that, for typical electron density profiles, the error in the reconstructed profile is bounded by the error in the data. Furthermore, the ability to reconstruct profiles substantially above the maximum (i.e., above the "F region" peak) in the presence of realistic amounts of noise is demonstrated. To the author's knowledge, this is the first indication that such a capability may be possible using a simple ground-based sounder. The analytical reasons for this behavior are discussed, as well as other considerations of the practical application to ionospheric sounding.

B4-5
1600 BISTATIC LOW FREQUENCY INVERSE SCATTERING: Norbert N. Bojarski, 16 Pine Valley Lane, Newport Beach, CA 92660

The monostatic acoustic and electromagnetic low frequency inverse scattering solutions of this author (1980) are generalized to the bistatic case. Specifically, derived are bistatic acoustic and electromagnetic low frequecy direct scattering approximations in terms of the characteristic function of a scatterer. Unlike the monostatic case, for which the acoustic and electromagnetic low frequency direct scattering approximations are identical, and for which the electromagnetic low frequency direct scattering approximation fails to yield depolarization information, the bistatic acoustic and electromagnetic low frequency direct scattering approximations are different, and the electromagnetic bistatic low frequency direct scattering approximation does yield depolarization information. An inverse scattering solution for the complete set of moments tensors of this characteristic function is obtained. It is shown that this bistatic inverse scattering solution is a bistatic generalization of Rayleigh's monostatic law, yielding the Rayleigh volume of the scatterer for the tensor of rank zero. The moments tensors of rank one and two are shown to be the spatial position centroic and the principal dimensions (and their spatial orientation) o the scatterer respectively.

B4-6
1630 K-SPACE FORMULATION OF THE SCATTERING PROBLEM IN THE TIME DOMAIN: Norbert N. Bojarski, 16 Pine Valley Lane, Newport Beach, CA 92660

The arbitrary direct scattering problem is solved numerically in closed form in the time domain and spatial Fourier transform space. This solution consists of casting the general basic global laws (i.e., the second order partial differential wave equation or its integral representation) as a local algebraic equation in the spatial Fourier transform space, and leaving the specific local constitutive equations (i.e., the algebraic boundary conditions, which specify a given structure, which are conventionally imposed on the differential or integral representation of the genaral basic global wave equation) as a local algebraic equation in real space, thereby reducing the scattering problem to a statement of two simultaneous local algebraic equations in two unknowns (the fields and the induced sources) in two spaces connected by the spatial Fourier Transform. By virtue of causality, a numerically efficient closed form solution to this set of equations is obtained that utilizes the fast Fourier transform algorithm as the transformations between the two spaces. By virtue of the numerically efficient fast Fourier transform algorithem and the local algebraic representation, the number of required complex multiply-add operations and storage allocation is of the order of $N\log_2 N$ and N per temporal descretization respectively (where N is the number of spatial cells into which the scattering problem is descretized). The solution is thus practical for very large scatterers. Some numerico-experimental results are presented.

DIGITAL HF: EQUALIZATION AND RELATED TECHNIQUES
Wednesday afternoon, 13 Jan., CRO-30
Organizer and Chairman: Martin Nesenbergs,
U. S. Department of Commerce,
NTIA/ITS, Boulder, CO 80303

C2-1
1400

A UNIFIED THEORY OF EQUALIZATION:

J. Salz, Bell Laboratories,
Crawford Hill Laboratory,
Holmdel, NJ 07733

A unified theory is presented for data-aided equalization of digital data signals passed through noisy linear dispersive channels. The theory assumes that some past and/or future transmitted data symbols are perfectly detected. We use this hypothesis to derive the minimum mean-square error receiver. The optimum structure consists of a matched filter in cascade with a transversal filter combined with a linear intersymbol interference canceller which uses the ideally detected data symbols. The main result is an expression for the optimized mean-square error as a function of the number and location of the canceller coefficients, the signal-to-noise ratio, and the channel transfer function. When the number of canceller coefficients is zero, we get the well known result for linear equalization. When the causal or postcursor canceller approaches infinite length, we obtain the well known decision feedback result. When both the precursor and postcursor cancellers become infinite, we obtain the very best result possible, namely, the matched-filter bound dictated from fundamental theoretical considerations.

Neither the decision feedback nor the matched-filter results can be achieved in practice since their implementation requires infinite memory and storage. Our theory is used to calculate the rate of approach to these ideals with finite cancellers. Numerical examples for some channel models reveal the surprising result that the approach to these ideals is very fast and only a few canceller coefficients are sometimes enough to achieve satisfactory results.

C2-2
1430

A REAL-TIME HF CHANNEL MODEL

P.E. Argo and I.J. Rothmuller
Linkabit Corporation
San Diego, CA 92121

Methods for estimating propagation path loss for HF frequency selection for ambient and naturally disturbed conditions have been developed to operate on small computers. Using microprocessor technology, these frequency selection methods can be integrated into real-time link operating procedures at each independent HF terminal.

The channel model developed for use during disturbed conditions includes the effects of solar x-ray flares, Polar Cap Absorption Events (PCA), ionospheric storms, and auroral activity. The models compute the parameters needed for intelligent frequency selection. Once a path is chosen, the parameter that can be obtained is signal-to-noise ratio as a function of, for example, time of day. Inputs to the model include, propagation path, time of day, season, 10.7 cm solar flux, and solar x-ray flux. To compute the signal-to-noise ratio use is made of a noise model as well as allowing the user to specify the characteristics of the transmitting and receiving equipment (e.g., power, required SNR).

The model has been adapted for use in a variety of applications including scenarios with jammers, and for LPI purposes. Future work includes adapting developed ray-tracing techniques to the microcomputer environment to extend the channel model to account accurately for the dispersive and multipath characteristics of the channel.

C2-3
1530

DATA DIRECTED EQUALIZATION FOR HF CHANNELS:

Earl F. Smith and Daniel D. McRae,
Harris Corporation, Advanced Technology Department
P. O. Box 37, Melbourne, Florida 32901

In recent years interest in serial transmission approaches to digital HF has led to renewed investigation of equalization techniques applicable to a fading medium. Performance improvement by modems utilizing linear equalizers for HF channels is limited because of in-band nulls resulting from multipath. Greater improvement can be obtained with a decision feedback equalizer by making use of "known" (previously decided) data preceding the unknown data being estimated. Still greater improvement can be obtained with data-directed equalization utilizing known data both preceding and following blocks of unknown data. This technique requires transmission of known (overhead) data which not only aids greatly in the estimation and decision process, but also provides means of channel tracking recovery from deep fades, an important consideration for HF channels.

Comparison of these techniques and their performance for HF channels is discussed, and measured performance results for a modem utilizing the data-directed technique are presented.

C2-4
1600 RELIABLE HF COMMUNICATIONS AT GREATER THAN 1 BPS/HZ - AND THE EVOLUTION OF A DIGITAL MODEM THAT DOES IT. P.H. Anderson, Senior Engineering Specialist, Communication Systems Division, GTE Products Corp., Needham, MA 02194

Successful digital communication at rates above 1 bps/Hz at HF is possible if an adaptive equalizer is used to track the fading time-dispersive channel. This paper will review an investigation of this tracking problem leading to the selection of a square-root Kalman algorithm to update the coefficients of a decision feedback equalizer (DFE). The design of a new HF modem utilizing the Kalman DFE in conjunction with a continuous GO BACK N ARQ strategy will be described.

The results of extensive performance testing at data rates from 2400 to 9600 bps using the DICEF real-time HF channel simulator will be presented. Both low error rate and high throughput are achieved using the combined equalization/ARQ techniques. Preliminary test results from a live link will also be reported.

EM NOISE IN THE SEA
Wednesday afternoon, 13 Jan., CR1-40
Organizer and Chairman: E.F. Soderberg,
Naval Underwater Systems Center, New London, CT 06320

E1-1
1330 COMPONENT GEOMAGNETIC FIELD FLUCTUATIONS IN MONTEREY BAY:

P.H. Moose, Department of Electrical Engineering
O. Heinz, Department of Physics & Chemistry
Naval Postgraduate School, Monterey, CA 93940

Vertical and horizontal components of the magnetic field fluctuations have been measured on the floor of Monterey Bay in 60 to 100m water depth. Measurements in the .05 to 20 Hz frequency range indicate that the vertical components are significantly lower (10 - 20db) than the horizontal components in most portions of the spectrum. Significant differences have also been noted between normal day or night time activity and sunset when magnetic background levels increased 20db or more.

Work is now in progress to correlate these undersea data with data from a land station located in a remote mountain site 40 miles southeast of Monterey.

E1-2
1355

POWER SPECTRA AND CROSS COHERENCE OF MAGNETIC FLUCTUATIONS RECORDED ON LAND AND UNDERSEA

D. M. Bubenik, R. Abileah, SRI International, Menlo Park, California 94025

Time series of geomagnetic fluctuations were recorded simulaneously on land and undersea by DTNSRDC in sourth Florida during 5-day intervals in January, July, and September 1980. The land site utilized a helium scalar field magnetometer located near the shoreline; the undersea data were collected using an identical sensor in a nonmagnetic body towed 75 m below the surface at a velocity of 3 m/s. Nominal interstation separation was 30 km. Data were recorded digitally in the 0-12 Hz band on shore, and in the 0.01-4 Hz band undersea.

The ground station time series show clearly the Sq variation, with superposed random fluctuations. Because of the bandpass filter used in recording the undersea data, these time series exhibit only random variations. Spectra derived from the shore data at a resolution of 0.21 mHz shows an inverse-frequency-squared characteristic at frequencies below 0.05 Hz; the white sensor noise level (0.01 $\gamma/\sqrt{Hz}$) dominates above this frequency. The undersea power spectra exhibit this same trend at lower frequencies, but are dominated by magnetic signals generated by surface waves above 0.1 Hz. The identification of the surface wave signature is confirmed by comparing its spectral form with that of wave height spectra derived from wave rider buoy data recorded immediately before commencing the magnetic measurements.

The magniture-squared coherence (MSC) function was computed between the two data streams in the 0-4 Hz band at a resolution of 0.006 Hz. Significant MSC levels were found in the 0.02-0.05 Hz band in most of the 2 hour data segments analyzed, with a mean MSC level of 0.025 in the remainder of the spectrum. This latter value corresponds to that expected for uncorrelated data given the quantity of data processed. A value of 0.16 indicates that mutual coherence exists at the 99.9% confidence level. The observed 0.6 level of coherence would permit a noise power reduction of about 3 dB if a suitable noise cancelling algorithm were implemented between the two stations.

E1-3
1420

UNDERWATER MEASUREMENTS OF EM FIELDS

J.C. Solinsky
Physical Dynamics, Inc.
La Jolla, CA 92038

E1-4 1445 PROPAGATION MEASUREMENTS FROM A CALIBRATED SOURCE IN THE OCEAN:

J. A. Giannini and D. L. Thayer,
The Johns Hopkins University,
Applied Physics Laboratory, Laurel, MD 20707

An experiment was performed to measure the subsurface-to-subsurface propagation of magnetic fields from a horizontal electric dipole (HED) source. Measurements were taken in the ocean in the quasi-static regime in a frequency range from 1 to 10 Hz. Horizontal source/sensor separations from 180 to 450 meters and depths from 46 to 100 meters were used.

Comparisons are made between the data and theoretical model predictions relative to range dependence and magnetic field strength. The model accounted for propagation paths through the water as well as paths to the surface, over the water and back down to the sensor. The ocean floor in the area where the measurements were made was uniformly deep and the source/sensor separation was electrically small compared to ocean depth to avoid bottom reflections, possible paths through the weaker conductive bottom crust and coastline effects. Model predicted magnetic fields are found to agree with the experimentally measured fields approximately within experimental uncertainty (±20%).

E1-5
1530 PROPAGATION OF AN ELF, TRANSIENT PULSE IN THE OCEAN:

J.W. Sari and D.A. Bowser, both at:
The Johns Hopkins University/Applied Physics Laboratory, Laurel, Maryland 20707

Propagation of a transient pulse in a dissipative conductive medium has been examined using an electric dipole source and a magnetometer receiver submerged in seawater. The shape of the pulse was designed to match the dispersive properties of the conductive medium, similar to the prescription described in Connor and Felsen (Proc. IEEE, 62, 1586, 1974). That is, the pulse was generated with a variable frequency sweep rate such that initially the time envelope of the propagated pulse would tend to compress, rather than disperse. Observed pulse shapes for subsurface-to-subsurface propagation were compared to a numerical simulation of the pulse shapes for propagation in an infinite conducting ocean. Pulse compression is observed in the experimental data and the observed pulse shapes match reasonably the numerical simulation results for the input pulses and source/receiver separations.

E1-6
1555

VERTICAL COHERENCE OF GEOMAGNETIC NOISE PROPAGATING THROUGH SEAWATER:

D. A. Bowser, L. W. Hart, J. W. Sari
The Applied Physics Laboratory/
Johns Hopkins University
Johns Hopkins Road, Laurel, MD 20707

The vertical coherence of ultra-low frequency geomagnetic noise (0.005-0.1 Hz) propagating through seawater is investigated. Measurements of geomagnetic noise were made by two subsurface cesium vapor total field magnetometers. The theoretical depth dependence of geomagnetic noise is used to quantify the small but finite amount of phase shift and amplitude attenuation occurring in the signal received by two sensors separated in depth. Theoretical spectra of the gradient are calculated based on the measured output of one of the sensors and the theoretical depth dependence; and the results are compared to the experimental gradient spectra calculated from the subtraction of the two sensor outputs. Ordinary coherence between the two sensor outputs is calculated and compared to theoretical predictions. Comparisons of the results obtained via coherence and gradiometry support the theoretical predictions of the effects of propagation through seawater on ultra-low frequency geomagnetic noise.

E1-7
1620

SPECTRA OF GEOMAGNETIC FIELD FLUCTUATIONS FROM OCEAN SURFACE WAVES:

D. A. Bowser, J. W. Sari, H. W. Ko,
The Johns Hopkins University/
Applied Physics Laboratory
Laurel, MD 20707

Measurements of magnetic fields induced by the movement of ocean surface waves have been made by a subsurface total-field magnetometer system. The experimental system consisted of two Cesium vapor magnetometers towed at 3 m/sec at nominal depths of 100m and 175m. Calculations of ocean wave height spectra were made from data measured by a stationary wave height gauge located near the towing vessel. Theoretical predictions of doppler-shifted magnetic field spectra are based on the surface wave gauge data. The theoretical predictions are compared to computed magnetic field spectra from the magnetometer data. For the frequency range $0.05>f>1$ Hz, spectral peaks are noted in the magnetic field data which can be associated with surface wave activity. The measured spectral amplitudes and their scaling with magnetometer depth are found to agree with the theoretically predicted spectra.

E1-8
1640

ELECTROMAGNETIC ACTIVE SOURCE SOUNDING NEAR THE EAST PACIFIC RISE

P.D. Young and C.S. Cox
Scripps Institution of Oceanography
University of California at San Diego
La Jolla, CA 92093

An active source electrical conductivity sounding was carried out near the East Pacific Rise at 21°N. The average electrical conductivity from 2 km beneath the seafloor into the upper mantle was found to be about 0.004 S/m. There is no evidence of fully molten magma at a distance of 7 km from the spreading axis. The inferred conductivity with depth of the crustal rock is consistent with Brace's model of connected, seawater filled pores in rocks heated from beneath.

GROUND-BASED REMOTE SENSING
Wednesday afternoon, 13 Jan., CR2-26
Chairman: Robert K. Crane,
Dartmouth University, Hanover, NH

F2-1
1400 OBSERVATIONS OF RADAR SCATTER FROM THE ENTIRE ALTITUDE REGION TO 97.5 KM ABOVE JICAMARCA, PERU: C.R. Cornish and D.T. Farley, School of Electrical Engineering, Cornell University, Ithaca, NY 14853; B.B. Balsley, Aeronomy Laboratory, NOAA, Boulder, CO 80303; and R.F. Woodman, Instituto Geofisico del Peru, Apartado 3747, Lima 100, Peru

We report here the first successful observations of radar backscatter from the entire lower atmosphere. It is particularly difficult to obtain echoes from altitudes in the vicinity of 40-50 km, a region which is too high to have significant refractive index fluctuations due to the neutral gas and too low for electrons to make much of a contribution. The results presented here, however, show that a sufficiently powerful radar at a sufficiently long wavelength can obtain useable data even in this altitude range. The 50 MHz Jicamarca Observatory radar has an antenna area of $8.3 \times 10^4 m^2$ and transmitted a peak power of somewhat more than 2 MW for these experiments. The altitude resolution was 2.5 km and a 4-baud complementary code pulse compression scheme was used; hence the total pulse length was 67 μs. The integration time was approximately 6 minutes and these preliminary observations were made with the antenna pointed either vertically or on axis (1° off vertical). At the more oblique angles (3°) required to measure horizontal winds the signal may well prove to be somewhat weaker.

F2-2
1425

PROBING OF OPTICALLY CLEAR AIR AT NSSL

D.S. Zrnic, National Severe Storms Lab.,
Norman, OK 73069
J.W. Bilbro, Electronics and Control Lab.
NASA Marshall Space Flight Center
Huntsville, AL 35612

Over the last several years the National Severe Storms Laboratory has been engaged in studies of nonprecipitating air flows with a 10 cm pulsed Doppler radar. The efforts are geared towards deducing as much as possible about these flows from Doppler velocity and reflectivity fields obtained with a single radar. Such phenomena as gust fronts, cold fronts, and stationary frontal boundaries have been consistently observed. For gust fronts the equivalent reflectivity factors are quite variable, and often an increase in reflectivity at the crest of the front suggests that debris is airborne and carried by the moist air inflow over the top of cold air outflows. In a joint experiment with NASA, velocities measured by an airborne Doppler lidar are compared with the Doppler radar and tower data. Finally, some examples of divergence fields in prestorm environment show that storm development can be predicted, and the velocity field reveals flows associated with frontal boundaries.

F2-3
1510

THE MICRO-STRUCTURE OF VERY STABLE ATMOSPHERIC LAYERS AS REVEALED BY CLEAR-AIR RADARS AND IN-SITU SENSORS.

EARL E. GOSSARD, NOAA/ERL/WPL, R45x6
325 Broadway, Boulder, CO 80303

The use of ground-based clear-air radars to observe the structure of elevated atmospheric layers and associated flux quantities is described. Case studies in which FM-CW radar, acoustic sounder, tower and balloon data were available are described and analysed. Applications in which surface-based sensors might be used to deduce the gradients in elevated refractive layers are suggested and the conditions under which the methods are likely to succeed or fail are discussed.

F2-4
1545 THE USE OF THE THREE NOAA PULSE DOPPLER RADARS IN CCOPE.

R.A. Kropfli, W.R. Moninger, and F. Pasqualucci
NOAA/ERL/Wave Propagation Laboratory, R45x6
325 Broadway, Boulder, CO 80303

The Cooperative Convective Precipitation Experiment (CCOPE) was a three month long observational program on all aspects of convection near Miles City, Montana during the summer of 1981. The overall mission of CCOPE was to document with state-of-the-art research tools all stages of convection from the pre-storm, dry planetary boundary layer, to the development of clouds, early storms, and through the mature storm phase. To accomplish this ambitious task, a network of seven pulse-Doppler radars, 13 instrumented aircraft, 120 surface stations, a long-range surveillance radar and five radiosonde stations were operated and maintained by a team of several hundred scientists, engineers and technicians.

The primary NOAA contribution to this experiment was the system of two pulse-Doppler X-band radars and one dual-polarization, pulse-Doppler radar at K-band. Within the context of the overall experiment NOAA's research objectives were to evaluate the ability of these three radars to monitor thermodynamic and kinematic changes in early storms so that future dynamic seeding operations can be successfully evaluated. The primary analysis emphasis at NOAA will be the comparison of the K-band polarization signature with microphysical measurements from the instrumented aircraft and the relationship of these data to cloud kinematics. Favorable weather patterns provided an unexpectedly large number of good case studies. An overall view of the experiment and some preliminary results will be presented.

F2-5
1610

COMPARISON OF DUAL-POLARIZATION RADAR MEASUREMENTS OF RAIN WITH GROUND-BASED DISDROMETER MEASUREMENTS;

J.W.F. Goddard and S.M. Cherry, Rutherford and Appleton Laboratories, United Kingdom; V.N. Bringi, Colorado State University, Fort Collins, CO; and T.A. Seligan, Ohio State University, Columbus, OH

Dual-polarization radar measurements of Z_H and Z_{DR}, where $Z_{DR} = 10 \log Z_H/Z_V$ and Z_H, Z_V are the radar reflectivity factors for horizontal and vertical polarizations respectively, are compared with values derived from rain drop-size distributions measured by a Joss-Waldvogel disdrometer. The measurements were made simultaneously, with the radar pulse volume situated 120 m above the ground-based disdrometer.

Despite the difference in size of the respective sampling volumes, agreement between the radar and disdrometer measurements was generally good. The radar estimates of Z_H exceeded the disdrometer estimates by 1.6 dB on average, well within the expected experimental error. The disdrometer estimates of Z_{DR} based on the equilibrium raindrop shapes exceeded the radar estimates by 0.3 dB on average. This was somewhat larger than could be accounted for by experimental error, and further analysis suggested that some modification to the theoretical ratios of horizontal and vertical back-scattering cross-sections was required, for drops of diameter less than 2.5 mm. An empirical modification to these ratios due to drop oscillations enabled the difference to be reduced to 0.15 dB on average.

F2-6
1635

PLANETARY PROBE SIGNAL STRENGTH MONITORING TO OBTAIN ATMOSPHERIC INFORMATION

Thomas A. Croft
SRI International
Menlo Park, California 94025

During the descent of a space probe into the atmosphere of a planet or satellite, its radio signal strength gradually diminishes due to the combined action of refractive defocusing and absorption. Because both of these phenomena have an effectiveness that depends on the structure of the atmosphere, theory indicates that a measurement of descent probe signal strength should yield atmospheric information much like that acquired from conventional radio occultations. Moreover, this novel approach would provide information about the lower atmosphere all the way to the surface whereas occultations are inherently blind to the region below the critical level: 33 km in the case of Venus.

Such a measurement was tried for the first time during the descents of the four probes of Pioneer Venus on December 9, 1978 (L. Colin, J. Geophys. Res., 85, A13, 7575-7598, 1980). In analyzing the results, it became clear that a lack of preflight calibrations was compensated somewhat by the availability of signals from four probes, three of which were identical, being received by common equipment. The multiplicity provided not only the advantages of averaging but also a basis for recognizing anomaloies that might otherwise have contaminated the data base. The derived loss-height curve clearly favors a nominal atmospheric model over either of the hot or cold models that were selected as representative extremes in a pre-Pioneer Venus study conducted for NASA. As to the matter of degree, however, it does not appear that the method has enough accuracy to add to our existing detailed knowledge about Venus. For a probe to a less-explored body, signal strength monitoring preceded by adequate calibration promises to provide an avenue for obtaining valuable atmospheric information, particularly below the critical level.

VLF-ELF WAVE INJECTION INTO THE MAGNETOSPHERE
Wednesday afternoon, 13 Jan., CR1-46
Chairman, C.T. Russell,
University of California, Los Angeles, CA

H1-1
1330

VLF WAVE INJECTION EXPERIMENTS ON THE MAGNETOSPHERE FROM SIPLE STATION, ANTARCTICA

R. A. Helliwell, Radioscience Laboratory,
Stanford University, Stanford, CA 94305

Coherent VLF waves injected into the magnetosphere from Siple Station, Antarctica, may be amplified 30 dB or more and may trigger narrowband whistler-mode emissions that closely resemble the elements of chorus. The mechanism of generation is thought to be doppler-shifted cyclotron radiation from counter-streaming energetic electrons that are trapped in the earth's radiation belts. Observations of interest include:

(1) Temporal growth of a coherent signal is suppressed by added noise.
(2) Temporal growth can be suppressed at frequencies just below that of the test signal.
(3) Temporal growth can be started only if the intensity of the injected coherent signal exceeds a certain value. This 'threshold' value varies widely with time.
(4) After saturation is reached the stimulated signal often breaks into 'pulsations,' in which amplitude and frequency may vary over ranges of ~6 dB and ±50 Hz, respectively. A typical period is ~40 Hz.
(5) Triggering of both rising and falling tones nearly always begins with an increase in frequency.
(6) Two signals spaced by as many as 120 Hz sometimes appear to be strongly coupled, from the lower to the higher frequency.

A new model of the interaction is discussed in the light of these results.

H1-2 1400 SATELLITE OBSERVATIONS OF VLF SIGNALS AND ASSOCIATED EMISSIONS FROM GROUND BASED TRANSMITTERS

U. S. Inan
Radioscience Laboratory
Stanford University
Stanford, California 94305

A substantial portion of the energy radiated by a ground based VLF transmitter enters the magnetosphere and propagates as either a ducted or a non-ducted whistler mode wave. While ducted signals follow geomagnetic field lines and may emerge from the ionosphere at the conjugate point and be observed on the ground, much of the wave energy propagates in the non-ducted mode following complicated raypaths; these tend to remain above the lower boundary of the ionosphere and can only be observed in situ with satellite based VLF receivers.

Observations on IMP-6, S3, ISEE-1 and EXOS-B satellites have shown that signals from a ground based transmitter are commonly observed in a region covering a longitude range of (+,-)30 around that of the transmitter and over L-shells of 1.5-5.0. On occasion, signals are observed at points that can be as much as 60 away in longitude from the tranmitter location. The transmitter signals generally reach the satellite through a number of raypaths with different time delay, thus resulting in a pulse duration that can be 3-5 times larger than that is transmitted.

VLF emissions triggered by these predominantly non-ducted signals were found to be usually triggered by the later coming pulses and had a broader frequency spectrum; characteristics quite different than those of ducted emissions. This finding suggests that the mechanism of emission triggering by non-field aligned signals could be qualitatively different. ISEE-1 observations of emission triggering showed that these events tend to occur during midnight-dawn local times whereas EXOS-B observations showed that probability of emission triggering is enhanced during the few days that follow a geomagnetic disturbance.

A review of these observations is presented with a view towards identifying the important questions that remain to be answered. Upcoming measurements on the DE-1 satellite is also discussed.

H1-3
1430

THE EFFECT OF MAN-MADE VLF SIGNALS ON RADIATION BELT PARTICLES:

W. L. Imhof, J. B. Reagan, E. E. Gaines, Space Sciences Laboratory, 3251 Hanover Street, Building 255, Lockheed Palo Alto Research Laboratory, Palo Alto, CA 94304
R. R. Anderson, Department of Physics and Astronomy, University of Iowa, Iowa City, Iowa 52242

Over the years there has been considerable speculation and controversy regarding the possible precipitation of electrons by man-made VLF waves, including the radiation generated by power lines at high harmonics of the power line frequency (e.g. Helliwell et al., J. Geophys. Res., 80, 4249, 1975; Park, J. Geophys. Res., 82, 3251, 1977). The frequent observation of peaks in the energy spectra of precipitating electrons that decrease in energy with increasing L value in a manner consistent with cyclotron resonance with waves of a constant frequency has led to the suggestion that the waves may originate from ground-based VLF transmitters (Imhof, Gaines and Reagan, J. Geophys. Res., 79, 3141, 1974; Vampola and Kuck, J. Geophys. Res., 83, 2543, 1978; Koons, Edgar, and Vampola, J. Geophys. Res., 86, 640, 1981). From high resolution measurements Imhof, Gaines and Reagan (J. Geophys. Res., 86, 1591, 1981) set extremely narrow limits on the widths of the peaks, further suggesting the possible importance of monochromatic waves generated by man-operated VLF transmitters. Recently Imhof, Anderson, Reagan and Gaines (J. Geophys. Res., in press) measured the wave frequencies, electron peak energies and plasma density profiles in coordination and found the data to support strongly the conclusion that the narrow peaks in the electron spectra result from cyclotron resonance interactions with the narrow band waves produced by ground-based VLF transmitters. These past experimental measurements will be reviewed along with assessing the possible overall importance of transmitters in the loss of radiation belt electrons. In addition, a new satellite experiment (SEEP: Stimulated Emission of Energetic Particles) scheduled for launch in 1982 will be discussed in which it is planned to operate VLF transmitters with distinctive on-off patterns and to observe associated variations in the electron precipitation.

H1-4
1530 A COMPARISON OF TERRESTRIAL AND PLANETARY VLF EMISSIONS:

W. S. Kurth, Department of Physics and Astronomy, University of Iowa, Iowa City, IA 52242

The Voyager missions to Jupiter and Saturn have provided the first observations of VLF wave phenomena in non-terrestrial magnetospheres. Perhaps the most important analysis to be performed with the Voyager observations is a comparison of plasma wave phenomena found in the Jovian and Saturnian magnetospheres with those detected in the terrestrial magnetosphere. This comparison not only advances the identification and understanding of the non-terrestrial emissions, but also greatly enhances our knowledge of the terrestrial counterparts. At first glance, this comparison yields the somewhat extraordinary result that the terrestrial and non-terrestrial plasma wave "zoos" are quite similar in many respects. Virtually all phenomena observed at Jupiter and Saturn have close terrestrial cousins. Conversely, there are few, if any, terrestrial emissions which are not detected in the magnetospheres of Jupiter and Saturn. These similarities exist despite obvious differences between the solar wind-dominated magnetosphere of the earth and the magnetospheres of the giant planets which are dominated by internal plasma sources (such as Io) and driven largely by the rotational energy of the planet.

Of course, one other major difference between earth and the two giant planets is the presence of man and civilization on the former. Now, at least in theory, it is possible to compare VLF emissions in the terrestrial magnetosphere with those of another magnetosphere not affected by civilization in order to begin to sort out which phenomena at the earth are naturally occurring, and which are triggered, modulated, or even generated by man. Some preliminary results of such a comparison will be given.

H1-5
1600

HIGH POWER ACTIVE STIMULATION OF THE AURORAL PLASMA:
A.Y. Wong and J. Santoru, Department of Physics, University of California, Los Angeles, CA 90024; and J.G. Roederer, Geophysical Institute, University of Alaska, Fairbanks, AL 99701

A recently completed facility for the active stimulation of the auroral plasma using a high power pulsed HF radio wave transmitting system is described. A unique feature of a pulsed modular system is that it can be upgraded to very high power capability (e.g., 10-100 MW). This pulsed HF system would be used in the excitation of short-term nonlinear plasma phenomena, such as resonant enhancement, particle energization, electron density profile modification, excitation of VLF plasma waves, and the modification of auroral optical emission. This excitation is predicted on the basis of previous experience, which includes laboratory simulation experiments at high-pulsed power, excitation of the ionospheric plasma at low latitudes, and theoretical calculations.

Research supported by ONR Contract #N00014-78-C-0754.

VERY LONG BASELINE INTERFEROMETRY-JOINT WITH AAS
Wednesday afternoon, 13 Jan., UMC 157
Chairman: J.M. Moran, Center for Astrophysics, Cambridge, MA 02138

J2-1 1330 VERY LONG BASELINE INTERFEROMETRY: 1967-2000: Mark Reid, Center for Astrophysics, Cambridge, MA 02138

In 1967, groups of radio astronomers in the U.S. and Canada obtained interference fringes from cosmic radio sources using telescopes separated by thousands of kilometers. This technique, named Very Long Baseline Interferometry or VLBI, produced a three order-of-magnitude improvement in the angular resolution of radio sources compared to that obtained with "conventional" interferometers. Astronomers are now constructing images with an angular resolution of 0.0003 arcsec, and VLBI stands as an unparalleled tool for studying the structure and origins of the great variety of bright sources in the Universe.

VLBI is the only technique that can resolve the compact components in the centers of QSO's and the nuclei of active galaxies. The compact components supply the enormous amounts of energy these objects radiate. VLBI results have shown that the compact components are often aligned with the extended structures, suggesting the existence of massive central objects. The discovery of relative motions among the compact components which exceed the speed of light has been one of the most significant results in astronomy of the last decade.

VLBI observations have led to significant discoveries in Galactic astronomy. VLBI is the best tool to probe the detailed and complex structures of molecular maser sources which are associated with the formation of massive stars and with red giant and super-giant stars. Recently, relative proper motions within clusters of H_2O masers have been measured. These measurements give three-dimensional kinematic information and allow distances to be determined via statistical parallax techniques to star-forming regions anywhere in the Galaxy.

VLBI observations have been used to study many astrophysical problems including the gravitational bending of light and the detailed structure of hydrogen absorption in galactic and extragalactic sources. Also, VLBI is becoming an ultra-accurate astrometric and geodetic tool.

At present, most VLBI observations are conducted with a half-dozen telescopes whose geographic distribution is not optimal for making high quality images. Plans are being made in Canada and the U.S. for the construction of arrays of telescopes designed for VLBI observations in the late 1980's. Many other nations are currently building or planning VLBI stations to compliment and extend arrays. Finally, great advances in sensitivity, resolution, and image quality will be possible with the addition of telescopes in space. Plans are being made to link a telescope in space with a ground-based array later in this decade. In the 1990's, the possibility of a complete array in space opens up many new and exciting research areas.

J2-2
1430

MARK III VLBI OBSERVATIONS OF THE NUCLEUS OF M81 AT 2.3 AND 8.3 GHz

N. Bartel, B. E. Corey, I. I. Shapiro, MIT, A. E. E. Rogers, A. R. Whitney, NEROC, Haystack Observatory, D. A. Graham, J. D. Romney, MPIFR, R. A. Preston, JPL

The "normal" spiral galaxy M81 (Sab) is at a distance of ∿3.3 Mpc, the nearest galaxy with a compact core detected with VLBI (Kellermann et al., 1976, Ap. J. Lett. 210, L121). Its flat radio spectrum which is variable on the time scale of days implying a core dimension of ∿1000 AU, its detectable x-ray radiation, its deficiency in infrared radiation, and its broad but weak Mg II and Hα emission lines, all make it an intriguing candidate for an "active" galactic nucleus which could be studied in detail.

We report here on simultaneous VLBI observations made with the Mark III system at 2.3 and 8.3 GHz utilizing the telescopes of MPIFR (100 m), NRAO (43 m), and OVRO (40 m). The total flux density of the core region is 130±30 mJy at 2.3 GHz and 83±12 mJy at 8.3 GHz per MPIFR beam area. The best fit elliptical-Gaussian model has peak flux densities of 58.2±2.6 and 76.0±4.9 mJy, corresponding to peak brightness temperatures of $(18\pm1)\times10^{10}$ and $(6.9\pm0.4)\times10^{10}$K, major axes of 1.3±0.1 and 0.53±0.03 mas (FWHM), minor axes of 0.6±0.1 and 0.36±0.03 mas, and position angles (PA's) of major axes of 75°.0±3°.4 and 50°.±4°.9 at 2.3 and 8.3 GHz, respectively. The slightly inverted spectrum of the compact core suggests a variable optical depth in the nuclear region. The dimension of the core is ∿1000 AU. The PA of the compact core, though apparently frequency dependent at the 4σ level, is closely aligned with the rotation axis of the galaxy (PA = 62°±3°). (References in Bartel et al. 1982, Extragalactic Radio Sources, IAU Symposium No. 97.)

J2-3 1440

KINEMATICS OF THE SUPERLUMINAL QUASAR 3C 345

S.C. Unwin, Owens Valley Radio Observatory,
California Institute of Technology,
Pasadena, CA 91125

VLBI hybrid maps of the compact radio structure associated with the quasar 3C345 (z=0.595) have been made at 2.8 and 6.0-cm wavelength, at intervals of a few months for the last 4 years. At all epochs the source has a dominant unresolved "core" with a spectral index $\alpha \sim +1$, and a curved "jet" extending ~ 10 milli-arcsec from it in PA $\sim -77^{\circ}$. Although the jet continues to bend out to 2 arcsec, most of the rotation occurs within a few milli-arcsec of the core. The jet is very strongly one-sided, and any compact emission on the eastern side is at most 5% of the core. Embedded in the jet are "knots" which move away from the core with apparent speeds > $\underline{c}$. We have observed two such knots, both moving at $\sim 8/\underline{h}$ c ($H_o = 100\ \underline{h}$ km/s/Mpc, $q_o = 0.05$); if this motion is the result of relativistic beaming, then the jet must point within $14\ \underline{h}^{\circ}$ of the line of sight. Since their positions and proper motions are independent of frequency, the knots represent discrete components in the source. The knots decay as they move out, with half-lives of roughly a year at 2.8 cm and about 3 years at 6 cm. Knot spectra steepen from $\alpha \sim 0.5$ at the point where they can be resolved from the core to $\alpha \sim -1$ at the detection limit of about 5% of the core brightness. From presently available data, there is no obvious relation between outbursts in total flux density and the appearance of new knots in the jet.

J2-4
1455 STRUCTURAL VARIATIONS AT 329 MHz in 3C147: R.S. Simon, Owens Valley Radio Observatory, California Institute of Technology, Pasadena, CA 91125

The compact radio structure associated with the quasar 3C147 (z=0.545) has been mapped using VLBI, at 329 MHz at two different epochs: 1975.21 (R.S. Simon, et al., Ap.J., 236, 707-713, 1980) and 1981.09. The first observations used only three stations, with no short baselines. A map with low dynamic range (~8:1) was made with a resolution of 0.020 arcseconds. In 1981 a seven station interferometer was used to produce a map with ~25:1 dynamic range and the same resolution. Due to the large amount of data (long tracks on 21 baselines), this is the highest quality VLB map produced thus far. In addition to revealing the full extent of the jet in 3C147, definite variations in the source structure between the two epochs were observed. 3C147 exhibits a core-jet morphology with a flat-spectrum core that has become synchrotron-self-absorbed at this frequency and a jet that extends ~0.2 arcsecond (~2kpc, for H_0=55 Km/s/Mpc, and q_0=0.05). It is the core which exhibits low frequency variability. In addition, there is a larger (~0.5 arcsecond) halo which accounts for about 50% of the flux in the source. The jet in 3C147 bends through a large angle near its end, before merging into the diffuse halo.

Large changes in the visibility amplitude and closure phase were observed in 1981.09, as compared to 1975.21, on the three baselines and single closure phase in common between the two sets of observations. Hybrid maps made from the two data sets imply that the core has undergone a substantial increase in flux density, by about a factor of two. Since the source is dominated in flux density by the jet and halo, these variations in the core have only a small effect on the total flux density; the expected change in total flux density is less than 5%.

J2-5
1505

Hybrid Maps of 3C84 and 3C345 at 22.2 GHz

A.C.S. Readhead, D.H. Hough, M.S. Ewing,
California Institute of Technology
R.C. Walker, National Radio Astronomy Observatory
J.D. Romney, Max Planck Institut fuer Radioastronomie

Recent advances in hybrid mapping have made it possible to make proper maps of astronomical radio sources from poorly calibrated visibility data (Readhead et al., Nature, 285, 137, 1980). This has opened up the wavelength range accessible to aperture synthesis mapping through 1 cm to the millimeter regime. This technique has been tested by application to observations at 22.2 GHz. The powerful extragalactic radio sources 3C84 and 3C345 have both been mapped by this method using VLBI. These are the first proper VLBI maps at 22.2 GHz. Both maps have interesting implications for the theory of the formation of extragalactic radio sources.

J2-6
1520

DETECTION OF MILLIARCSECOND RADIO CORES IN ALL MEMBERS OF A COMPLETE SAMPLE OF RADIO QUASARS:

R.A. Preston and D.D. Morabito,
Jet Propulsion Laboratory, Pasadena, CA 91109
D.L. Jauncey, C.S.I.R.O., Canberra, Australia

VLBI observations have been performed on 31 radio quasars from the Parkes $\pm 4^{o}$ catalog. The selected sources form a complete radio sample and include all radio quasars within a 0.33 steradian sky area with total finding flux densities ≥ 0.5 Jansky at 2.7 GHz. The sample includes both flat and steep spectrum objects. The VLBI observations were performed between pairs of NASA Deep Space Network antennas on California-Australia and California-Spain baselines utilizing Mark II and Mark III VLBI systems. Only limited u,v coverage was obtained for each source. Fringe spacings were $\sim$3 milliarcseconds.

All 31 quasars were detected, indicating that each source possessed a radio core no larger than about a milliarcsecond in angular extent. For our sample, one milliarcsecond is equivalent to a linear size of order 1 to 10 parsecs. For each source, correlated flux density exceeded 0.05 Jy and the fringe visibility exceeded 0.04. This result suggests that all radio quasars, regardless of spectral index, have core components with angular sizes of one milliarcsecond or less.

J2-7
1540

A SEARCH AT THE MILLIJANSKY LEVEL FOR MILLIARCSECOND CORES IN A COMPLETE SAMPLE OF RADIO GALAXIES:

A.E. Wehrle, R.A. Preston, D.L. Meier,
Jet Propulsion Laboratory, California Institute of Technology, Pasadena, CA 91109
M.V. Gorenstein, I.I. Shapiro, Earth and Planetary Sciences, Massachusetts Institute of Technology, Cambridge, MA 02139
A. Rius, NASA Deep Space Network, Madrid, Spain

A complete sample of 26 radio galaxies was observed in March 1981 at 2.3 GHz using the Mark III VLBI system. A single 10 minute observation of each source was performed on a baseline between the 64-meter antennas of the NASA Deep Space Network at Goldstone, California and Madrid, Spain. The fringe spacing was $\sim$3 milliarcseconds with a detection limit of $\sim$1 millijansky. We believe these observations represent the most sensitive search for VLBI cores performed to date.

The sample of 26 radio galaxies was chosen from the set of bright galaxies identified with radio sources in the B2 catalog. The selection criteria included all galaxies within a sky area of 0.22 steradians with flux densities at 408 MHz greater than 0.25 Jansky and apparent visual magnitudes brighter than 16.5. All galaxies in the sample are elliptical galaxies.

A majority of the galaxies were found to possess milliarcsecond radio cores. We will discuss the relationship between the optical and radio properties of the galaxies and the characteristics of the cores.

J2-8
1555

MARK III VLBI: HIGH SENSITIVITY MAPPING OF WEAK RADIO SOURCES:

Marc V. Gorenstein
Irwin I. Shapiro
Nathaniel L. Cohen
Emilio E. Falco
Juan M. Marcaide
Massachusetts Institute of Technology
Cambridge, Massachusetts 02139
Alan E.E. Rogers
Alan R. Whitney
Hans F. Hinteregger
Roger J. Cappallo
Haystack Observatory
Westford, Massachusetts 01886
Richard W. Porcas
Max Planck Institut fur Radioastronomie
5300 Bonn 1, West Germany
Robert A. Preston
Jet Propulsion Laboratory
Pasadena, CA. 91103

The sensitivity of VLBI can be improved by using the wideband Mark III system, a calibration source for a phase reference, and simultaneously combining data from all baselines. A theoretical expression for the detection sensitivity is given along with some examples of weak sources mapped using the Mark III. Sub-milliJansky sensitivity has already been achieved. Large areas, of the order of an arcminute in linear dimension, can, in principle, be mapped at milliarcsecond resolution. However, in practice our maps have so far been restricted to regions of about 0".3 x 0".3.

J2-9
1610

A PHASE-COHERENT LINK BETWEEN VLBI STATIONS VIA SYNCHRONOUS SATELLITE

S. H. Knowles, W. B. Waltman
E. O. Hulburt Center for Space Research
Naval Research Laboratory, Washington, D.C. 20375
W. H. Cannon, D. A. Davidson, W. T. Petrachenko
York University, Toronto, Canada
Y. L. Yen
University of Toronto, Toronto, Canada
J. Popelar
Earth Physics Branch
Department of Energy Mines and Resources,
Ottawa, Canada
D. N. Fort
Herzberg Institute of Astrophysics, Ottawa, Canada
and
J. Galt
Dominion Radio Astrophysical Observatory
Penticton, B. C. Canada

A joint Canadian - U.S. experiment is in progress to demonstrate the capabilities of phase-coherent VLBI for the measurement of geodetic parameters including Universal Time and polar motion. In order to do this, we have developed a high-precision phase-coherent link between VLBI stations in British Columbia, Ontario and Maryland using the synchronous satellite ANIK-B.

The system uses the 12/14 GHz transponder of ANIK-B in a shared-user mode with television transmissions, and makes only modest power and bandwidth demands on the satellite channel. A two-tone transmission format eliminates the necessity for a coherent satellite local oscillator, and two-way transmission enables elimination of satellite position changes as well as atmospheric effects.

Data obtained on link performance during a first experiment lasting several days show a measured phase stability of 2×10^{-15} for a period of one day. This is superior to typical VLBI measurements of the performance of separated hydrogen masers. A complete measured Allen variance vs. averaging interval curve has been computed, and clearly demonstrates the long-term stability of the link. It also demonstrates the accuracy relationship of the link to various types of frequency standards over different time intervals. Our first results indicate an internal precision that verifies the ability of this technique to improve on the short-baseline interferometer technique currently used.

J2-10 MARK III VLBI:
1625 ASTROMETRY AND EPOCH J2000.0

C. Ma and T. A. Clark, NASA Goddard Space Flight Center and D. B. Shaffer, Phoenix Corporation, for the Goddard/Haystack/MIT/Onsala/UBonn VLBI group

The IAU has recommended that celestial positions be referenced to the FK5 equinox and equator of the Julian year 2000.0 ("J2000.0"). We have determined the J2000.0 positions for a set of extensively observed extragalactic radio sources from X-band and S-band VLBI data provided by NASA's Crustal Dynamics Project. The observations were treated as a single data set and all parameters, including station positions, UT1/polar motion, solid Earth tides, clocks, and tropospheric zenith delays, were adjusted simultaneously. Typical 3-sigma formal errors are less than 0".005 in declination, except for nearly equatorial sources, and 0".002 in right ascension. J2000.0 positions of some 75 other sources with fewer observations have been determined with somewhat poorer precision from individual experiments.

We have taken the J2000.0 position of 3C273 (12h 29m 6.6997s), derived from the Besselian year 1950.0 ("B1950.0") position of Hazard et al., as our right ascension reference. Our reduction procedures used the IAU 1976 constants for precession to/from J2000.0 as developed in expressions by Lieske et al. A new sidereal time expression from Aoki et al. reflecting the equinox offset and rate between FK4 and FK5 was applied. We derived the initial positions of sources other than 3C273 by adding 0.0376s to our B1950.0 right ascensions and then rotating from B1950.0 to J2000.0 using the matrix developed by Lieske. The RA offset reflects 1) the difference between FK4 and FK5 and 2) the effect of our using the IAU 1976 precession constant with Newcomb's expression for sidereal time in estimating B1950.0 positions. The IAU 1980 (Wahr) nutation series was used with fundamental arguments from Van Flandern. We used MIT's planetary ephemeris rotated to J2000.0 to reduce positions to the solar system barycenter.

J2-11
1640

MARK III VLBI: UT1, POLAR MOTION, AND BASELINES

T. A. Clark and J. W. Ryan, NASA Goddard Space Flight Center, and D. B. Shaffer, Phoenix Corporation, for the Goddard/Haystack/MIT/Onsala/UBonn VLBI Group

UT1, Polar Motion, and baseline vectors have been measured with X-Band or dual S/X-Band VLBI from 36 experiments spanning September 1976 through July 1981. These observations were carried out as a part of the NASA Crustal Dynamics Project. Experiments consisted typically of day-long sessions during which a dozen or so radio sources were observed repeatedly in order to achieve a wide sampling of baseline projections. Scan lengths were typically two minutes, and the different sources were observed as rapidly as the telescopes could be slewed from one source to the next. Bandwidth synthesis was used to increase delay observation precision. The resulting delay and delay rate observations were analyzed with an interactive, multi-parameter least-squares program by which source and antenna positions, atmospheric delays, earth tides, and UT1 and polar motion were simultaneously determined.

Experiments after May 1978 were carried out with the Mark-III VLBI system. These experiments produced measurements of the Earth's rotational position, UT1-UTC, with formal errors of less than 0.1 millisecond of time; and the VLBI values show the existence of systematic, annual errors in the current BIH data which are as large as 3 milliseconds of time. Polar motion was determined to about 1-2 milliarcseconds. Transcontinental U.S. baselines are sensitive to the X-component of polar motion, and baselines to Europe are necessary for an accurate determination of the Y-component.

A concentrated period of observations in September/October of 1980, as part of the MERIT campaign to measure earth rotation, showed typical baseline length deviations of 3-4 cm on 14 different baselines. Some of the baselines were determined 14 separate times. This was a period of unusually high solar activity and accurate results were obtained only because the dual-frequency system allowed removal of ionospheric effects. The length of the Haystack-Owens Valley Radio Observatory baseline shows no significant change between 1976 and 1981, with a limit of less than 1 cm per year.

J2-12 MARK III VLBI:
1655 FROM "LIGHT BULB" TO AP.J. OR J.G.R.

N. R. Vandenberg and D. B. Shaffer,
Phoenix Corporation, and T. A. Clark,
NASA Goddard Space Flight Center, for the
Goddard/Haystack/MIT/Onsala/UBonn VLBI Group

The Mark III VLBI system is now in routine use for NASA Crustal Dynamics Project measurements. However, astronomers have shown some reluctance to use the Mark III. We believe the apparent complexity of the system has scared potential users away. While the record terminal is indeed more complex than previous VLBI terminals, there is a set of software that makes the Mark III very easy to use. We discuss these programs and show examples, from scheduling to making use of correlator output.

An interactive program, SKED, creates an observing schedule and then prepares floppy disks with schedule and procedure files, printed schedules, and tape labels for use in the field. SKED provides selection of sources and stations, and then keeps track of tape usage and tape change times, telescope limits and slew times, and what sources are "up" at the moment. When the floppy disk schedule is used at the telescope, the terminal and tape recorder configuration are controlled by the observer, in absentia. The telescope operator need do nothing more than change tapes. Correlator control files are also made from the SKED files. Correlator output from the FRNGE program contains all the familiar VLBI results: (equivalent analog) correlation coefficient, phases (baseline and geocentric), delay, and delay rate; as well as other information. This flood of numbers may be bewildering at first, but is useful for checking the quality of data, and some of it is essential for geodesy and astrometry. Source mapping with Mark III data is no different from mapping with Mark II data, although current programs for mapping directly from Mark III data are rather rudimentary. Mark III output has been translated into the Caltech VAX mapping system. Another interactive program, SOLVE, is used for multi-parameter least-squares source position and baseline estimations.

All stages of Mark III analysis have been implemented at Goddard on an HP1000 mini-computer. A VLBI Data Base Handler provides convenient access to whatever subset of data is desired from individual scans. The data base handler is currently implemented on several HP systems. It is available for IBM 360 systems as well, and is being readied for VAX and Univac machines.

J2-13
1710

FREQUENCY RESPONSE OF A SYNTHESIS ARRAY: PERFORMANCE LIMITATIONS AND DESIGN TOLERANCES

A.R. Thompson, National Radio Astronomy Observatory, Socorro,New Mexico 87801, and L.R. D'Addario, National Radio Astronomy Observatory, Edgemont Road, Charlottesville, VA 22901

The frequency responses of the receiving channels of a radio astronomy synthesis array, and in particular the variations between them for different antennas, are factors which limit the accuracy and sensitivity of the instrument. A response that approximates a rectangular passband as closely as possible is advantageous from considerations of maximizing sensitivity within a given frequency band and minimizing the smearing of detail in the outer regions of a map. Tolerance on slopes, ripples, and other bandpass distortions can be determined by examining their effects with regard to loss in sensitivity and the introduction of errors in the assignment of complex gain factors for individual antennas using calibration observations. These calibration errors are generally larger in amplitude than in phase , and their effect is usually more serious than the loss in sensitivity. Errors in adjustment of compensating time delays affect the phase responses of of the signal channels and are also included. The effects discussed are relevant to both very-long baseline and conventional arrays. Implementation of the tolerances derived is discussed for the Very Large Array radio telescope of the National Radio Astronomy Observatory.

USE OF SPACECRAFT AND SATELLITE LINKS FOR SCIENTIFIC MEASUREMENTS
Commission A, Session 3, CR1-42
Chairman: Gerald S. Levy,
Jet Propulsion Laboratory, Pasadena, CA 91103

A3-1
0830

Radio Science Measurements Utilizing the Deep Space Network Radio Science System

B. J. Buckles, Radio Science System Engineer
Jet Propulsion Laboratory
California Institute of Technology
Pasadena, CA 91109

The Deep Space Network (DSN) has supported for many years radio science investigations that utilized radio metric data normally generated by the DSN Tracking System. However, due to the increasingly stringent requirements of proposed radio science experiments during the mid-nineteen seventies the present DSN Radio Science System was conceived as a means to perform future radio science investigations. The first phase of implementation was completed in 1978 and was used to support the Pioneer-Venus radio occultation experiments (Berman-Ramos, Pioneer Venus Occultation Radio Science Data Generation, IEEE Trans. on Geosci. and Remote Sensing GE-18, 11-14). Since then two additional phases of implementation have been completed in order to support the Voyager radio science experiments at Jupiter and Saturn.

Key characteristics of the present Radio Science System in addition to acquisition of the traditional radio metric data are (1) highly phase stable open loop receivers (2) reduction of recorded data bandwidth by using computer controlled receivers (3) realtime digitization and recording of data on computer compatible tape for narrow bandwidths and nonrealtime bandwidth reduction of wider bandwidth data and (4) realtime measurement and recording of system temperature information.

This paper describes the capabilities and performance characteristics of the DSN Radio Science System of today and addresses the goals and drivers for future implementation.

A3-2
0855

JUPITER AND SATURN AS SEEN WITH S- AND X-BAND

G. L. Tyler
Stanford University
Center for Radar Astronomy
Stanford, California 94305

Voyager radio science observations of the Jovian and Saturnian systems included:

1) Occultation measurements of the atmospheres of Jupiter and Saturn to the level of the clouds (1-bar pressure at Jupiter, 1.4 bar pressure at Saturn), and the atmosphere of Titan to the surface,
2) Determination of the ionospheric profiles at the occultation points,
3) Determination of the figures of Jupiter and Saturn and the radius of Titan to high precision (approximately 1 kilometer),
4) Measurement of the principal gravitational harmonics of the primaries and the masses of several Saturnian satellites,
5) The microwave extinction and scattering phase function of Saturn's rings - - which leads to estimates of the particle size distribution, and
6) a significant test of the general relativistic red shift in the potential well of Saturn.

These results were obtained through early scientific inputs to a carefully engineered radio tracking system and special trajectory considerations.

A3-3
0920

THREE YEARS OF RADIO SCIENCE WITH PIONEER VENUS

A. J. Kliore
Jet Propulsion Laboratory
California Institute of Technology
Pasadena, CA 91109

Since Venus orbit insertion on December 4, 1978, the Pioneer Venus Orbiter has been used to obtain a large number of radio occultation measurements of the ionosphere and atmosphere of Venus at S-band (13.05 cm) and X-band (3.56 cm) wavelengths. More than 140 profiles of electron density in the Venus ionosphere have been obtained, covering solar zenith angles (SZA) from 26^{0} to 167^{0}. On the dayside, the peak electron density peak behaves in accordance with Chapman theory, while the peak altitude does not. It remains fairly constant at about 140 km to SZA 70^{0}, then dips to about 138 km between SZA 70^{0} and 85^{0} in response to the rapidly decreasing density near the terminator, before rising to about 145 km on the terminator between SZA 85^{0} and 100^{0}. On the nightside the peak electron density displays great variability from orbit to orbit, having a mean of $20.5 \times 10^{3}\ cm^{-3}$ and a standard deviation of $8.3 \times 10^{3}\ cm^{-3}$. The altitude is also more variable, having a mean of 143 km and a standard deviation of 7 km. Over 100 profiles of the temperature structure of the Venus lower atmosphere between the altitudes of 40 and 90 km have also been obtained. The temperature structure has been found to vary mostly with latitude, with the tropopause height remaining at about 55 km from the equator to 45^{0} latitude, and then rising to about 64 km between latitudes of 55^{0} and 80^{0}, corresponding to the "collar cloud" region. In this region a strong temperature inversion above the tropopause is also observed. In the polar regions the tropopause altitute is either 55 km or 62 km, depending on whether or not the measurement was made inside or outside of the polar "dipole" features. The strong correspondence of temperature structure with observed visual features suggests that both are consequences of the general circulation pattern.

This work was performed under NASA contract NAS-7-600.

A3-4
1005

RADIO RELATIVITY EXPERIMENTS

R. W. Hellings
Jet Propulsion Laboratory
Pasadena, CA 91109

The remarkable precision of routine range and Doppler measurements to deep-space spacecraft has turned the solar system into a laboratory for testing the predictions of General Relativity. The experiments are of two types: those which probe the gravitational field of the sun and those which search for gravitational waves from cosmic sources.

By combining range data to the Viking lander with other astrometric data types, the relativistic effects of the sun's gravity on planetary orbits and on the propagation of electromagnetic tracking signals may be detected. The non-linear effect of the sun's self-gravity (PPN parameter β) has been measured to 0.5%; the curvature of space (PPN parameter γ) has been measured to 0.1%; and the time rate of change of the effective Newtonion gravitational constant ($\dot{G}/G$) has been shown to be zero to within a few parts in 10^{11} per year. The improvement in the determination of these parameters is mainly the result of the unprecedented accuracy of our knowledge of Mars' orbit, derived from ranging to the Viking lander. The orbit has now been modelled to within 8 m over the nearly five years of data.

In an attempt to produce a first direct detection of gravitational waves, we use the superior frequency stability of Deep Space Network to detect the tiny Doppler shift produced when a gravitational wave affects the spacetime through which a spacecraft tracking signal is passing. With accuracies of 10^{-2} mm/sec over 500 sec integration times obtainable in two-way tracking the Voyager spacecraft, a sensitivity to waves of dimensionless amplitude 3×10^{-14} is realized. The limiting error source in this measurement is scintillation in the interplanetary plasma. This limit may be improved by about an order of magnitude when an X-band uplink is available to replace the present S-band uplink.

A3-5 1030 CLUES FOR PLANETARY STRUCTURE: B.W. Williams and W.L. Sjogren, Jet Propulsion Laboratory, Pasadena, CA 91009

Extracting gravity field information from radiometric tracking (Doppler) data of orbiting spacecraft has provided constraints on planetary interiors. Over the last two decades, planetary explorations of the Moon, Mars, Venus, Jupiter, Saturn, and even planetary satellites have supplied opportunities for deducing the mass properties of these bodies. An overview of results from various planetary explorations will include the Ranger and Surveyor missions from which the mass parameter (GM) of the Moon was determined and the Apollo 15 and 16 orbits which resulted in confirmations of lunar mass concentrations (mascons). The Apollo 15 and 16 spacecraft included small unmanned subsatellites which, after release, came to within 15-20 km. of the lunar surface and thus provided the highest resolution thus far for a portion of the lunar surface.

The Mariner IX mission to Mars yielded preliminary Martian global gravity models which were initially used to model the large orbit perturbations encountered by the Viking I and II spacecraft. The Viking orbiters were eventually used to improve the global model of Mars gravity and also to pro-provide high-resolution surface gravity maps near their periapsis latitudes. A unique application of gravity reduction from doppler tracking occurred when the mass parameters of the Martian moons, Phobos and Deimos, were determined during encounters with the Viking spacecrafts. Meanwhile, the Pioneer Venus Orbiter provided the first detailed look at the Venusian gravity field. Both direct and indirect methods were again used to obtain gravity information, but the task was complicated by the relative insensitivity of the PVO orbit to Venus gravity perturbations. These gravity maps correlate very well with radar maps of surface topography obtained from PVO even though this does not occur for the Earth.

A quite different approach to the inference of Earth's gravity perturbations on two orbiting spacecraft will be presented in a summary of the GEOS-3/ATS-6 experiment. The analysis of the relative tracking between the low orbit of GEOS-3 and the much higher orbit of ATS-6 resulted in measures of local gravity anomalies which were free from errors associated with spacecraft tracking from Earth-based stations. Finally, the recent determinations of mass parameters of Jupiter and Saturn from the fly-bys of Voyager I and II will be presented. The results obtained from single encounters such as these, while more limited than orbiter results, can nevertheless yield constraints on planetary structure.

A3-6
1055

IONOSPHERIC RADIOWAVE PROPAGATION MEASUREMENT TECHNIQUES

J.A. Klobuchar, Air Force Geophysics Laboratory, Hanscom AFB, MA 01731
C.L. Rino, SRI International, Menlo Park, CA 94025

Various military and civilian satellite systems including NASA-JPL Deep Space Probes require correction for the time delay effects of the earth's ionosphere. Satellite communication systems require a knowledge of the statistics of ionospheric amplitude and phase scintillation for system design and operational planning purposes. Since satellites specifically designed for ionospheric monitoring purposes would be very expensive, the ionospheric community has taken advantage of the signals transmitted from various operational navigation and communications satellites to make measurements of the amplitude and phase fading as well as time delay produced by the ionosphere. These measurements have used telemetry beacon signals from 137 MHz to communications carriers at frequencies in excess of 10 GHz. The standard amplitude scintillation measurement simply requires determining the normalized RMS statistics of the received signal as a function of time, while the phase measurement requires detrending the diurnal curve from the received phase changes and determining the RMS fluctuations remaining after a suitable detrend interval has been chosen. The absolute ionospheric time delay can only be determined by measuring the difference in phase of modulation received on two carriers such as the method used in the NAVSTAR-Global Positioning System (GPS) satellite navigation system currently under development. Other two frequency satellite systems, such as the TRANSIT 150-400 MHz low orbit satellite navigation system are able to correct only for range rate errors due to changes in the relative ionospheric time delay from one satellite position to another.

Still another technique for determining relative ionospheric time delay, weighted by the earth's magnetic field, is the measurement of Faraday polarization rotation of linearly polarized VHF radio signals transmitted from telemetry signals from suitable geostationary satellites. While Faraday rotation is a relative ionospheric time delay measure, the ambiguity in determining the absolute number of turns of polarization rotation due to the ionosphere generally is not difficult to resolve.

While various techniques have been developed for near-real-time measurement of the amplitude, phase and time delay characteristics of trans-ionospheric paths, the use of signals from the NAVSTAR-GPS satellites shows the most promise for future near-real-time user requirements.

A3-7
1120

TECHNIQUES FOR DETERMINING ELECTRON CONTENT CORRECTIONS FOR INTERPLANETARY SPACECRAFT NAVIGATION

H. N. Royden, T. E. Litwin, and R. A. Norman
Jet Propulsion Laboratory
California Institute of Technology
Pasadena, CA 91109

Determination of the orbits of interplanetary spacecraft at the Jet Propulsion Laboratory (JPL) is performed by using Doppler and range measurements from the radio link between spacecraft and Earth, augmented by optical measurements near the target planet. The high precision of radio navigation arises from the fact that these measurements determine angles (right ascension and declination), not just radial velocity and distance. Free electrons along the signal path introduce errors in Doppler and range measurements that result in significant errors in the angles derived from those measurements. The angular errors due to the earth's ionosphere, in particular, are systematic.

Most of the deleterious effects of ionospheric and solar-plasma electrons on orbit-determination accuracy can be removed by applying computed corrections for total electron content along the line of sight to each data point. These corrections are based on Faraday-rotation ionospheric electron content mapped from geostationary satellites and on dispersive (S- and X-band) downlink Doppler directly from the spacecraft. The techniques used at JPL to determine these corrections will be described, along with both direct and indirect applications to radio science measurements.

INTERFACE AND SURFACE EFFECTS
Thursday morning, 14 Jan., CR2-28
Chairman: Allen Q. Howard,
Department of Electrical Engineering, University of Arizona, Tucson, AZ 85721

B5-1
0830 SINGLE INTEGRAL EQUATION FORMALISM FOR SCATTERING AND TRANSMISSION AT A ROUGH INTERFACE:

J.A. DeSanto, Electro Magnetic Applications, Inc., 1978 S. Garrison St., Denver, Colorado 80226

We discuss the problem of scattering and transmission by a rough interface separating homogeneous semi-infinite media using Green's function methods. The media are either fluids (acoustic case) or dielectrics (TE and TM polarizations). Green's theorem applied to the upper medium (V_1) containing the source and field coordinates (for a scattering problem) yields an integral relation for the field value G, in terms of surface values G_{1S} and its normal derivative N_{1S}. Green's theorem in the lower medium (V_2) with source and field coordinates in V_1 yields an extended boundary condition or extinction coefficient relating surface values G_{2S} and N_{2S}. Using the usual continuity conditions at the interface, combining the equations, passing to the surface limit, and expressing the results in terms of a single layer integral density yields a single integral equation for this density. Analogous results hold for the transmitted field. In the limiting cases for Dirichlet and Neumann boundary conditions we recover the usual boundary integral equations from this single equation. In the flat surface limit the Fresnel reflection and transmission coefficients are derived.

B5-2
0850

COHERENT SCATTERING FROM GENTLY UNDULATING RANDOMLY ROUGH CONDUCTING SURFACES:

G. S. Brown, Applied Science Associates, Inc.
Apex, North Carolina 27502

A scattering solution which goes beyond physical optics or perturbation approximations is presented for the case of a randomly rough perfectly conducting surface having negligibly small slopes and curvatures but arbitrary height. The continuous surface is approximated by an infinite number of nonoverlapping large flat areas which are randomly elevated with respect to the mean planar surface. This approximation is justified by the small surface curvatures and slopes. Ignoring curvature and slope effects and using the above approximation for the surface, the magnetic field integral equation for the current induced on the discretized surface is solved exactly. The solution shows that only the lowest elevated flat area supports a nonzero current and this particular current is equal to the physical optics value. The average scattered field is found to depend upon the probability density function for the random surface height, its distribution function, and the effective number of surrounding flat areas N. For the case where decorrelation implies statistical independence, the average scattered field is given by one straightforward integration which is solved numerically for a Gaussian surface. For a given surface roughness or Rayleigh parameter, there is one and only one value of N which maximizes the average scattered field. The N which maximizes the average scattered field is found to vary as the Rayleigh parameter raised to the third power. In consonance with the physics of multiple scattering, this result is interpreted to represent the increasing area of interaction on the surface. That is, for N=0 there is no multiple scattering on the surface while for N>>1 there is strong multiple scattering or interaction on the surface. Thus, for the first time, it is possible to clearly relate the effective area of multiple scattering on the surface directly to the surface roughness.

B5-3
0910

COMPLETE ORTHOGONAL FUNCTIONS FOR COUPLED STRIP CONDUCTORS IN STRATIFIED DIELECTRICS:

Bing-Hope Liu, Electromagnetics Laboratory,
Department of Electrical Engineering,
University of Colorado, Boulder, CO 80309

Recently, the author has proposed a method for systematically constructing basis functions for two-dimensional field problems containing a strip conductor buried in stratified dielectrics (to appear in the Special Issue of RADIO SCIENCE on the 1980 Munich Symposium). In this paper, the method is generalized to the case of a pair of symmetrical conductor strips.

By applying a simplifying averaging process to the associated static problem, the structure of the specific kernel or Green's function can be determined approximately. An integral form of continuity equation is derived; general sets of even as well as odd quasi-eigenfunctions defined on the discrete interval $(-b,-a) \cup (a,b)$ are set up, which are orthogonal and complete in appropriate Hilbert spaces. On substituting into these sets the specific information obtained from the approximate kernel, the required quasi-eigenfunctions for the problem in question can be established.

Since both the edge condition and the continuity equation are satisfied simultaneously and the inhomogeneity of dielectric constants is duly taken into account, these resultant functions are a particularly suitable expansion basis for the series or moment solution to such physical quantities as scalar potential, induced surface charge, and surface current in wave guide or scattering problems involving a pair of symmetrical strips buried in stratified dielectrics.

B5-4
0930

RADIATION PATTERNS OF HF DIPOLES ON A SLOPING BEACH

K. S. Park, C. J. Teng* and R. J. King
Department of Electrical and Computer Engineering
University of Wisconsin, Madison, WI 53706
*M.I.T. Lincoln Laboratory, Lexington, MA 02173

The effect of a sloping beach on the radiation of a vertical electric dipole (VED) is of practical interest since antenna systems are often situated on an island or near a coastline. Recently, Teng and King (Electromagnetics, 1, 101-116, 1981) developed an integral formulation using the compensation theorem which can be applied to azimuthally symmetric ground structures on which the surface impedance can vary arbitrarily in the radial direction. Here, the radiation characteristics of a VED on a circular island-sloping beach-sea are numerically investigated using this method. As the formulation is based on the surface impedance concept, the surface impedance along the sloping beach is calculated using an overburden of uniform depth equal to the local depth of the sea water and parallel two-layer stratified media theory. It was found that the sloping beach does not have a profound effect on the radiation pattern, because the effective sloping beach only extends about $0.15\lambda_0$ at 10 MHz (ab). At this point (b) the impedance of the sloping beach is about 90% of that of the homogeneous sea. Also, the effects of various parameters such as the properties of the land (e.g., wetness), the distance between the VED and the coastline (a), the height of the VED and the operating frequency are discussed.

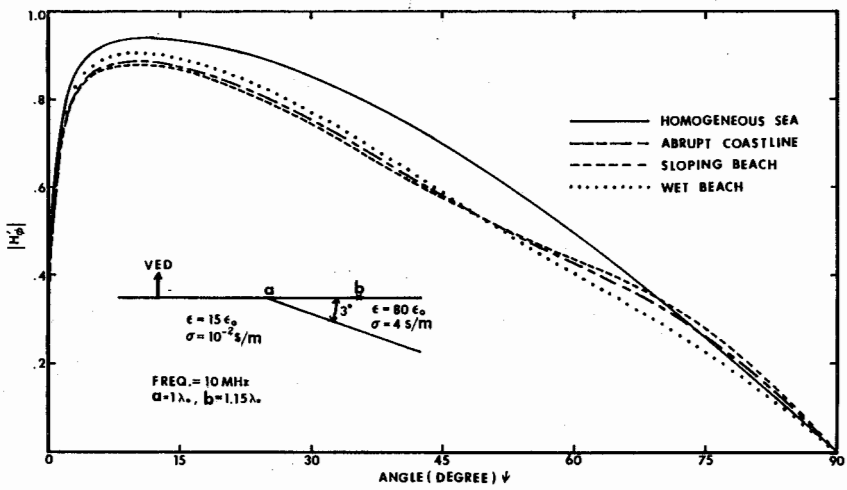

B5-5
1020 SCATTERING FROM A CONDUCTING STRIP LOCATED BELOW THE INTERFACE BETWEEN TWO HALF SPACES: C. M. Butler and A. W. Glisson, Department of Electrical Engineering, University of Mississippi, University, MS 38677

Attention in this paper is addressed to the determination of the scattering from a conducting strip that is embedded in a half space and is located near the planar interface between its host and a second half space. The axis of the strip is parallel to the interface but the plane of the strip need not be. Excitation is transverse magnetic to and invariant along the strip axis but otherwise may be general. An integral equation whose kernel contains a two-dimensional Sommerfeld integral is formulated for the strip current and is solved numerically. Care is given to accurate evaluation of the Sommerfeld integral. Results are compared with the analytic solution available for the current on a narrow strip that resides on the interface between the two media. For the general strip, current distributions for several cases of interest are presented and are interpreted physically. Far-zone field patterns, determined by asymptotic techniques, are given for various combinations of media contrasts and strip width, location, and orientation relative to the interface.

B5-6
1040 SCATTERING FROM A CONDUCTING STRIP ON A PLANAR INTERFACE BETWEEN TWO HALF SPACES: Chalmers M. Butler, Department of Electrical Engineering, University of Mississippi, University, MS 38677

The purpose of this paper is to report upon an investigation of scattering of a specified incident field by a conducting strip which resides on the planar interface between two semi-infinite, homogeneous half spaces of different electromagnetic properties. The perfectly conducting, flat strip is of infinite extent and the excitation of interest here is transverse magnetic to the strip axis. The formulation of an integral equation for the current induced on the strip is briefly outlined and it is mentioned that the Green's function can be expressed in closed form rather than as a two-dimensional Sommerfeld integral. For the electrically narrow strip, the integral equation is approximated and the approximate equation is solved analytically. In addition, results based upon a numerical solution of the integral equation are presented for wide and moderately-wide strips. From knowledge of the current on the strip, far-zone scattered fields are determined by an asymptotic evaluation of the two-dimensional Sommerfeld integrals. Far-zone field patterns are presented for various strip widths and half-space medium parameters.

B5-7
1100

AN EFFICIENT NUMERICAL METHOD FOR MODELING BURIED AND PARTIALLY BURIED ANTENNAS

G. J. Burke, W. A. Johnson, R. W. Ziolkowski,
E. K. Miller, J. N. Brittingham
Lawrence Livermore National Laboratory
P.O. Box 5504, L-156
Livermore, CA 94550

When an antenna near or penetrating an interface between two media is modeled by the numerical solution of an integral equation, the kernel includes Sommerfeld integrals. Solution by the method of moments can often be limited by excessive computation time and numerical difficulties. This paper describes a solution procedure that is an extension of a method used for antennas above the ground (G. J. Burke, et. al., Electromagnetics 1:29-49, 1981) combining interpolation in previously computed tables of Sommerfeld integrals with approximations valid at large separations of source and observer.

The above ground case involved bivariate interpolation for the Sommerfeld integrals. The singularity in the field was reduced analytically to permit modeling wires very close to the interface. This method was easily extended to buried antennas where the wave number in the source medium is complex. Extension to interactions across the interface required interpolation in three variables for the Sommerfeld integrals. At larger separations the field was evaluated by approximations involving ray optics and lateral wave formulas. Results have been obtained for antennas buried and penetrating the interface. The method is being incorporated into the method-of-moments computer code NEC.

B5-8
1120

EVALUATION OF SOMMERFELD INTEGRALS BY INTEGRATION ALONG THE REAL AXIS

W. A. Johnson
Lawrence Livermore National Laboratory
University of California
P.O. Box 5504, L-156
Livermore, CA 94550
D. G. Dudley
The University of Arizona
Tucson, AZ 85721

Efficient modeling of radiation and scattering problems in the presence of a lossy ground requires rapid, accurate, evaluation of Sommerfeld Integrals. Approximate techniques (A. Banos, Dipole Radiation in the Presence of a Conducting Halfspace, Pergamon, New York, 1966) are generally valid for specific ranges of parameters. Numerical techniques have generally been carried out along contours in the complex plane (G. J. Burke, et. al., Electromagnetics, 1, 29-49, 1981 and P. Parhami, et. al., IEEE Trans. on Antennas and Propagation, AP-28, 1, 100-104, 1980).

Few authors (D. Bubenik, IEEE Trans. on Antennas and Propagation, AP-25, 6, 904-906, 1977) have attempted direct evaluation of Sommerfeld integrals along the real axis. The advantage of rapid evaluation of Bessel functions of real argument is offset by the rapid oscillations and near singularities of the integrand. To overcome these difficulties subtraction of an asymptotic term and change of variables are used. The technique will be applied to typical earth parameters at frequencies of less than 100 Mhz. Although the region of practicality of this technique will be restricted by the distance between source and observation points, it is hoped that this region will compliment the region where asymptotic approximations are valid.

MULTIPLE BEAM SATELLITE ANTENNAS FOR COMMUNICATION SATELLITE SYSTEMS
Thursday morning, 14 Jan., CRO-30
Organizer and Chairman: J. Paul Shelton
Naval Research Laboratories, Washington, D.C. 20375

C3-1
0830 SOME FACTORS THAT INFLUENCE EHF SATCOM SYSTEMS;
Dr. Leon J. Ricardi, M.I.T. Lincoln Laboratory, Lexington, MA 02173

Frequency management problems, scarcity of orbital position assignment and resistance to interfering signals are projected to become serious problems for satellite communications (SATCOM) systems operating below about 15 GHz. International frequency allocations in the 15-50 GHz range permit SATCOM system operation with increased frequency bandwidth and hence may eliminate significant frequency management problems. This paper addresses some of the salient factors that influence SATCOM systems operating over the range 7-50 GHz. Propagation losses, frequency variation of a terminal's EIRP, spatial discrimination, and bandwidth available for spread spectrum AJ are presented as a guide to choosing the operating frequency of an EHF SATCOM system.

*This work was sponsored by the Defense Communications Agency.
"The U.S. Government assumes no responsibility for the information presented."

C3-2 SURVEY OF NASA ANTENNA TECHNOLOGY DEVELOPMENT PROGRAMS:
0900 L.B. Holcomb, NASA Headquarters, Washington, DC 20546

NASA's major antenna technology development programs include: (1) 30/20 GHz Multibeam Antenna; (2) Phase Array-Fed; and (3) Large Space Antenna.

The 30/20 GHz Multibeam Antenna program includes two parallel industry contracts with Ford Aerospace and TRW to design, develop, test and evaluate breadboard components for a 30 GHz receive and 20 GHz transmit proof of concept models by early 1983.

The phase array-fed antenna program currently involves parallel industry system study contracts to evaluate the use of monolithic amplifier and phase shift modules for multi-beam and/or scanning beam offset fed antenna systems. In support of this program, variable phase transmit and variable power amplifier monolithic modules are under development. Future efforts will involve the development, test and evaluation of a breadboard phase array-fed antenna system by the end of 1985.

NASA's large space antenna program involves parallel industry technology development programs to permit deployment of a 100-meter diameter space antenna serving as a mobil communications satellite. Two competing systems concepts are the hoop/column and the offset wrap-rib configurations. A companion technology program is focused on developing and testing a breadboard 30 foot diameter UHF feed.

C3-3
0930 LARGE APERTURE REFLECTORS - NEAR TERM TECHNOLOGY: A.A. Woods, Jr., Lockheed Missiles and Space Company, Inc., Sunnyvale, CA 94088

Multiple-beam space based communications missions have been postulated which require offset apertures with diameters in the region of 500 to 1,000 wavelengths. These missions, as a result of the aperture requirements, have been relegated to the post year 2000 time frame where they await space construction technology. Recent activities at Lockheed Missiles and Space Company, Inc., under partial sponsorship of Jet Propulsion Laboratories and The National Aeronautics and Space Administration, Office of Aeronautics and Space Technology, have shown that apertures in the 500 to 1,000 wavelength class are obtainable near term. In fact these activities are culminating with the ground test proof of concept model of a potentially flyable 800 wavelength offset parabolic reflector and feed support tower. This system under study is designed as fully deployable, antonomous spacecraft segment capable of a late 1980's mission.

This paper presents an overview of this large aperture antenna design, fabrication, and test program. Emphasis is placed on the design approach, available performance and technology limits.

C3-4
1030

REVIEW OF ANTENNA DESIGN TECHNIQUES FOR COMMUNICATION SATELLITES

J. P. Shelton
Naval Research Laboratory
Washington, DC 20375

The current status of design techniques for synchronous-orbit communication satellite antenna systems is reviewed. The requirement for high-gain, limited angular coverage, polarization diversity systems is considered. Two general configurations are discussed, one in which simultaneous multiple beams are formed to cover the desired angular region and one in which a single scanning beam achieves the desired coverage. Methods of realizing these configurations with offset multiple reflectors are described. Problems of minimizing the size of the subreflector and feed array and of achieving a satisfactory radiation pattern synthesis capability over the desired coverage region are addressed. It is noted that, because of the variety of requirements that may be placed upon antenna systems of this type and the numerous design parameters involved, an optimum design is difficult to define or derive. Opportunities for theoretical and applied research related to these systems are discussed.

C3-5
1100

A COMPARISON OF CONVERGENCE PROPERTIES IN TWO LINEAR ADAPTIVE RECEIVING ARRAYS: C.W. Jim and L.J. Griffiths, Department of Electrical Engineering, University of Colorado, Boulder, CO 80309

A new approach to linearly constrained adaptive beamforming has been suggested previously [1,2]. The new structure is designed for used with arrays which have been time delay steered such that the desired signal of interest appears approximately in phase at the steered outputs. The system includes signal distortion constraints which are implemented using simple hardware differencing amplifiers at the element outputs. Under certain conditions, the steady-state performance of this structure has been shown [3] to be identical to the linearly-constrained adaptive structure proposed by Frost [4].

In this paper, it is shown that different eigenvalue spectra will be encountered by the adaptive filter in the two systems. As a result, although the two processors adapt to the same steady-state solution, the coefficient trajectories and adaptive learning rates will be different. This paper provides both an analytical framework and simulation results which show how to choose the system which will optimize performance of the overall adaptive array processor for a particular signal and interference environment.

NON-GAUSSIAN NOISE: MEASUREMENT AND THEORY
Thursday morning, 14 Jan., CR1-40
Chairman: G.H. Hagn
SRI International, Arlington, VA 22209

E2-1
0900 THE MEASUREMENT OF SHIPBOARD RFI AT MICROWAVE FREQUENCIES: K.G. Gray, Electrical Engineering Department, Naval Postgraduate School, Monterey, CA 93940, and J.E. Ohlson, Stanford Telecommunications, Inc., Sunnyvale, CA 94086

A system is described for making radio frequency interference (RFI) measurements at microwave frequency bands near 7, 20, and 40 GHz. The system is used aboard U.S. Navy ships in support of the Navy EHF Satellite Communications Program (NESP). The measurement environment involves sensing RFI and identifying its source in a dense population of high-power emitters. The RFI system uses spectrum analysis to locate emissions in frequency. It can also resolve pulses in the time domain. The RFI system is described in terms of its purpose and the interesting features of the shipboard RFI environment are summarized.

E2-2
0930

RELIABILITY OF ATMOSPHERIC RADIO NOISE PREDICTIONS

D.B. Sailors, EM Propagation Division
Naval Ocean Systems Center,
San Diego, CA 92152

Measured radio noise values at widely separated geographical locations are compared with predicted values for five frequencies between 0.495 and 20.0 MHz. The measured noise data were the seasonal 4-hr time block values, averaged over each 4-hr period for the 3 months of the season and were for the years 1960 and 1965. The 1960 measured noise data included that reported by Herman (J.R. Herman, J. Res., NBS, 65D, 1961).

Atmospheric noise values were predicted using noise models with their worldwide atmospheric noise representation at 1 MHz, as presented in CCIR Report 322 (1963), produced by numerical mapping techniques developed by D.H. Zacharisen and W.B. Jones (OT/ITS Research Report 2, 1970). Included in these models was a simplified atmospheric noise model suitable for use in estimating noise on a minicomputer. The frequency dependence in these models was represented by a power series of least squares fit to the frequency dependence curves in CCIR Report 322 (D.L. Lucas and J.D. Harper, NBS Tech. Note 318, 1965).

It was found that the predicted and measured noise levels were in good agreement except at some places, times, and frequencies, where large discrepancies occurred. During 1960, the largest bias was 5.7 dB low; during 1965 the largest bias was 7.4 dB low. At Thule, discrepancies as large as 30 dB low were not uncommon. Large discrepancies were noted both at the lowest frequency 0.495 MHz and the largest frequency 20.0 MHz. The former is due primarily to use of the frequency dependence model below the lowest frequency of its intended use. The latter is due to the presence of man-made and galactic noise in the measured data. Reasons for the disagreements are discussed.

E2-3
1030

NEW RESULTS IN THE CANONICAL THEORY OF OPTIMUM THRESHOLD SIGNAL DETECTION

David Middleton, 127 E. 91st, New York, New York 10028

Locally optimum Bayes Detectors (LOBD's) -- originally derived by the author in 1965, 1966 -- are threshold signal detection algorithms which possess certain optimal properties. The LOBD is constructed from a suitable expansion of the (known) optimum (or logarithm of the) unconditional likelihood ratio $\Lambda_n(\underline{x};\theta)$ about the null signal state $\theta = 0$. This expansion distinguishes between coherent reception ($\theta \neq 0$) and incoherent reception ($\theta = 0$) and requires a suitably chosen bias term, which is usually taken to be the next non-vanishing term in the Taylor series expansion of log Λ_n with respect to H_o (noise alone).

It is shown here by a modification of LeCam's theorem on asymptotic equivalence of two distributions that for independent noise samples (at least) the LOBD is also an asymptotically optimum detection algorithm (AODA) and hence is locally optimum for all sample sizes n ($\to \infty$) as well as for small samples. Sufficient conditions for this are given. Practical implications of these results and conditions are discussed and illustrated, along with a comparison of another type of AODA derived recently by B. R. Levin (1969-1976).

E2-4
1100

OPTIMUM AND SUBOPTIMUM RECEPTION OF THRESHOLD SIGNALS IN CLASS A AND B ELECTROMAGNETIC INTERFERENCE ENVIRONMENTS

David Middleton, 127 E. 91st, New York, New York 10028
A. D. Spaulding, NTIA/ITS, Boulder, Colorado 80303

Canonically optimum threshold detector structures (LOBD's) for weak input signals in all classes of EMI are presented for the following reception regimes: (1), coherent detection; (2), incoherent detection; with binary, as well as "on-off" signal waveforms, and with a variety of fading and doppler-spread conditions on the desired signals. These LOBD algorithms are not only locally optimum (for all sample sizes), but are asymptotically optimum algorithms (AODA's) as well, convergent to the strictly optimum results for weak signals.

Canonical and specific optimum performance are evaluated for Class A and B EMI and for weak-signal conditions [which must be appropriately specified to insure that: (i) the AODA condition is obeyed, and that, (ii), coherent detection is never worse than incoherent reception (with the same input signal waveforms and sample sizes)]. The performance of conventional detectors (i.e., auto- and cross-correlators) is also obtained and shown to be significantly inferior to the LOBD performance under corresponding conditions. The optimum receiver is shown to require (1), suitable nonlinear filters to "match" to the noise, and (2), appropriate linear filters to match to the signal, in the now "matched" noise. Canonical system diagrams illustrate the processing algorithms, and performance measures show typical results for Class A and B interference (as well as for Gaussian noise).

SURFACE SENSING FROM AIRBORNE AND SPACE PLATFORMS
Thursday morning, 14 Jan., CR2-26
Chairman: Richard K. Moore,
University of Kansas, Lawrence KS 66045

F3-1
0840 UNUSUAL SAR OCEAN IMAGES ASSOCIATED WITH UNSTABLE ATMOSPHERIC CONDITIONS: T.W. Thompson, Planetary Science Institute, Science Applications, Inc., 283 S. Lake, Suite 218, Pasadena, CA 91101; D.E. Weissman, Dept. of Eng. Science, Hofstra University, Hempstead, NY 11550; W.T. Liu, Space Science Div., Jet Propulsion Laboratory, Pasadena, CA 91109

Synthetic Aperture Radar (SAR) images of the Gulf Stream and adjacent waters off the coast of Florida on 10 December 1975 show unusual radar features probably related to unstable atmospheric conditions. At the time of the observations, a moderate (10m/s) but cold, northwest wind (following the passage of a cold front on the previous night) was blowing over the ocean. The air-sea temperature difference was 10^{o}C. The ocean surface under these unstable atmospheric conditions had SAR image where radar-bright splotches appeared when the radar was looking nearly upwind or downwind. These splotches disappeared from the image when the radar was looking cross-wind. Also, these splotches were strongest for the warm Gulf Stream and they disappeared when near shore where the fetch is small. The radar data suggests that short (16cm-36cm) ocean waves preferentially form in the direction of the wind under these atmospheric conditions. Also, measurements of backscatter coefficients during this period show an unusually strong dependence upon wind direction.

F3-2
0900

SPATIAL EVOLUTION OF SEASAT SAR SPECTRA FROM HIGH PRECISION DIGITAL TRANSFORMS

Robert C. Beal, Applied Physics Laboratory, Johns Hopkins Road, Laurel, MD 20707

The Seasat SAR spectra of ocean wave systems contain information on storm generation history, deep and shallow water ocean currents, and coastal bathymetry. The optimal extraction of this information from the SAR spectra, however, requires a proper accounting for and removal of several types of systematic error sources. Precision digital transforms which have been corrected for major SAR system-induced biases have now been performed over a major portion of Seasat pass 1339, which occurred over the U.S. East Coast on September 28, 1978.

The corrected spectra graphically illustrate a systematically evolving set of two separately-generated ocean wave systems. The two-dimensional wave number spectra of each wave system appear to be accurately monitored by the SAR when the highest quality digitally-processed data are used. The uniqueness of the SAR spectra are somewhat tempered, however, by the attenuation of azimuth-traveling waves in high sea states. This observed attenuation, although serious for the Seasat SAR geometry, need not be as destructive in future SAR systems orbiting at a lower altitude.

F3-3 0920 MOVING SCATTERER RESOLUTION LIMITATIONS ASSOCIATED WITH WAVE IMAGERY USING SYNTHETIC APERTURE RADAR: Frank M. Monaldo, Applied Physics Laboratory of The Johns Hopkins University, Laurel, MD 20707

A synthetic aperture radar (SAR) achieves azimuthal resolution by using the movement of the SAR platform during a finite integration time to create a large effective aperture. Movement of the scatterers during the integration time introduces complications. Radial scatter acceleration results in defocusing which blurs the image (Alpers and Rufenach, IEEE Trans. Antennas Propag., 27, 685-690). Radial velocity results in a simple azimuthal displacement of the scatterer in the image. A surface like the ocean has a random radial velocity at each point and hence a random azimuthal displacement. This results in positional uncertainty in the azimuthal direction. Thus far such velocity effects have been largely ignored in considering resolution degradation in wave imagery.

In order to predict the azimuthal resolution degradation inherent in SAR imagery, a modified Pierson wind wave spectrum is assumed to exist on the surface. This spectrum is used to predict a radial v_{rms} and a_{rms}. These, in turn, are used to predict azimuthal resolution degradation as a function of wind speed. These results compare favorably with wave resolution degradation measured from Seasat SAR imagery. Results show velocity as well as acceleration effects must be considered in predicting this degradation. Results are presented in the context of the total wave imagery modulation transfer function.

F3-4
0940

THE POTENTIAL USE OF TWO DIMENSIONAL SAR SPECTRA IN OCEAN WAVE FORECASTING

Ella B. Dobson, Applied Physics Laboratory, Johns Hopkins University, Laurel, Maryland 20707

The field of ocean wave forecasting has progressed significantly during the last several years to the state where several first order wave forecasting models are in operational use in the United States and other countries. While research in this area is steadily evolving, theoretical and practical problems are inhibiting a rapid and complete solution which is sufficiently accurate and reliable to satisfy the needs of those communities needing the service. In terms of practical problems, the two most outstanding are: 1) the lack of measured winds over the world oceans and, 2) the unavailability of insitu or remote ocean wave measurements with which the predicted forecast wave parameters can be compared. This paper reports on an investigation to determine the usefulness of synthetic aperture radar in providing two dimensional wave spectra to test wave forecast models and guide modelers in the future development and refinement of models.

The impetus for this work was provided by studies of Seasat Synthetic Aperture Radar (SAR) spectra of the ocean surface which were measured during 1978. The paper will discuss comparisons of the SAR spectra and forecast spectra. Using winds provided by the Fleet Numerical Ocean Center, two forecast models have been used to estimate the ocean spectra along the Seasat flight path.

If measured two dimensional ocean wave spectra are available at regularly spaced intervals throughout an ocean area, it is possible to use these spectra for initialization of models and as correctors during the forecast period. A discussion will be given on the potential benefits and problems associated with incorporating measured ocean wave parameters into forecast models.

F3-5
1020

SIMPLIFIED METHODS FOR REMOVAL OF CERTAIN BIASES AND ERRORS FROM SEASAT MICROWAVE ALTIMETER ECHO

Donald E. Barrick
NOAA, ERL, Wave Propagation Laboratory
Boulder, Colorado 80303
Belinda J. Lipa
CODAR Research
165 Harcross Road
Woodside, California 94062

The SEASAT microwave altimeter was intended to measure ocean significant waveheight, mean sea surface position, normalized radar cross section at vertical incidence (from which surface wind speed is derived), and possibly waveheight skewness. Recent works have shown that the entire waveheight probability density can also easily be extracted from the altimeter echo leading edge. However, at least five types of biases/errors can contaminate extraction of the desired parameters. These are tracker bias, waveheight skewness bias, satellite pointing error, rain effects, and electromagnetic bias.

This study deals with the first three, and shows that they can be easily measured and removed by maximum-likelihood methods that employ models linear in these three parameters. Therefore, time-consuming grid-search or multi-dimensional minimization procedures are avoided. That these methods work effectively is demonstrated both by analysis of SEASAT data and by separate theoretical analysis of the SEASAT tracking system.

F3-6
1040 THE EFFECT OF RAIN THAT PARTIALLY FILLS A RESOLUTION CELL ON OCEANIC MEASUREMENTS WITH SPACEBORN SCATTEROMETERS AND RADIOMETERS: R.K. Moore, A.H. Chaudhry, I.J. Birrer, Remote Sensing Laboratory, University of Kansas Center for Research, Inc., Lawrence, KS 66045

When rain partially fills a resolution cell for a microwave radiometer, estimates of oceanic parameters such as wind speed and atmospheric parameters such as water-vapor content are seriously degraded. When the radiometer is used to estimate the attenuation experienced by a radar scatterometer, the effect is to degrade the "correction" so much that wind speed cannot be accurately determined. This paper presents results of simulations using artificial "rain cells" for both radar and radiometer and using conditions actually experienced during a hurricane for the radar-correction problem.

F3-7
1100

REMOTE SENSING OF ICE AND SNOW IN FINLAND

Martti Hallikainen
Radio Laboratory, Helsinki University of Technology
02150 Espoo 15, Finland

Four remote sensing projects are briefly described: (1) UHF radiometry of low-salinity sea ice, (2) CW-FM radar measurements of lake ice and frost, (3) microwave radiometry of snow-covered terrain and (4) interpretation of Nimbus-7 SMMR data for determining the thickness and water equivalent of snow cover.

Measurements of low-salinity ($S \leq 2^0/_{00}$ by weight) sea ice by an airborne multi-channel UHF radiometer were made along the Finnish coast in 1974-1978. The experimental and theoretical results show that the thickness of dry sea ice can be determined with reasonable accuracy. However, even a thin water layer upon the ice will prevent the determination of the ice thickness. A CW-FM radar, operating at 1-1.8 GHz, has been developed for monitoring the thickness of fresh-water ice and frost on lakes and bogs. The radar may be installed on a vehicle and thus a continuous recording of the ice thickness is obtained. The correlation between the actual thickness (up to one meter in 1980) and the experimental value is 0.99 for lake ice and 0.81 to 0.85 for frost, depending on its wetness.

Radiometer measurements of snow-covered terrain have been made continuously since 1978. The frequencies are 5 and 12 GHz and, occasionally, 37 GHz. The radiometers, installed in a tower, are looking towards the snow at an angle of 15 degrees from vertical. Since 1980, the ground under the snow has been covered with metal sheets to eliminate its emission. The observed snow parameters (wetness, particle size, density and temperature) have been included in the theoretical snow model. The spectral behavior of the brightness temperature of snow can be employed for determining the thickness and water equivalent of snow cover. However, the distinctive behavior of the brightness temperature of snow may be shadowed by forests and various types of surfaces. Microwave brightness temperature data from Nimbus-7 satellite, made available by the NASA Goddard Space Flight Center for data validation and testing of retrieved algorithms, was used to study the effects of forests, farmlands, boglands and lakes. In order to determine the water equivalent of dry snow cover, the surface effects should be taken into account by comparison with observations before snowfall.

F3-8
1120

SEASONAL RADAR RESPONSE OF SEA ICE

R.G. Onstott, R.K. Moore, S. Gogineni, Y.S. Kim
Remote Sensing Laboratory
University of Kansas Center for Research, Inc.
Lawrence, Kansas 66045

Measurements of the radar response of ice in October 1981 provided the first example of backscattering-coefficient measurement for fall ice. The variation in radar backscatter from ice in spring, summer, and fall is compared in this paper.

IONOSPHERIC PHENOMENA AND PROPAGATION
Thursday morning, 14 Jan., CR1-46
Chairman: George Millman,
General Electric Company, Syracuse, NY

G1-1
0900 RECENT AURORAL BACKSCATTER OBSERVATIONS AT OTTAWA

L.E. Montbriand
Communications Research Centre
Box 11490, Station H,
Ottawa, Ontario K2H 8S2

The SARA receiving facility of the Communications Research Centre, Ottawa in conjunction with a transmitting facility at Rome, New York has been used during 1980-1981 to make bistatic backscatter radar observations of auroral zone irregularities in a region north of Ottawa. FMCW sweeps with widths ranging from 1.25 to 5.00 KHz were used at frequencies from 7.9 to 24.5 MHz. Doppler spreads from auroral echoes, not necessarily at the range of ground backscatter, occasionally exceeded $\pm$ 100 Hz, while shifts of the median doppler occasionally reached 30 Hz. A large change in the doppler shift with range was often observed. A few cases when measured doppler spreads and shifts could be attributed to auroral clutter present at the range of ground backscatter are also discussed. Using echoes received on both arms of the SARA array, an attempt has been made to study the elevation angles of the auroral clutter returns.

G1-2
0930 MF SKYWAVE OBSERVATION AT COBA ROJO, PUERTO RICO:

J. Washburn, R. Espeland, G. Wasson, J. Carroll, and C. Rush, National Telecommunications and Information Administration, Institute for Telecommunication Sciences, Boulder, CO 80303

A program to monitor long-distance medium frequency skywaves from emitters in South America has recently been initiated at Coba Rojo, Puerto Rico. The Coba Rojo site was chosen specifically because of the availability of highly directional Beverage antennas that permit isolating the location of the observed signals. Observations of signals from seven different broadcasting stations spanning the frequency range 870 kHz to 1220 kHz are continuously made in one minute intervals between the times of local midnight at the receiving site and local sunrise.

The data are being used as a basis for developing an improved method of predicting the field strength of long-distance MF radio signals in the Western Hemisphere. Initial observations indicate considerable day-to-day variability in the strength of the received signals which must be taken into account by any realistic prediction method. Examples of the observations will be described, and the possibility of MF signals from Central and South American giving rise to interference to AM broadcast stations in the United States will be discussed.

G1-3
1030

A SCATTERING THEORY OF TRANSEQUATORIAL PROPAGATION IN THE VHF BAND

Jerry Alan Ferguson
EM Propagation Division
Naval Ocean Systems Center
San Diego, CA 92152

Transequatorial propagation in the VHF band can occur when the ionosphere does not support such propagation by refraction. The phenomenon is closely associated with the scattering phenomenon known as equatorial spread-F. This scattering is caused by the presence of irregularities in the ionization density of the F-layer. A spectrum of irregularities is used which has horizontal scales spread from tens of kilometers down to the electron gyroradius. A model of scattering from long curved irregularities, aligned along the earth's magnetic field, is presented. For transequatorial propagation, the curvature of the irregularities causes convergence of the scattered rays in the magnetic meridian in many situations of practical interest. Received power, while less than that coresponding to free-space propagation, considerably exceeds that corresponding to scattering by isotropic irregularities. Results of scattering calculations representative of experimental transequatorial propagation paths are presented. Power law spectra having spectral indices between 2 and 3 are found to be satisfactory.

G1-4
1100

WINTER ANOMALY OF L CURRENTS IN THE IONOSPHERE:

S. Matsushita, High Altitude Observatory, NCAR,
P.O. Box 3000, Boulder, CO 80307

Equivalent ionospheric L current systems produced by the lunar gravitational tides, which can be estimated by spherical harmonic studies of geomagnetic data, often show an anomaly at middle latitudes in winter (see the figure below). This indicates winter anomaly in ionospheric winds, namely, upward propagation mode of lunar tides. In fact, lunar semidiurnal winds at 90-100 km in altitude measured by the Kyoto meteor radar show almost reversed phase between winter and other seasons: namely, the maximum variation occurs at 10.1 h in winter, 5 h in equinox, and 5.8 h in summer. The winter anomaly also presents longitudinal dependences: it is clearer in Europe and Japan than in North America. Detailed behavior needs to be examined by IS radar.

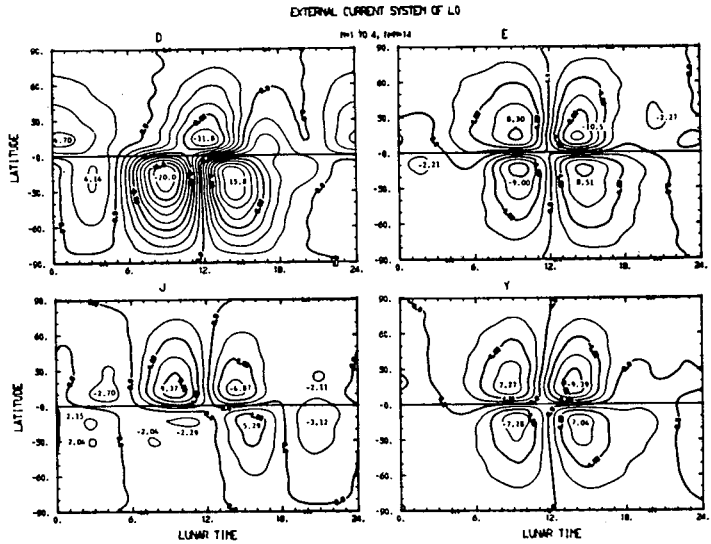

Ionospheric L current systems in December solstitial (top left), equinoctial (top right), and June solstitial months (bottom left), with their yearly average (bottom right). The contour interval is 2 kiloamperes.

DATA PROCESSING IN RADIO ASTRONOMY WITH EMPHASIS ON THE USE OF ARRAY PROCESSORS

Thursday morning, 14 Jan., CR2-6

Chairman: W.R. Burns, National Radio Astronomy Observatory, Charlottesville, VA 22903

J3-1
0900 ARCHITECTURE OF THE NEW J.P.L.-C.I.T VLBI PROCESSOR

M. Ewing, California Institute of Technology, Pasadena, CA 91125; D. Rogstad, Jet Propulsion Laboratory, Pasadena, CA 91103

J3-2 0920 MARK III VLBI: THE USE OF AN ARRAY PROCESSOR IN THE CORRELATOR: A. Whitney, A. Rogers, J.C. Webber, Haystack Observatory, Westford, MA 01886

The Mark III VLBI processor uses a CSPI MAP 300 array processor interfaced to a Hewlett-Packard 1000 mini-computer to perform Fourier transforms.

The maximum likelihood detection of "fringes" is accomplished by performing a 2-dimensional Fourier transform on the array of correlation functions in time and frequency to delay and delay rate. The array of delay and delay rates are then searched for the peak magnitude to find the interferometer delay, delay rate, and phase. This and other uses of the array processor for VLBI are discussed in this paper.

J3-3
0935

THE VLA ARRAY PROCESSOR BASED MAPPING SYSTEM

W. Brouw, Netherlands Foundation for Radio Astronomy, R. Payne, National Radio Astronomy Observatory, Socorro, N. M. 87801

J3-4
1000

AN OVERVIEW OF THE NRAO-AIPS IMAGE PROCESSING SYSTEM

E. Greisen, National Radio Astronomy Observatory
Charlottesville, VA 22903

J3-5 THE NEW CLASS OF ARRAY PROCESSORS
1025 Author not yet specified

Commission J Session 4

REMOTE OBSERVING AND DATA TRANSFER PROBLEMS IN RADIO ASTRONOMY
Thursday morning, 14 Jan., CR2-6
Chairman: W.R. Burns, National Radio Astronomy Observatory, Charlottesville, VA 22903

J4-1 1110 RECENT EXPERIENCE IN REAL TIME MONITORING OF A VLBI NETWORK
M. Reid, M. Schnepps, J. Moran, S. Rosenthal,
Center for Astrophysics, Cambridge, MD 02138

J4-2
1125

THE MARK III DATA BASE-HANDLER

J. Ryan, C. Ma, NASA/Goddard Space Flight Center
Greenbelt, MD 20771; B. Schupler, Computer Science
Corporation

J4-3 THE PLANNED NRAO DIGITAL NETWORK

1145 A. Shalloway, R. Burns, National Radio Astronomy Observatory, Charlottesville, VA 22903

J4-4 1330 CURRENT STATUS OF J.P.L.-C.I.T. HIGH DENSITY VLBI RECORDING

B. Rayhrer, Jet Propulsion Laboratory, Pasadena, CA 91103

J4-5 1350 DEVELOPMENT AT HAYSTACK OF DENSITY UPGRADE FOR MARK IV RECORDER

H. J. Hinteregger, Haystack Observatory, Westford, MA 01886

NEAR FIELD MEASUREMENTS-1

Commission A, Session 4, CR1-42
Chairman: Carl F. Stubenrauch,
Electromagnetic Fields Division, National Bureau of Standards, Boulder, CO 80303

A4-1 1330 **ANTENNA GAIN OBTAINED FROM NEAR-FIELD MEASUREMENTS;**
A.C. Newell, Electromagnetic Fields Division, National Bureau of Standards, Boulder, CO 80303

Although near-field measurements have been done for some time, there still appear to be questions and uncertainties with some users concerning the determination of gain. In this paper we discuss in detail for planar near-field measurements three different methods of obtaining gain, each method employing the "gain standard" in a different way. Each method has certain advantages and problems which will be described, but in each case the gain of the test antenna is determined without the need for simplifying approximations. The extension of these techniques to cylindrical and spherical near-field measurements will be outlined.

The first method requires only one near-field measurement, and the probe, whose gain must be known, serves as the gain standard. An auxillary gain standard is used in the second method where two near-field scans are required, but the probe gain need not be known. In the third technique, essentially a three antenna procedure, the gains of the probe, auxillary standard, and test antenna are all determined without a priori knowledge of any of the three gains. It does however require three near-field scans.

In each method, one or more insertion loss measurements must be made between the ports of the test antenna, the probe and/or the auxiallary gain standard.

In choosing a specific method for a given application, one must consider the required accuracy, the availability of calibrated probes or gain standards, the amount of time required, the ease of implementation, and the effects of sources of error.

A4-2
1355

FUNDAMENTAL THEOREMS ENABLING THE EFFICIENT COMPUTATION OF NEAR-ZONE ANTENNA FIELDS AND COUPLING

Arthur D. Yaghjian
Electromagnetic Fields Division
National Bureau of Standards
Boulder, Colorado 80303

For applications such as determining the mutual interference between co-sited antennas, gain-correction factors for two antennas, or potentially hazardous fields in the vicinity of antennas, it is desirable to perform the calculation inverse to the near-field measurement problem - namely computing near-field coupling between two antennas given the far field of each antenna. Two programs are presented emphasizing the theory on which they are based.

The first program computes coupling (or fields) versus transverse displacement of the antennas using a plane-wave representation and capitalizing on the result that, in most practice, only the far fields within the solid angle mutually subtended by the antennas is required. The second program computes coupling (or fields) versus separation distance throughout the Fresnel region using a spherical-wave representation made possible by a fundamental theorem for the coupling function between two antennas; it like each component of electric and magnetic field in free space, satisfies the homogeneous scalar wave equation.

A4-3
1420

PROBE EFFECTS IN SPHERICAL NEAR-FIELD MEASUREMENTS:

F. Holm Larsen, Electromagnetics Institute, Technical University of Denmark, DK-2800 Lyngby, Denmark

Since 1976 an experimental facility for spherical near-field antenna testing has been under development at the Technical University of Denmark (TUD) in cooperation with the European Space Agency. The spherical near-field scanning method is advantageous in the way that the far field can be determined in all directions from a single scan. Furthermore, the scanning can be carried out by rotating the test antenna only; thus the probe can be fixed in space. The purpose of the research program has been general development of the spherical near-field method, accurate indoor testing of satellite antennas, and definition studies for other test ranges. In addition, the facility is being used for accurate calibration of antenna standards. A potential use of the facility is measurement of feed-systems which have a wide beam and where accurate phase measurements are desirable.

As special features of the TUD near-field range can be mentioned accurate alignment of the two rotation axes. These must be perpendicular to each other and intersect in order to measure accurate phase patterns. The probe antenna is dual polarized such that it in connection with a Scientific-Atlanta 1774 three-channel receiver can measure the $\hat{\theta}$ and the $\hat{\phi}$ components of the field simultaneously. The control and data collecting software has been written in house in order to obtain a high degree of flexibility and allow for future modifications. The near-field to far-field transformation with probe correction is carried out in a HP1000 minicomputer allowing measurements with sampling increments down to $\Delta\theta = \Delta\phi = .5^{\circ}$ to be treated. This corresponds to maximum antenna diameter of 110λ. The directivity of the test antenna is automatically found in the data processing when the full near-field pattern has been measured. Directivity values for the same antenna measured at different distances agree within two or three hundredths of a dB.

A point which has attracted particular interest is the influence of the probe characteristics and the possibility of correcting for them. The probe in a spherical near-field measurement must be a rotationally symmetric antenna, and therefore its influence on the measurement can conveniently be broken down into the following probe effects:

- Multiple scattering
- Directive probe pattern
- On-axis cross polarization
- Difference between E-plane and H-plane patterns
  = off-axis cross polarization
- Amplitude and phase ratio between $\hat{\theta}$ and $\hat{\phi}$ components

Most of these effects can be corrected for in the data processing as will be illustrated by measured patterns.

A4-4
1505

THE ALIASING ERROR IN NEAR-FIELD SPHERICAL SCANNING DUE TO THE FFT--EQUAL TO ZERO?

Richard L. Lewis, Electromagnetic Fields Division,
National Bureau of Standards, Boulder, CO 80303

In this paper we wish to discuss how one can use the FFT to calculate a correlation embedded within the near-field spherical scanning algorithm. This idea is not new, as it was first introduced by Larsen (Elect. Letters 15, (19), 588-590, 1979 Sept.). Thus, the so-called Π-matrix data-matrix product (cf. Wacker, NBSIR 75-809, p. 32, 1975 June) was shown by Larsen to be efficiently calculated as a correlation using two 4N-term FFTs. Here we present a new formulation, that reduces by half the number of terms summed by these FFTs without introducing any aliasing error, assuming that the field radiated by the test antenna is completely described using N-1 spherical modes.

In a previous paper (Lewis, 1981 IEEE/AP-S Symposium, Los Angeles, CA, 246-249), a modified near-field spherical scanning algorithm was presented that promises to halve the spherical data-processing computations when the back-hemisphere radiation from the test antenna is negligible. One of our goals here is to expand on one computational step in that algorithm, using the same notation for the present discussion as in the previous paper. The application of our formulation to the full-sphere scanning algorithm can be regarded as just one part of the single-hemisphere scanning algorithm, in the sense that we discard half of the terms in the latter algorithm's formulation to arrive at the analytically simpler but computationally more difficult full-sphere scanning algorithm.

The integral, $\int_0^{\pi} W_m^{\mu}(\theta) d_{m\mu}^{n}(\theta) \sin\theta \, d\theta$, can be expressed as a double sum by utilizing a Fourier-series expansion for the quantities in the integrand. Here, $W_m^{\mu}(\theta)$ denotes the azimuthal angle ($e^{im\phi}$) Fourier transform of the measured data, while $\mu=\pm 1$ describes the polarization. The function $d_{m\mu}^{n}(\theta)$ can be expressed for $\mu=\pm 1$ as a linear combination of an associated Legendre function, of order m and degree n, and the derivative of that Legendre function. If we consider just half of this double sum: in particular that single sum whose terms contain the Fourier-transform coefficients of the measured data, we see that this sum can be expressed as a pair of discrete Fourier transforms (DFT's). By using Silverman's (FFT Methods, IBM Research Report RC3347, 1972 Feb.) "circulant matrix" formulation and the already established periodicity of the measured-data's Fourier-transform coefficients, it is shown that our representation of the sum as a pair of DFT's is an identity. Finally, we combine the pair of DFT's into a single DFT by utilizing an identity between $W_m^{\mu}(\theta)$ and its Fourier series expansion. The final result allows the computation of the sum to be obtained as two 2N-term FFTs, rather than as two 4N-term FFTs, with the added assurance that no aliasing error has been introduced.

A4-5
1530

SPHERICAL AND CYLINDRICAL NEAR FIELD TESTING OF ELECTRICALLY LARGE ANTENNAS:

S. Sanzgiri and K. Lee, Antenna Laboratory,
Texas Instruments Inc., Dallas, Texas

Compact and near field ranges have been considered as alternatives to long outdoor far field ranges to provide better utilization of the existing land and to centralize antenna test facilities. Large antennas with shaped beam patterns can be tested only in the spherical or cylindrical near field scanning mode. This paper presents the results of recent experiments carried out to confirm the feasibility of the spherical and the cylindrical near field testing of such large antennas. In particular, the spherical near field test results of a L band open array antenna and the cylindrical near field test results of a X band model of a ATCRBS antenna are presented. The transformed far field patterns are shown to correlate very well with the measured far field patterns.

A4-6
1555

RANGE SELECTION CONSIDERATIONS FOR CYLINDRICAL NEAR-FIELD MEASUREMENTS

C. P. Burns, V. V. Jory, D. G. Bodnar, D. F. Tsao
Microwave Systems Division
Systems and Techniques Laboratory
Engineering Experiment Station
Georgia Institute of Technology
Atlanta, Georgia 30332

Georgia Tech has been involved in the research and development of near-field antenna measurement techniques for over a decade and has had an operational planar near-field scanner since 1974. To be discussed here is a recently designed and implemented cylindrical near-field antenna range at the Cobb County Research Facility of the Engineering Experiment Station. Automated procedures for acquisition of measured near-field data and computation of probe compensated far-field radiation patterns from sampled cylindrical near-field data are described.

Factors determining the selection of the cylindrical geometry for the basic range design are discussed together with the versatility of the design which accommodates planar-polar and spherical measurements as well as cylindrical. Also included are experiences in the utilization of the range as a general purpose anechoic chamber for various measurements of antennas and feeds. Emphasis is given to range parameters, instrumentation, system-equipment interfacing, time required for data collection and reduction, and error analysis and control.

Results from the on-going validation of the system in the form of comparisons between the actual measured far-field radiation patterns of several antennas and the far-field patterns of those antennas predicted from probe compensated near-field measurements will be presented.

A4-7
1620

DEVELOPMENTS IN NEAR-FIELD MEASUREMENTS AT THE UNIVERSITY OF SHEFFIELD :

E.P. Schoessow, J.C. Bennett and N.E. Muntanga, University of Sheffield, Department of Electronic and Electrical Engineering, Mappin Street, Sheffield S1 3JD, U.K.

The current near-field work at the University of Sheffield is divided primarily between two related projects. The first of these has involved the development of a novel approach to the problem, termed Plane Wave Synthesis. This relies upon the computational weighting of a portion of a set of spherical near-field measurements to synthesise a radiating aperture producing an effective plane wave incident upon the test antenna. This scheme can provide all-space pattern predictions from a full sphere of data and can also produce rapid predictions of single plane cuts, if required. In addition, because only a restricted part of the data sphere is needed to produce any one prediction point, it is not necessary to obtain a full data sphere (or to carry out the complete all-space prediction process) to obtain predictions over a limited area. Another attractive aspect of Plane Wave Synthesis, again because of this limited data requirement, is that, if the technique is implemented in a suitable on-line system, predictions can start to become available quite early in a scan (thus facilitating early diagnosis of problems, preview of results etc.).

A technique which has evolved out of Plane Wave Synthesis is one in which a suitably fed linear probe (such as a linear array) is used to provide one dimension of the required weighting function whilst the other is implemented computationally. This means that a single data scan can provide a single pattern cut with extremely simple and rapid processing.

Encouraging results are emerging from both of the above projects and examples of such results will be provided in the presentation. In addition, we would briefly draw attention to the large-antenna metrology work at Sheffield which, although primarily a diagnostic tool can also be used for near-field/far-field transformation with very large antennas.

SINGULARITY EXPANSION METHOD
Thursday afternoon, 14 Jan., CR2-28
Chairman: L. Wilson Pearson, Department of Electrical Engineering, University of Mississippi, University, MS 38677

B6-1
1330 TIME-DOMAIN TECHNIQUES IN THE SINGULARITY EXPANSION METHOD

D. J. Riley and W. A. Davis
Department of Electrical Engineering
Virginia Polytechnic Institute and
State University
Blacksburg, VA 24061

Recent time-domain techniques in SEM by Cordaro and Davis (IEEE Trans. Antennas Propagat., AP-29, May, 1981) have reduced the pole extraction problem to an algebraic eigenvalue problem for which many efficient and numerically stable algorithms exist. The most desirable of these algorithms is full eigensolution by similarity transformations. However, to implement this method a general matrix must be stored in full storage mode. The difficulty with the method of Cordaro and Davis is that the order of a matrix (A) whose eigensolution is sought, increases approximately as the square of the number of unknowns and thus the class of solvable problems is restricted to very simple geometries if solution by similarity transform techniques is desired.

As is true with most large matrices which describe physical phenomenon, the matrix (A) is sparse and real. However, as is unlike many physically related matrices, A is unsymetric in the sense that it is its own block companion matrix. No algorithms exist for the complete eigensolution of a large matrix of this form. Several methods do exist, however, which yield a partial eigensolution. The merits of power related and root searching techniques are discussed, and a useful method for the partial eigensolution of very large systems is developed. Both computer running time and storage requirements are considered.

B6-2
1350

SOME INTERPRETATIONS OF TIME AND FREQUENCY DOMAIN FORMS OF THE SINGULARITY EXPANSION: L. Wilson Pearson and D. R. Wilton, Department of Electrical Engineering, University of Mississippi, University MS 38677

Withdrawn

The large complex frequency asymptotic behavior of the resolvent kernel of an integral equation of electromagnetic scattering bears heavily on both the time and frequency domain singularity expansion of its solution (D. R. Wilton, Nat'nl Rad. Sc. Mtng., January 1978; L. W. Pearson, *Electromagnetics* V. 1, No. 4). The asymptotic form of the resolvent to the magnetic field integral equation for large S in the right half of the Laplace transform plane was rigorously determined by Marin (*IEEE Trans. Ant. & Prop.*, Ap-21, 809-819, 1973) and is consistent with other high frequency asymptotic formulations--i.e. geometrical and physical optics. The determination of the counterpart left-half-plane result has proven more problematic. Recently Wilton has given a non-rigorous development of the needed asymptotic forms based on a discretized electric field operator (*Electromagnetics* V. 1, No. 4). The result is consistent with that of Marin in the right half plane and decays as $\exp[-|\mathrm{Re}\ s|\ |\bar{r}-\bar{r}'|]$ in both half planes.

The consequences of this form are discussed as they bear on both time and frequency domain expansions in the resonances of the scatterer. It is shown that considerable lattitude for alternative coupling coefficient representations is allowed by this asymptotic behavior. It is shown, too, that the frequency domain expansion may be constructed in terms of a pole series alone, thus obviating the ubiquitous concern over a "possible entire function," provided one allows the resolvent to set the turn-on time naturally. Futhermore, the frequency domain expansion is uniformly convergent so that termwise operation on the infinite series is permissible and the time domain forms ensue from simple operational calculus.

B6-3
1410 ON THE EXISTENCE OF BRANCH POINTS IN THE EIGENVALUES OF THE ELECTRIC FIELD INTEGRAL EQUATION (EFIE) OPERATOR IN THE COMPLEX FREQUENCY PLANE, Donald R. Wilton, Krzysztof A. Michalski, and L. Wilson Pearson, Department of Electrical Engineering, University of Mississippi, University, Ms 38677

The SEM representation for the current density on a scattering object can be derived formally from the eigenfunction expansion involving eigenvalues and eigenfunctions of the associated integral operator (C.E. Baum, AFWL Interaction Note 229, 1975). It is usually assumed that the inverse eigenvalues are analytic in the complex frequency s-plane except for pole singularities. Indeed, it was shown by Marin and Latham (L. Marin, R.W. Latham, Proc. IEEE, 60, 640-641, 1972) that in the case of finite extent perfectly conducting bodies in lossless media, poles are the only singularities in the SEM expansion. However, it has been suggested (L.W. Pearson, D.R. Wilton, IEEE Trans. Antennas Propagat., AP-29, 697-707, 1981) that this does not preclude the possibility of the occurence of branch point contributions which cancel in the SEM series. In fact, only for bodies such as the sphere or circular loop antenna, in which geometrical symmetry completely determines the eigenfunctions (and they are frequency independent), can it be shown that branch points cannot occur. Although the existence of branch integral contributions in the SEM representation has been speculated upon, no specific examples of their occurrence have been cited. The aim of this presentation is to fill this gap.

To gain some insight, we first demonstrate simple circuit and transmission line examples in which the eigenvalues of the impedance matrix have branch points. At a branch point in the s-plane two or more eigenvalues become degenerate and the inclusion of root vectors (A.G. Ramm, IEEE Trans. Antennas Propagat., AP-28, 897-901, 1980) in the expansion may be necessary. Next we consider the scalar scattering problem from a prolate spheroid and demonstrate the occurrence of branch points in the eigenvalues of the associated integral operator. This follows from the analysis of the spheroidal wave equation (T. Oguchi, Radio Sci., 5, 1207-1214, 1970). Similar analysis of the Mathieu's differential equation (G. Blanch, D.S. Clemm, Math. Comp., 23, 97-108, 1969) leads us to the conclusion that branch points besides the well-known branch point at the origin occur in the eigenvalues of the EFIE operator for the infinite elliptical cylinder. (The branch point at the origin results from the infinite extent of the object. These examples suggest that branch points may always be present when sufficient object symmetry is lacking.

B6-4
1430

A HYBRID CREEPING WAVE AND SEM APPROACH TO TRANSIENT FIELD SCATTERING BY A CIRCULAR CYLINDER

E.Heyman and L.B.Felsen, Department of Electrical Engineering and Computer Science,
Polytechnic Institute of New York,
Farmingdale, New York 11735

SEM complex resonances are useful for analyzing transient illumination of smooth convex bodies at long observation times but inconvenient near the time of arrival of the first response. In that regime, creeping waves provide a more effective description. It has, in fact, been shown [H.Uberall et al., IEEE Trans.& Prop.AP-28 pgs.924-927, 1980] that there is an analytic connection between the SEM resonances and the creeping waves, and that numerical summing of SEM contributions generates a creeping wave response [K.N.Chen & D. Westmoreland, Proc. IEEE Vol.69 pgs.747-750, 1981]. The interrelation between these two descriptions can be systematized and generalized by applying partial Poisson summation either to the creeping wave series or to the SEM resonance series. In this fashion, one may generate a hybrid formulation wherein, within a single analytical framework, a certain number of creeping waves dominates for early times and a correspondingly determined number of SEM resonances for later times. The method is illustrated for two-dimensional scattering by a perfectly conducting circular cylinder.

B6-5
1520 INCIDENT-WAVEFORM SYNTHESIS FOR MONOMODE SCATTERING BY AN INFINITE CYLINDER AND ITS APPLICATION FOR TARGET DISCRIMINATION: C-I Chuang, D. P. Nyquist, and K-M Chen, Dept. of Elect. Engrg.; B. C. Drachman, Dept. of Mathematics; Michigan State University, East Lansing, MI 48824

The waveform-synthesis method for detection of unknown radar targets is investigated for long, thick cylindrical targets. It is desirable, for the purpose of identifying and discriminating a radar target, to selectively excite a specific natural-resonance mode of that target. Incident radar-signal waveforms are synthesized to excite return signals consisting of a single natural mode in the late-time period. If the transient waveform synthesized to excite monomode backscatter from a preselected target is incident upon a different target, the resulting return signal differs significantly from the expected single natural mode; the wrong target is consequently sensitively discriminated. The narrow-band spectrum of a monomode return signal facilitates simplified signal processing.

The impulse response of an infinite, perfectly-conducting cylinder to normally incident, transversely-polarized illumination is first obtained. Spectral-domain analysis reveals that this response consists of a discrete series of natural-resonance modes (distribution of complex natural frequencies is computed) augmented by a series of continuous-spectrum terms (approximately decaying exponentials). An approximate method for summing an infinite number of natural modes leads, outside the immediate early-time period, to an accurate impulse response which includes the creeping-wave contribution. It is found that the late-time impulse response can be approximated by a finite number of terms. The late-time backscatter field is determined in terms of this latter impulse response, and is exploited to synthesize the incident-field waveform required to excite a monomode return signal.

Numerical examples are obtained to demonstrate the required incident waveforms which excite various monomode responses. When the waveform synthesized to excite monomode backscatter from a preselected cylinder is incident upon a cylinder of different radius, the return signal differs from the expected natural mode. The sensitivity of target discrimination based upon this method is studied.

B6-6
1540

APPROXIMATE CHARACTERISTIC EQUATIONS FOR SIMPLE STRUCTURES

D.L. Moffatt, J.G. Bagby
ElectroScience Laboratory
Department of Electrical Engineering
Ohio State University, Columbus, OH 43212

In this paper, geometrical and physical considerations are shown to lead to useful approximations of the characteristic equations and corresponding natural frequencies of oscillation of several simple structures. For thin wires, simple approximations for path attenuation and phase delay, junction reflection and transmission and end reflection and radiative coupling are stressed. These approximations are applied to various wire configurations including curved and bent wire segments, loops and multi-legged structures.

For solid conducting objects, the application of a characteristic equation procedure using GTD (E.M. Kennaugh, IEEE Trans. AP-29, 327-331, 1981) to the case of a circular disc is discussed.

B6-7
1600

EXCITATION OF SINGLE-MODE BACKSCATTERS FROM TWO SKEW COUPLED WIRES

Che-I Chuang, K. M. Chen and D. P. Nyquist
Department of Electrical Engineering and
Systems Science
Michigan State University, E. Lansing, MI 48824

For the purpose of identifying and discriminating a radar target, it is desirable to have capacity to selectively excite natural modes of the target. To do so, it is necessary to synthesize an aspect-independent waveform for the incident radar signal in such a way that it excites a single-mode backscatter from the target in the late-time period.

A system of two isolated wires oriented at an angle and being illuminated by a pulse of radar signal is considered. The induced currents in the wires in the late-time period can be expressed in terms of natural modes of the system. The natural modes of the system can be divided into symmetrical and anti-symmetrical modes. The natural frequencies and spatial variations of the natural modes are found as functions of the separation and the orientation angle between the wires. After the natural frequencies of the major natural modes, which have low damping coefficients, are determined, it is possible to synthesize a required, aspect-independent waveform for the incident radar signal to excite a single-mode backscatter from the system in the late-time period.

A special case of these study results can be used to explain the experimental results on the excitation of a single-mode backscatter from an arbitrarily oriented wire above the ground plane. For this case, the wire and its image form a pair of skew coupled wires carrying only the anti-symmetrical modes of induced currents. Since the natural frequencies of the wire are dependent on the orientation angle with the ground plane, the aspect-independent excitation of a single-mode backscatter from the wire is only possible when the spacing between the wire and the ground plane is large and that the coupling between the wire and its image can be neglected.

B6-8
1620

DEGENERACY IN THE NATURAL MODES OF A LOADED THIN-WIRE ANTENNA:

Ahmad Hoorfar and David C. Chang,
Electromagnetics Laboratory, Department of Electrical Engineering, University of Colorado, Boulder, CO 80309

Equipped with an accurate analytical expression in the frequency-domain for the current induced on a thin-wire dipole antenna, previously obtained by Chang, Lee and Rispin(IEEE-APS, 26,5; 683-690, 1978), we have recently derived simple closed-form expressions for the SEM poles, natural mode current and coupling coefficient of an unloaded thin-wire antenna. Excellent agreements with the numerical works for both the transmitting and receiving antennas were demonstrated. In the present work, the problem is extended to include the transient response of a loaded thin-wire antenna. Locations of the first-layer SEM poles (i.e., natural frequencies) in the complex ω-plane can be determined from the modal equation:

$$D(\omega_s) = 1 - R^2(\omega_s) I_\infty^2(\omega_s;L) + Z_\ell(\omega_s) f(\omega_s;d,d) = 0$$

where R is the current reflection coefficient from the end of the antenna; $I_\infty(\omega;z-z')$ is the current at z along an infinitely-long antenna, of radius a, eminating from a source at z'. The function $f(\omega,z,z')$ is the corresponding normalized input admittance of an antenna of finite length L in the absence of the load; finally, Z_ℓ is the load impedance located at $z=d$ on the antenna. Natural mode current and admittance function can also be determined explicitly. For a center-loaded antenna, the natural frequencies of this structure varies from ones corresponding to the symmetric modes of an antenna of length L when $Z_\ell = 0$, to ones corresponding to an antenna having half of the length, i.e. $L/2$, when $Z_\ell \to \infty$. In this transition the natural frequencies $\omega_s, s = 0,1,2,\ldots$, pass through points with maximum attenuation (i.e., where $I_m(\omega_s)$ is maximum). We have been able to show that for a very thin wire antenna these points occur when $Z_\ell \simeq |Z_c(\omega)|$, where $Z_c(\omega)$ is the input impedance of the corresponding infinitely-long thin-wire antenna. In addition, as the values of a resistive load increases from 0 to ∞, the natural frequencies of the first two modes transverse in opposite directions in such a manner that for some specific values of a/L and Z_ℓ, degeneracy of the two modes occur. A detailed structure of this degeneracy, and the associated current distributions of two near-degenerate modes will be discussed in the presentation. Transient response for a loaded antenna that satisfies the degeneracy condition will also be presented.

COMMUNICATION SATELLITE SYSTEMS INCORPORATING MULTIPLE BEAM ANTENNAS
Thursday afternoon, 14 Jan., CRO-30
Organizer and Chairman: Douglas O. Reudink, Bell Telephone Laboratories, Holmdel, NY 07733

C4-1
1330

AN EXPERIMENTAL RAPID SCANNING PHASED ARRAY REPEATER FOR HIGH-SPEED DIGITAL SATELLITE COMMUNICATION:

A. J. Rustako, Jr.
Bell Laboratories
Holmdel, New Jersey 07733

An experimental phased array satellite repeater capable of rapidly scanning independent receiving and transmitting beams between multiple pairs of ground stations is described. The array repeater can interconnect these stations by re-orienting the beams in less than 10 nsec. permitting efficient use of time division multiple access techniques at high data rates (600Mb/s). Both receiving and transmitting arrays can be automatically co-phased under microprocesser program control from any ground station. The array implementation and performance are described.

C4-2
1400

MOTIVATION FOR MULTI-BEAM SATELLITES

D. O. Reudink
Bell Laboratories
Crawford Hill Laboratory
Holmdel, New Jersey 07733

A simple fundamental relationship is derived between antenna gain and transmitter power which maximizes the effective radiated power in mass-limited satellite systems. In the most common case, maximum effective radiated power is achieved when the payload mass is divided equally between the antenna system and the power system. Although this may have been known intuitively to satellite designers, to the author's knowledge this relationship has never been published. Example calculations show that considerable increases in performance can be expected for satellites which employ high-gain multibeam antennas.

C4-3
1430 30/20 GHz EXPERIMENTAL FLIGHT SYSTEM DEFINITION:

David L. Wright, Head, Systems Engineering Section,
Space Communications Division, NASA Lewis Research Center
Cleveland, OH 44135

The 30/20 GHz Satellite Communications Program has been developed in concert with the communications industry. Phase I of the program defined the characteristics of the operational system and identified the associated critical technologies which must be developed before viable, spectrum-conservative operational systems can be implemented by the common carriers. During Phase II the final experimental flight system requirements and definition were developed through the in-house synthesis of five system studies which were conducted with the U.S. satellite communications suppliers (Ford, General Electric, Hughes, RCA and TRW). These requirements are consistent with the critical technologies identified in Phase I. In this paper, which focuses on Phase II system requirements, results are presented for the space and ground segment requirements of the experimental flight system for both trunking and customer premise services (CPS). The technology development program which is responsible for creating the required technology for operational systems has been previously reported and will not be considered in this paper.

C4-4
1530

A FOUR-PHASE COMMUNICATION SYSTEM EMPLOYING ADAPTIVE ANTENNAS*

J. H. Winters
Bell Laboratories, Holmdel New Jersey 07733

This talk discusses a four-phase communication system employing adaptive antennas. A system is described that provides protection against interference (including repeat jamming) with rapid acquisition of the signal at the receiver. A method is shown for generating reference signals required by the adaptive array from the received signal. With these reference signals, the received antenna pattern can be adapted to maximize desired signal to interference and noise power ratio at the receiver. The signal acquisition technique is also described. Analytical and experimental results demonstrate both the rapid signal acquisition and interference protection of this system.

---

*The work reported in this talk was supported, in part, by Contract F30602-79-C-0068 between the Rome Air Development Center and the Ohio State University Research Foundation.

C4-5 1600 A NARROW MULTIBEAM, DUALLY POLARIZED GROUND STATION ANTENNA EMPLOYING A LINEAR ARRAY WITH A GEOSYNCHRONOUS ARC COVERAGE OF 60°

N. Amitay and M. J. Gans
Bell Laboratories
Holmdel, New Jersey 07733

We have investigated various schemes for utilizing a linear scan in narrow multibeam ground station antennas employing phase arrays. The feasibility of using an appropriately squinted linearly scanned antenna was demonstrated. We have done this by deriving formulas for optimum (in the mean square sense) antenna orientation. This orientation yields an accurate mapping of a 60° segment of the geosynchronous equatorial arc (GEA) onto a plane parallel to a cardinal plane in the antenna directional cosine coordinates.

Calculations for properly oriented, linearly scanned, and narrow ($\leq$0.5°) multibeam antennas placed at selected cities in the USA are very encouraging. They indicate that the peak beam pointing deviation in the 70°W to 130°W GEA segment is under 5/1000th of a degree. Even higher beam pointing accuracy exists for shorter segments.

For a 300 Mbaud rate at 11.95 GHz, a relatively simple time equalization can be used to minimize PSK bit error rate degradation due to array dispersion.

These ground station antennas, with relatively simple mechanical structure, are suitable for multi-satellite communication systems, intersatellite systems communication, multi-satellite receive only stations, etc.

We examined various implementation alternatives for the above mentioned antenna system. The current antenna structure, for the 11.7-14/5 GHz band, consists of cut horns. There are approximately 250 closely spaced horn elements in the array feed so as to eliminate the formation of grating lobes when the beams are scanned over a 60° segment of the geosynchronous equatorial arc. The present antenna design possesses a dual polarization capability. A linear array feed is required per single polarization. In order to utilize the same feed design for both polarizations, a wide angle polarization rotator is used in conjunction with the vertical polarization feed.

RADAR OCEANOGRAPHY
Thursday afternoon, 14 Jan., CR2-26
Chairman: Donald E. Barrick,
NOAA/ERL/WPL, Boulder, CO 80303

F4-1
1330

ATTENUATION RATES OF AN HF RADAR OVER THE SEA

R.S. Lyons
NOAA, ERL, Wave Propagation Laboratory
Boulder, Colorado 80302
D.E. Barrick
NOAA, ERL, Wave Propagation Laboratory
Boulder, Colorado 80302

The attenuation rates of an HF radar, CODAR (Coastal Ocean Dynamics Applications Radar), are studied as a function of wave height and orientation with respect to the radar beam direction. These empirical propagation losses are compared to a model of HF surface-wave attenuation based on theoretical sea-surface impedance calculations. The radar system transmits at 25.4MHz and includes directional antennas which show variations of attenuation rates depending on wave as well as wind direction. The propagation losses in dB/km were calculated from data on sea-echo spectral signal-to-noise ratio taken at the ARSLOE experiment during October-November, 1980 at Duck, N.C. where sea conditions varied from calm to wave heights of 4.5m. Besides the simple situation when only wind waves are present, conditions were analyzed when both swell and wind waves from different directions existed simultaneously. These empirical attenuation rates agree with the model of ocean waveheight directional spectrum effects on HF propagation losses.

F4-2
1400

REAL-TIME SEA-STATE SURVEILLANCE WITH HF SKYWAVE RADAR

T.M. Georges,
NOAA, ERL, Wave Propagation Laboratory,
Boulder, CO 80303
J.W. Maresca, Jr.,
SRI International,
Menlo Park, CA 94025
J.P. Riley,
NOAA, ERL, Wave Propagation Laboratory,
Boulder, CO 80303
C.T. Carlson,
SRI International
Menlo Park, CA 94025

A NOAA/SRI team has conducted tests of the coverage efficiency of HF skywave (ionospheric) radar for mapping ocean waveheight and surface wind direction at ranges between 1200 and 3000 km. We found that surface wind direction can be mapped routinely in less than two hours over the entire radar coverage area, and that rms wave height can be mapped in 3 to 6 hours, depending on ionospheric conditions. Two brief tests with the SRI-WARF radar showed that skywave radar can cover either large or small selected regions of ocean with about 60 percent efficiency. Greater efficiencies could be expected operationally with more sophisticated radars. We show for the first time how on-line waveheight processing algorithms and real-time ionospheric diagnostics help select space-time-frequency windows with low ionospheric distortion.

F4-3 1430 IONOSPHERIC DISTORTION OF SKYWAVE SEA-ECHO DOPPLER SPECTRA

R.M. Jones,
NOAA, ERL, Wave Propagation Laboratory
Boulder, CO 80303

Skywave (ionospheric) radar gives more coverage of the ocean than does surface-wave radar, but ionospheric motions often distort the received signal so much that it is difficult to extract the sea-state information that the sea-echo Doppler spectra contain. The most significant ionospheric distortions of sea-echo spectra are (1) contamination of the second-order part of the spectra, and (2) an increase in variance of the spectra by a factor of two to three. The main causes of the ionospheric distortion are (1) multilayer multipath, (2) ordinary-extraordinary wave multipath, (3) traveling-ionospheric-disturbance multipath, (4) Doppler spreading from a time-varying frequency shift on a single path, and (5) ionospheric reflection coefficient variability.

Measurements in October, 1980 of ionospherically propagated ground-backscatter spectra (which represent in most respects a direct measure of the ionospheric distortion) show (1) Doppler spectra that are more continuous rather than made up of a small number of discrete spectral components, (2) significant ionospheric distortion (as measured by contamination of second-order sea echoes) most of the time, and (3) large variability in ionospheric distortion with time and place.

The larger variance of individual spectra with skywave requires longer incoherent averaging to get the necessary variance reduction for average spectra. That the ionospheric distortion cannot be accurately modeled by a small number of propagation paths prohibits the use of simple deconvolution schemes to remove the distortion. That the distortion is significant most of the time implies that sophisticated algorithms for reducing the effect of distortion are nearly always necessary. Because the average ionospheric distortion spectrum varies much more rapidly than the average sea-scatter spectrum, and because the average effect of the distortion is to increase the second-order part of the spectrum, the average spectra with the smallest second-order part are probably the least distorted. Georges et al (NOAA Technical Memorandum ERL WPL-73) discuss this and other techniques for reducing the effects of ionospheric distortion of skywave sea-echo spectra. The ionospheric distortion measurements presented here are for only about two hours of F-layer propagation. Future measurements should include a variety of ionospheric conditions, including sporadic E.

F4-4
1500 REMOVAL OF CURRENT DOPPLER DISTORTION FROM SECOND-ORDER HF BROAD-BEAM SEA ECHO BEFORE SEA-STATE DETERMINATION

Belinda J. Lipa
CODAR Research
165 Harcross Road
Woodside, California 94062
Donald E. Barrick
NOAA, ERL, Wave Propagation Laboratory
Boulder, Colorado 80303

Methods have been developed and demonstrated that allow extraction of the ocean waveheight directional spectrum from second-order HF sea-echo Doppler spectra. The frequency resolution obtainable in the derived wave spectrum is for all practical purposes the same as the frequency resolution of the echo spectrum. If a current is present in a narrow-beam radar, it shifts all parts of the echo spectrum (first and second order) uniformly, and is therefore easily identified and removed. In a broad-beam system (such as the compact CODAR crossed-loop system developed by NOAA), however, variation of the radial component of current across the resolution cell produces a smearing of the echo spectrum that can represent an intolerable degradation in frequency resolution.

We demonstrate a technique whereby the first-order echo is used to measure the radial current pattern over the scatter area. This pattern is then employed in the frequency relationship in the equation for the theoretical second-order sea-echo to remove this distortion. Thus the resulting waveheight directional spectra obtained have the same frequency resolution as if no currents had been present.

F4-5
1545

COMPARATIVE RESULTS OF DELTA-K OCEAN WAVE SPECTROMETER MEASUREMENTS WITH A VARIETY OF SURFACE ILLUMINATION GEOMETRIES

J. W. Johnson and H. F. Thornton, NASA Langley Research Center, Hampton, VA 23665; and D. E. Weissman, Hofstra University, Hempstead, NY 11550

Measurements of the relative strength of ocean surface wave spectral components have been made from an aircraft using the two-frequency microwave resonance technique. A coherent Ku-band radar was used to study the Bragg type resonance matching (at the difference frequency, Δf) to the surface wave components. The spatial spectrum of the surface reflectivity modulation was then computed as the value of Δf was varied over a matching range of approximately 15 - 150 m in surface wavelength. This paper contains experimental results from flights conducted during the 1979 MARSEN project and the 1980 ARSLOE project, and the objective here is to present the radar results in terms of the variety of surface illumination geometries encountered.

In MARSEN, a .5° x 25° fan beam antenna at a fixed angle of incidence was used with the aircraft flying at three different altitudes. A 3.5° pencil beam antenna was used during ARSLOE at incidence angles of 15°, 25°, 40°, 50°, and a variety of altitudes. The experimental results will be presented in terms of the effect of incidence angle, along track footprint length, and footprint area on both the strength of individual resonances and the shape of the modulation spectrum. It will be shown that the MATSEN results, with the narrow footprint, are consistent with a one-dimensional theroetical approach and that the ARSLOE results, with a symmetric beam pattern, agree well with the existing two-dimensional theory.

F4-6
1615

DISTRIBUTIONS OF CAPILLARY-WAVE ON LARGER WAVES AS MEASURED BY RADAR

R.K. Moore, S. Barkeshli, I.J. Birrer, G.J. Dome
Remote Sensing Laboratory
University of Kansas Center for Research, Inc.
Lawrence, Kansas 66045

The modulation of capillary-wave amplitudes on the ocean govern the production of radar images of the ocean, particularly those using synthetic-aperture systems. Simultaneous radar measurements of wave height and radar backscatter were made from a tower in the North Sea. Correlations between the radar signal and the wave heights are used to deduce the relationships between positions of the capillary wave maxima and the wave crests, taking slope modulation into account.

F4-7 1645 MEASUREMENTS OF THE CAPILLARY-WAVE SPECTRUM FOR THE OCEAN BASED ON RADAR SCATTEROMETER MEASUREMENTS FROM A TOWER

R.K. Moore, G.J. Dome, I.J. Birrer
Remote Sensing Laboratory
University of Kansas Center for Research, Inc.
Lawrence, Kansas 66045

Measurements of radar backscatter from a tower in the North Sea over a wide range of frequencies and angles of incidence permit determination of the capillary-wave spectrum. The capillary wave spectrum produced by using Bragg-resonance theory on the observations is similar to that based on wave-tank observations and previously used in radar backscatter theory, but it differs enough that the theoretical radar backscatter curves vs wind speed and angle of incidence must be modified.

TROPOSPHERIC PROPAGATION
Thursday afternoon, 14 Jan., CR1-40
Chairman: Juergen H. Richter, Naval Ocean Systems Center, Electromagnetic Propagation Division, San Diego, CA 92152

F5-1
1400

RELIABILITY OF THE EVAPORATION DUCT FOR OVER-THE-HORIZON PROPAGATION

K. D. Anderson, EM Propagation Division, Code 532
Naval Ocean Systems Center
San Diego, CA 92152

The analytical models describing propagation in the presence of an evaporation duct are well known, but several practical questions remain unanswered. First, can the duct reliably support propagation to ranges of twice the horizon? Second, what are the short and long term fading rates? Lastly, what is the probability of significant enhancement on a worldwide basis? This talk presents preliminary results from an ongoing effort to answer these specific questions.

F5-2
1425

PROPAGATION STUDY FOR A TROPOSPHERIC TRANSHORIZON RADAR:

K. Toman, Propagation Branch
Electromagnetic Sciences Division
Hanscom AFB, MA 01731

Derived from an early NBS tropospheric transhorizon propagation data base, a particular loss term defined as path attenuation was used in the radar equation to estimate the behavior of signal-to-noise ratio with frequency, distance including percentile variability. This loss term depends on frequency, distance, climate, refractivity and an empirically derived attenuation function which takes into account effects of antenna heights. Equivalent antenna temperatures are assumed to be due to galactic noise. Receiver noise is characterized by noise figure F. For conveniently chosen system parameters, signal-to-noise ratio behavior is illustrated for several known target cross sections as a function of frequency, distance, variability for particular climates. Conversion to other system parameter combinations is simple. For the conditions considered above, an attempt is made to assess detectability in terms of realistic parameter ratios.

F5-3
1510

SEA CLUTTER UNDER ATMOSPHERIC DUCTING CONDITIONS

F. Perry Snyder
EM Propagation Division
Naval Ocean Systems Center
San Diego, CA 92152

Atmospheric ducting phenomena can seriously influence radar coverage, significantly extending radar ranges or causing radar "holes." Such atmospheric ducting conditions influence not only the radar target return signal, but also the signal returned from other objects, i.e., radar clutter. Expected improvements in radar performance due to some ducting conditions can be seriously diminished, if not converted to degraded performance, due to clutter effects. An "onboard" capability to sensor performance has been developed in the IREPS (Integrated Refractive Effects Prediction System) project at NOSC. Presently, the IREPS, or any other known general purpose performance assessment system, does not adequately consider clutter.

Radar clutter return has been investigated extensively, both theoretically and experimentally, and several empirical models for sea clutter have recently been developed. These sea clutter models have many features in common, particularly the consideration of only standard atmospheric conditions. A sea clutter effects model, capable of consideration of non-standard atmospheric conditions, has been developed for intended usage in the IREPS. The model, which couples a classical ray-optics propagation formulation with an empirical sea clutter cross-section model, is discussed. Also presented are predicted effects on radar coverage due to a variety of atmospheric ducting environments. The clutter effects model is most appropriate to a propagation environment resulting from an elevated refractive layer producing a ground based duct. For such ducting conditions, the clutter effects model predicts the occurrence of discretely spaced "clutter rings," in agreement with observations.

F5-4
1545

EHF ATTENUATION AND DELAY PROPERTIES OF MODEL ATMOSPHERES

H. J. Liebe, National Telecommunications and Information Administration, Institute for Telecommunication Sciences, Boulder, CO 80303

A complex transfer function for radio wave propagation through moist air at frequencies below 1000 GHz has been formulated (H. J. Liebe, Radio Sci., 16(6), 1981). This model is applied to calculate and plot EHF attenuation and delay rates for ten model atmospheres encompassing tropical to arctic height profiles of pressure, temperature, and relative humidity. Homogeneous (horizontal radio path) and inhomogeneous (e.g., zenith paths) air masses are evaluated with the following objectives:

(a) optimizing computer run time by reducing the number of molecular (H_2O and O_2) absorption lines (typically between 30 and 80 lines) and limiting the number of height intervals (typically 20 to 60 for h = 0 to 100 km);
(b) demonstrating the influence of total precipitable water vapor (w) and cloud water (W) contents within a radio path;
(c) correlating cumulative quantities with meteorological surface conditions; and
(d) estimating the anisotropic behavior of mesospheric O_2 spectral lines caused by Zeeman-splitting in the geomagnetic field.

For example, an evaluation of zenith path transfer properties between 1 and 300 GHz with three values of w (0 to 70 mm) and two values of W (0 to 3 mm) requires about 10^7 individual summations excluding the Zeeman effect.

The results are useful to analyze signal impairments due to deterministic amplitude and/or phase variations within the signal bandwidth. This problem gains importance with the advent of gigabit-rate data links employing EHF carriers.

F5-5
1610

THEORETICAL AND CALCULATIONAL ASPECTS OF THE RADIO REFRACTIVE INDEX OF MOIST AIR

R.J. Hill, Wave Propagation Laboratory
Environmental Research Laboratories
National Oceanic and Atmospheric Administration
Boulder, Colorado 80303

According to the Kramers-Kronig relation, an absorption resonance produces a frequency-dependent refraction. This refraction is nondispersive at frequencies much lower than the resonance frequency. For instance, the ultraviolet electronic resonances provide the refraction at visible frequencies. These induced-dipole type transitions produce refraction that is proportional to the number density of molecules. The radio refraction is caused by the infrared as well as the ultraviolet transitions. Classically, the infrared rotational resonances (permanent-dipole transitions) of water vapor provide a radio refraction proportional to water vapor number density divided by temperature. The quantum theory shows that this classical notion is true provided that no transitions involve energy changes of the order of the thermal energy. The water-vapor rotational resonances certainly include strong transitions involving energy changes near the thermal energy. Thus, it is expected that the radio refractive index caused by the rotational resonances of water vapor is not precisely proportional to number density divided by temperature.

The radio refractive index is calculated by summing the refraction due to the infrared resonances of the water vapor monomer. Although this calculated refraction agrees well with measured values, its temperature dependence departs significantly from the measured variation with temperature. As expected, the rotational resonances of water vapor give a contribution to the radio refractive index that does not vary precisely as number density divided by temperature. The vibrational-rotational resonances contribute a radio refraction that is nearly, but not precisely, proportional to number density of water vapor. This vibrational-rotational contribution is much smaller than that by the rotational resonances.

It has been hypothesized that the term proportional to number density in the radio refractive index equation should be equal to its counterpart in the optical refractive index equation, and that this relationship can be used to improve the values of the coefficients in the radio refractive-index equation for moist air. The hypothesis is found to be false, and it is suggested that it is best to use the empirical coefficients of the refractive-index equation.

F5-6
1635

OPTICAL, RADIATIVE, AND MICROPHYSICAL INHOMOGENEITIES IN CLOUDS

V.E. Derr, Office of Director, and Wave Propagation Laboratory, Environmental Research Laboratories, Boulder, Colorado 80303

The performance of many radar and lidar systems is influenced by cloud microphysical properties, such as dropsize distribution.

Clouds modulate solar influx and terrestrial and atmospheric thermal emission. The lack of uniformity of cloud concentration and characteristics from global to microscopic scales affects transmission of electromagnetic radiation over a wide range of frequencies. Experimental data are presented on optical, radiative, and microphysical properties of clouds, and statistical properties of spatial variations of clouds are presented. Data obtained in many flights of the NOAA P-3 research aircraft include radiative and microphysical parameters. Hemispherical downward and upward fluxes were measured in four spectral bands from .3 to 50 μm as functions of depth of cloud under various conditions. Simultaneous measurements of liquid water content and drop-size distributions were made as well as standard meteorological variables. Relations between liquid water content and optical attenuation and the effect of clouds on solar flux at the ocean surface will be presented.

TRANSIONOSPHERIC RADIO
Thursday afternoon, 14 Jan., CR1-46
Chairman: K.C. Yeh, University of Illinois
Urbana, IL 61801

G2-1
1330 TOTAL ELECTRON CONTENT STRUCTURE IN THE MIDDLE EAST

Haim Soicher, Center for Communications Systems
U.S. Army Communications-Electronics Command
Fort Monmouth, N.J. 07703

Polarization rotation data recorded from the geostationary satellite SIRIO at Haifa, Israel, have been used to study the structure and variability of the total electron content (TEC) during the maximum phase of the current solar cycle. In addition to the overall diurnal and seasonal variation, the TEC is regularly modulated by the effects of travelling ionospheric disturbances (TIDS). The behavior of TIDs in terms of their frequency of occurrence, amplitude, period, and time of occurrence is seasonally dependent.

G2-2
1400 MODELING THE IONOSPHERIC ELECTRON CONTENT MEASURED BY ATS6: O.M. Grimalizzi and K. Davies, Space Environment Laboratory, NOAA, Boulder, CO 80303

A model that solves the time-dependent ion-continuity equation was used for comparison with total electron content data measured, with the ATS6 radio beacon, at Boulder, Colorado during sunspot minimum (June 1974 to May 1975). Calculated and observed critical frequencies (foF2) at Boulder were compared also.

With the inclusion of atomic oxygen ions O^+ only it was possible to obtain good agreement between model and observed foF2 by adjusting the neutral wind. However, under these conditions, the calaculated TEC were much below the observed TEC. Inclusion of molecular ions NO^+ and O_2^+ in the model gave better agreement with the observed TEC.

G2-3
1500

F LAYER IRREGULARITY PHENOMENA AT SUB-AURORAL AND AURORAL LATITUDES

Jules Aarons,* Air Force Geophysics Laboratory, Hanscom AFB, MA 01731

Both scintillation intensity and F layer clutter observed with HF backscatter radars are effects of the F layer irregularity electron density (ΔN) and the irregularity configuration. Using data obtained at Goose Bay, Labrador and the Sagamore Hill Radio Observatory in Hamilton, Mass. plots of continuous levels of scintillation intensity were developed for latitudes ranging from 53° CGL to 69° CGL.

For any individual night F layer scintillation activity similar to that of sub-storm activity is revealed with a longitudinal region affected for several hours while paths at the same CGL but 15° away in longitude remain unaffected. On other nights the boundary of F layer irregularity intensity is quite sharp across a range of longitudes.

Using other scintillation data taken over long periods of time, the role of sunspot cycle will be assessed. Lower median levels of scintillations have been noted with lower sunspot number at plasmaspheric, sub-auroral and auroral latitudes. The irregularity electron density, ΔN, in some regions appears to be affected by the relevant intability mechanisms in the same way that polar and equatorial irregularities are affected i.e. as a percentage of the ambient electron density, N. In years of relatively low electron density, i.e. the low sunspot years, ΔN in the irregularity will be smaller and scintillation levels for the same magnetic conditions lower than those at the peak of the sunspot cycle.

*At present at Boston University, Boston, MA

G2-4
1530 PROPAGATION OF BEAM WAVES THROUGH AN IONOSPHERIC IRREGULARITY LAYER

Yean-Woei Kiang, Department of Electrical Engineering, National Taiwan University, Taipei, Taiwan, Republic of China
C. H. Liu, Department of Electrical Engineering, University of Illinois, Urbana, IL 61801

The problem of a beam wave propagating through a turbulent layer is investigated. Applying the phase screen approach exact analytical expressions for beam wander and spread are derived for the case of a beam wave passing through a random slab containing irregularities with general power-law spectrum. The results are valid for all scintillation strengths including the strong cases. Depending on the parameters of the beam and the properties of the turbulent layer, the effects of irregularities on the beam wave may be appreciable. In particular, it is found that these effects are dependent on the spectral index p of the power-law spectrum for the irregularities. To further investigate the instantaneous behavior of the beam, a numerical approach is used to propagate the beam through a simulated irregularity layer based on in-situ ionospheric measurements. It is found that hot spots may develop in the beam when irregular structures with sharp spatial gradients drift across the beam. These results are applied to investigate the possible effects of ionospheric irregularities on the proposed solar power satellite systems.

G2-5
1600 TEMPORAL VARIATIONS OF EQUATORIAL IONOSPHERIC IRREGULARITIES DEDUCED FROM SCINTILLATION DATA

K. C. Yeh, T. R. Tyagi, A. W. Wernik, C. H. Liu,
Department of Electrical Engineering, University of Illinois at Urbana-Champaign, Urbana, IL 61801

In most ionospheric scintillation studies, the "frozen-in" assumption is made for which the irregularities are assumed to be frozen as they drift across the beam of radio wave. In reality, the irregularities will change with time as they move. Indeed, the temporal evolution of the irregularities is closely related to the generation mechanisms of the irregularities. In this paper, we attempt to investigate the temporal variations of the equatorial ionospheric irregularities using scintillation data received at two stations located in Natal, Brazil. The two stations are separated by 278 m in the East-West direction. Radio signal at 257.55 MHz from Marisat 1 was received at the stations. The scintillation signals at the two stations are found to be well correlated. Cross correlation analysis yielded the drift speeds of the irregularities. Cases were selected when the drift speed was near zero. The variations of the signals in these cases are assumed to be due to the temporal variations of the irregularities. Several such cases were analyzed. A theoretical analysis based on a temporal-spatial irregularity spectrum model has been carried out. The results will be used to interprete the experimental data.

G2
1630 PRESENTATION OF THE 1982 HARRY DIAMOND AWARD TO DR. JULES AARONS

RADIO ASTRONOMY (GENERAL) AND INSTRUMENTATION
Thursday afternoon, 14 Jan., CR2-6
Chairman: M. Ewing, California Institute of Technology, Pasadena, CA 91103

J5-1 1410 **A BEAM-RATIO TECHNIQUE FOR STUDIES OF SOLAR MICROWAVE SOURCES:** K.F. Tapping, NRC, Canada

The conventional beam-switching or beam-difference observing technique is highly effective in reducing the effects of tropospheric noise fluctuations upon the measurement accuracy. However, when very strong sources are observed, the direct effect of the varying tropospheric loss upon the source signal is much larger than the contribution from the tropospheric noise. In this case the beam-difference method is not useful.

In a study of the intensity variations of compact microwave sources on the solar disc, it was found that the time-varying, tropospheric attenuation, under most conditions, made total power observations rather suspect. These sources are bright, producing antenna temperatures ranging from $\sim 10^3$-10^6 K at 2.8 cm wavelength. The receiver and tropospheric noise contributions were insignificant compared with this. The background solar disc temperature was about 10^4 K. For observation of these sources, the beam-ratio technique was found to be highly effective. The system is set up so that the main antenna beam falls on the source under study and the reference beam on the background solar disc. The main and reference beam signal powers are given by:-

$$P_{main} = G[T_R + T_t(1 - \alpha_t) + \alpha_t T_s \omega_s/\Omega_o + \alpha_t T_{disc}\ (1 - \omega_s/\Omega_o)]$$

$$P_{ref} = G[T_R + T_t(1 - \alpha_t) + \alpha_t T_{disc}$$

Where T_R = Receiver noise temperature, G = Receiver gain-bandwidth product, Ω_o = Antenna beamsize; T_t = Mean tropospheric temperature, α_t = Overall transmissivity of troposphere^t ($0 < \alpha_t < 1$); T_S = Brightness temperature of compact source, ω_s = Angular size of source and T_{disc} = Temperature of background solar disc.

The receiver is switched between the main and reference feeds at a rate faster than the tropospheric fluctuations. The outputs are separated and filtered. The ratio P_{main}/P_{ref} is then derived. Since $T_s\omega_s/\Omega_o$, $T_{disc} \gg T_R, T_t$, we obtain:-

$$\frac{P_{main}}{P_{ref}} = \frac{T_s \omega_s/\Omega_o + T_{disc}(1 - \omega_s/\Omega_o)}{T_{disc}}$$

or, for compact sources small compared with the beam-size,

$$\frac{P_{main}}{P_{ref}} = \frac{T_s}{T_B}\frac{\omega_s}{\Omega_o} + 1$$

The tropospheric fluctuations are eliminated from the receiver output. In practice, the rejection of tropospheric and receiver fluctuations was found to be at least 100 times smaller compared with single beam, total power observations.

J5-2 1425 A COMPARISON OF TERRESTRIAL AND PLANETARY VLF EMISSIONS: W.S. Kurth, Department of Physics and Astronomy, University of Iowa, Iowa City, IA 52242

The Voyager missions to Jupiter and Saturn have provided the first observations of VLF wave phenomena in non-terrestrial magnetospheres. Perhaps the most important analysis to be performed with the Voyager observations is a comparison of plasma wave phenomena found in the Jovian and Saturnian magnetospheres with those detected in the terrestrial magnetosphere. This comparison not only advances the identification and understanding of the non-terrestrial emissions, but also greatly enhances our knowledge of the terrestrial counterparts. At first glance, this comparison yields the somewhat extraordinary result that the terrestrial and non-terrestrial plasma wave "zoos" are quite similar in many respects. Virtually all phenomena observed at Jupiter and Saturn have close terrestrial cousins. Conversely, there are few, if any, terrestrial emissions which are not detected in the magnetospheres of Jupiter and Saturn. These similarities exist despite obvious differences between the solar wind-dominated magnetosphere of the earth and the magnetospheres of the giant planets which are dominated by internal plasma sources (such as Io) and driven largely by the rotational energy of the planet.

Of course, one other major difference between earth and the two giant planets is the presence of man and civilization on the former. Now, at least in theory, it is possible to compare VLF emissions in the terrestrial magnetosphere with those of another magnetosphere not affected by civilization in order to begin to sort out which phenomena at the earth are naturally occurring, and which are triggered, modulated, or even generated by man. Some preliminary results of such a comparison will be given.

J5-3
1440

THE MODE SWITCHING PHENOMENON IN PULSARS

N. Bartel, M.I.T., D. Morris, IRAM,
W. Sieber, MPIFR, T. H. Hankins, NAIC,
Arecibo Observatory

We report on a multifrequency full polarization analysis of the two classical mode-switching pulsars PSR 0329+54 and PSR 1237+25 and compare properties of all known mode-switchers.

Simultaneous observations of PSR 0329+54 at 1.4 and 9.0 GHz show that the switch between modes is broadband as it occurs simultaneously at both frequencies. During a switch, components in the profile alter their longitudinal positions so that the total pulse width is reduced. The spectra measured at the peak of different pulse components have only slightly different spectral indices in the normal mode. The pulse component spectra steepen or flatten when the pulsar switches to the abnormal mode so that abnormal pulse profile shapes tend to be more frequency dependent than normal ones. All polarization properties, i.e. linear and circular polarization percentage and the polarization position angle sweep, are affected by a mode change; and furthermore the periodic intensity fluctuation from pulse to pulse, also known as the drifting phenomenon, changes its behavior dramatically from one mode to the other.

We interpret the moding phenomenon as a change in the inhomogeneous chemical composition and/or structure of the pulsar surface followed by an alteration of the electrostatic conditions in the polar cap region above the surface, which leads to a different distribution of the particles in the magnetosphere. In the abnormal mode the average plasma flow rate is apparently reduced so that radio emission is observed from lower levels in the magnetosphere. Comparison with other pulsars suggests that the sequence of drift bands A, B, C (PSR 0031-07) or A, B, ABN (PSR 2319+60), followed by nulls, is a sequence of increasing plasma flow. Thus, in contrast to modes, nulls may be associated with episodes of high plasma flow leading to overheating or changes in the composition of the pulsar surface.

J5-4
1455 HIGH RESOLUTION RADAR MAPS OF THE MOON AT 70 CM WAVELENGTH: T.W. Thompson, Planetary Science Institute, 283 S. Lake Ave., Suite 218, Pasadena, CA 91101

The long-range goal of this research is to produce a new radar map of the moon at 70cm wavelength with improved resolution and radarmetric calibration over the existing data which was obtained in the late 1960's. This is underway with five observations in May 1981 using the 430Mhz radar at the Arecibo Observatory. (Some eleven more observations are needed to map the lunar earthside hemisphere.)

The May 1981 observations had radar cell-sized of 2.5 to 4.0 kilometers; we used 10 to 15 microsecond pulses and spectra resolutions of 0.01hz. Radar pulses were transmitted from the main (1000 foot) antenna. Both polarized and depolarized echoes were simultaneously recorded using new 430Mhz radar equipment at an auxiliary (Los Caños, 100 foot) antenna. These data are currently being processed to produce digital images similar to those already existing at 70cm and 3.8cm wavelength. The new 70cm radar maps of the moon will have resolutions which are three times better than the existing 70cm data and which are near that of the existing 3.8cm Haystack Observatory radar maps. This will permit detailed study of lunar craters with diameters 7.5 kilometers and greater.

FRIDAY MORNING, 15 Jan., 0900-1200

NEAR FIELD MEASUREMENTS II
Commission A, Session 5, CR1-42
Chairman: Carl F. Stubenrauch,
Electromagnetic Fields Division
National Bureau of Standards, Boulder, CO 80303

A5-1
0830 COMBINING PLANAR AND CYLINDRICAL NEAR-FIELD MEASUREMENTS TO OBTAIN INCREASED ANTENNA PATTERN COVERAGE:
A.C. Newell, Electromagnetic Fields Division, National Bureau of Standards, Boulder, CO 80303

It has long been realized that for electrically large antennas, measurements on a planar surface normal to the boresight direction are the most efficient of the near-field techniques. One of the main limitations of the planar technique however, is that for measurements on one plane, the results are valid only for a cone of angles somewhat less than a full hemisphere as determined from the measurement geometry. If results are required for the back hemisphere, another measurement must be made on a plane behind the antenna and, in general, there will always be a region of angles close to grazing incidence to the measurement planes where reliable results are not available.

To overcome this limitation, it has been suggested that a combination of planar and cylindrical measurements be employed to extend the coverage to almost the full sphere. The planar technique would be used to obtain results for the main beam and first few sidelobes and the cylindrical technique used to obtain the additional sidelobes and into the backlobe region. Using this approach, pattern, gain, and polarization results would be available in all directions except near the axis of the cylinder on the back hemisphere.

To test this idea, a research program was undertaken to determine the feasibility of such a measurement approach. The study was devoted to the cylindrical measurement part, since the planar portion is already well developed and, in this application, is being used in the conventional way. The cylindrical measurements outlined above, however, are different than those usually employed since they are being used to determine the sidelobe and backlobe patterns only, with the boresight direction of the antenna parallel rather than normal to the axis of the measurement cylinder. The results of this research has shown that this cylindrical sidelobe measurement, as it has been called, can be quite successful. Results have shown that by using somewhat directive probes, and/or artifical extention of the measured data, the error producing effects of main-beam components of the spectrum are minimal. General relations are also obtained from the geometry of the measurement to predict the angular region of validity for these measurements and therefore ensure overlap of planar and cylindrical results.

A5-2
0855 AN ALGORITHM WITH ENHANCED EFFICIENCY FOR COMPUTING THE FAR-FIELD FROM NEAR-FIELD DATA ON A PARTIAL SPHERICAL SURFACE: Doren W. Hess and Joseph J. Tavormina, Scientific-Atlanta, Inc., 3845 Pleasantdale Road, Atlanta, GA 30340

Both the Wacker algorithm for the spherical near-field to far-field transform in its original form and the improved version devised by Larsen are conventionally applied to near-field data sets corresponding to complete spherical pattern coverage; if only partial coverage is of interest then zero-filling is typically used over those portions of the sphere where the near-field pattern levels are negligible. This paper describes an enhancement of the Wacker and Larsen algorithms which requires that only the significant portion of the near-field data set be processed.

The enhanced algorithm operates upon the simplifying assumption that the antenna's radiation pattern may be assumed to be periodic in the spherical coordinates. Periodicity in the azimuthal coordinate is especially important because it restricts the number of permissible spherical modes considered to comprise the pattern, and significantly reduces the number of scattering matrix elements that must be calculated. Efficiency in the running time is realized when the main beam of a radiation pattern lies on the equator of the spherical grid.

This enhanced partial sphere algorithm has been implemented on a minicomputer and its numerical results checked on measured data against numerical results for full spherical coverage. Reduction factors in running time of three to ten are easily obtained, depending on the measurement radius and the coverage area of the partial sphere.

A5-3
0920 PRACTICAL CONSIDERATIONS FOR NEAR-FIELD MEASUREMENTS AND THE USE OF PROBE CORRECTION:

Doren W. Hess, Scientific-Atlanta, Inc., 3845 Pleasantdale Road, Atlanta, GA 30340

A simplified case of spherical near-field scanning measurements occurs when the geometry of the near-field range configuration is arranged so that numerical correction for the finite dimension of the probe antenna can be avoided. This is accomplished by meeting the criterion that

$$R >> \frac{dD}{\lambda}$$

where R is the length of the range, λ is the wavelength of the radiation and D and d are the dimensions of the test antenna and the range antenna respectively. The criterion follows by requiring that the angle intercepted by the range antenna at the center of the scanning sphere be appreciably less than the sample increment at which near-field data is recorded. Avoiding the need to measure the directivity pattern of the probe antenna affords the important practical advantage of simplicity in the measurement procedure.

However a second consideration which is very important in range design -- that of signal power -- makes it difficult to meet the above criterion when the size of the test antenna becomes large. To appreciate the difficulty consider a near field range configuration that marginally meets the above criterion and which operates at the power capacity of its signal generator; then let the dimension of the test antenna increase, with the frequency held fixed. In order to maintain the same fraction of signal power transferred between the ports of the test antenna and the range antenna the dimension of the range antenna would have to be made larger. On the other hand, for a fixed range length, increasing the site of the test antenna reduces the angular sample increment; and, in order to avoid probe correction the dimension of the range antenna would have to be reduced. Clearly the desire to avoid probe correction and the desire to conserve signal power can come into conflict.

One is led then to the interesting conclusion that as the dimensions of antennas to be tested increase, probe corrected measurement procedures will be required unless either (a) larger range lengths are used, (b) longer measurement times are available, (c) more sensitive receivers are available or (d) more powerful signal sources are available.

A5-4
1005

HIGH PRECISION 6.7m x 6.7m NEAR-FIELD PLANAR SCANNER

C. A. Raquet, G.R. Sharp, and R. E. Alexovich
Space Communications Division
National Aeronautics and Space Administration
Lewis Research Center
Cleveland, OH 44135

A 6.7m x 6.7m near-field planar scanner is being constructed at the NASA Lewis Research Center. This facility, scheduled to be completed in early 1982, will be used to test and evaluate advanced space communication antenna concepts in support of the Center's space communication program. The near-field measurement technique offers several important advantages for testing present and future large, high frequency, complex space communication antennas for which the conventional minimum far-field probe-antenna separation distance $2D^2/\lambda$ (D=aperture diameter, λ = wavelength) exceeds several kilometers. The Lewis facility has been designed to measure high gain antennas with aperture diameters as large as 6.2m at frequencies from 0.8 to 60 GHz.

The scanner is configured to acquire near-field data on a vertical rectilinear planar grid. The two axes of scan are provided by the motion of the probe along a vertical gantry truss and the horizontal motion of the gantry and support structure along precision rails. Probe location along both axes in the vertical plane is determined with a laser interferometer system. The horizontal and vertical chain drive systems, for the gantry and probe respectively, use d. c. motors with precision tachometers and sychronous belt reduction drives and are operated by a computer controlled position programmer. Automatic data acquisition is under control of a computer in the test facility. Both the scanner and the wall surrounding the scanning plane on three sides will be covered with 46 cm (18 inch) thick microwave absorbing material.

In order to achieve the scanning plane flatness required for high frequency near-field measurements, an extremely rigid mechanical design providing high structural stability and the capability for easy and accurate adjustment has been developed. System alignment is performed using laser straightness measuring devices, a precise optical level and jig transits. Achievement of the surface flatness design goal of 0.01 cm will permit accurate measurements at 60 GHz. without corrections. First order corrections for deviations from a true plane will, in the future, permit extending the frequency capability beyond 60 GHz.

A5-5
1030 PLANE-POLAR NEAR-FIELD MEASUREMENTS FOR FAR-FIELD CONSTRUCTION: Y. Rahmat-Samii, Jet Propulsion Laboratory, California Institute of Technology, Pasadena, CA 91103

Far-field construction from near-field measurements has been shown to be a potentially powerful scheme, and the amount of work to justify this observation is voluminous. In constructing far-field patterns from near-field measurements, three basic geometrical surfaces surrounding the test antenna have been probed: 1) planar, 2) cylindrical, and 3) spherical. This presentation will focus on the planar scheme. In the past the planar configuration has been used with a probe scanning a rectangular geometry and computations have been done using FFT algorithms. Recently an alternate useful scan geometry based on the plane-polar configuration has been investigated (Rahmat-Samii, et. al, IEEE AP-S, March, 1980) and results have been presented to demonstrate its applications.

In this presentation, a short review of the plane-polar measurement technique will be made in order to demonstrate the application of the computational steps for constructing both the far and Fresnel fields using the Jacobi-Bessel series expansion. Results will be shown for both the far and Fresnel fields and the need for probe correction will be discussed. The usefulness of a method for measuring the absolute gain will also be addressed. Finally, some of the electrical and mechanical features of a newly constructed plane-polar near-field facility at JPL will be presented.

A5-6
1055

REVIEW OF GEORGIA TECH NEAR-FIELD SCATTERING MEASUREMENTS

Charles E. Ryan, Jr.,
Engineering Experiment Station
Georgia Institute of Technology
Atlanta, Georgia 30360

The Georgia Tech EES automated planar near-field scanner has been employed for scattering measurements since 1973. These measurements have included bi-static (J. L. Edwards, C. E. Ryan, Jr., and W. J. Storey, 1974 IEEE Ant. & Prop. Symposium Digest, 174-177) and forward scattering (C. E. Ryan, Jr. and E. E. Weaver, 1979 IEEE Ant. & Prop. Symposium Digest, 59-62) and measurements of the effects of model aircraft external stores on antenna performance (T. B. Wells, 1981 IEEE Ant. & Prop. Symposium Digest, 257-260). This paper will present a review of near-field scattering measurement techniques including measured results for model targets. Also, data processing methods to enhance the field-of-view of planar measurements of non-aperture limited fields will be suggested.

GUIDED WAVES
Friday morning, 15 Jan., CR2-28
Chairman: David A. Hill, NTIA/ITS, Boulder, CO 80303

B7-1
0830 **INTEGRAL-OPERATOR DESCRIPTION OF INTEGRATED DIELECTRIC WAVEGUIDES:** D. P. Nyquist, Dept. of Electrical Engineering and B. C. Drachman, Dept. of Mathematics, Michigan State Univ., East Lansing, MI 48824

A new integral-operator formulation is presented which provides an exact description for surface-wave eigenmodes supported by graded-index, integrated dielectric waveguides of arbitrary cross-section shape. As indicated in the figure, the waveguide core with cross section CS and graded refractive index $n(\vec{\rho})$ is deposited over a substrate of index n_s and embedded in a cladding overlay of index n_c.

If core/overlay contrast is described by $\delta n^2(\vec{\rho}) = n^2(\vec{\rho}) - n_c^2$, then surface-wave eigenfield $\vec{E}(\vec{r}) = \vec{e}(\vec{\rho}) \times \exp(-j\beta z)$ is found to satisfy the 2-d electric-field, polarization integral equation (EFIE)

$$\vec{e}(\vec{\rho}) - \left(k_c^2 + \nabla\nabla\cdot\right)\int_{CS} \frac{\delta n^2(\vec{\rho}\,')}{n_c^2} \overleftrightarrow{g}(\vec{\rho}\,|\,\vec{\rho}\,')\cdot\vec{e}(\vec{\rho}\,')\,dS' = 0$$

$$\ldots \text{ all } \vec{\rho} \in CS$$

where $k_c = n_c k_0$ and $\overleftrightarrow{g} = \overleftrightarrow{g}^p + \overleftrightarrow{g}^r$ is a 2-d Green's dyadic comprised of principal and reflected wave components (in integral representation) which depend upon unknown eigenvalue β. When applied to planar, asymmetric-slab waveguides, the above EFIE reduces to a pair of independent, 1-d, scalar IE's for resulting TE and TM modes; closed form solutions provide the well-known eigenvalue equations for step-index slabs.

Quasi-closed-form, exact solutions are obtained for the step-index, integrated rectangular dielectric waveguide. Unknown field $\vec{e}$ in its core is expressed exactly in terms of 4 integration constants and 2 eigenvalue parameters. Satisfaction of the x and z-component IE's leads to a pair of determinantal eigenvalue equations $D_x(\kappa_x,\kappa_y)=0$ and $D_z(\kappa_x,\kappa_y)=0$. These equations are solved numerically for κ_x and κ_y by a 2-d generalization of Newton's method, resulting in an exact quantification of the surface-wave mode. Extensive numerical results are obtained.

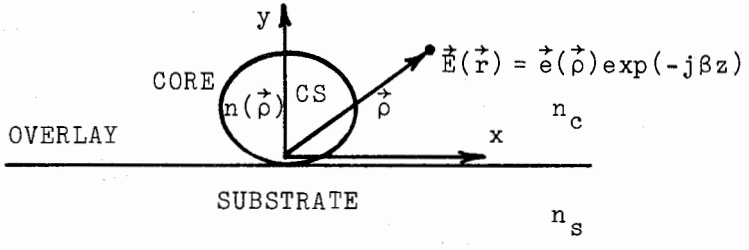

B7-2
0855

EVANESCENT WAVES AND COMPLEX RAYS FOR CURVED DIELECTRIC WAVEGUIDES

E.Heyman and L.B.Felsen, Department of Electrical Engineering and Computer Science,
Polytechnic Institute of New York,
Farmingdale, New York 11735

Evanescent wave theory has been shown to provide an effective tool for high-frequency asymptotic analysis of non-leaky guided waves in straight graded index slabs and fibers [J.M.Arnold and L.B.Felsen, J.Acoust.Soc.Am.67 (1980), 757-763]. It is therefore suggestive to seek extension of the theory to curved waveguides wherein radiation occurs. This problem has been studied on the prototypes of two-dimensional cylindrically curved surface impedance and dielectric layer configurations. Assuming weakly radiating modes, an attempt has been made to express the phase paths and phase fronts for the leaky case as perturbations of those for the non-leady case. This was unsuccessful because of the failure of the perturbation in the transition region between the essentially evanescent and essentially propagating fields near and far from the convex side of the waveguide, respectively. The difficulty may be overcome with the use of complex rays, which result upon extension of generating caustics and reflecting surfaces into a complex coordinate space. Complex rays are shown to accommodate smoothly the above-noted transition in real coordinate space, where an evanescent wave interpretation now provides the previously lacking connection between the non-leaky and leaky regimes. By invoking self-consistency between outgoing and incoming complex ray congruences, one may derive a resonance condition for the modal fields. Numerical examples for varying degrees of leakage furnish insight into the modal complex ray and evanescent wave behavior. Some difficulties are noted when one attempts to generalize these results for the canonical circular waveguide contour to configurations deviating weakly from the circular case.

B7-3
0920 RESOLVENT GREEN'S FUNCTION FOR A TAPERED DIELECTRIC WAVEGUIDE:

A.Kamel and L.B.Felsen, Department of Electrical Engineering and Computer Science,
Polytechnic Institute of New York,
Farmingdale, New York 11735

By the method of resolvents or characteristic Green's functions, one may construct general contour integral representations of Green's functions for separable geometries. From these general integral representations, one may derive a variety of alternative field representations, including those involving normal (discrete and continuous) modes, leaky modes, conventional and generalized rays, hybrid ray-mode combinations, etc. The method cannot be applied rigorously to non-separable problems such as a wedge-shaped dielectric. However, for small wedge angles, we have managed to construct an approximate characteristic Green's function integral based on the requirement that the resulting normal mode representation arising from residues at the resonance poles yields the properly normalized and symmetrized trapped local modes far from their cutoff points. For propagation toward the narrow portion, as a mode approaches cutoff, its resonance pole approaches a branch point and therefore couples strongly to its radiation field. In this transition region, the Green's function may be reduced asymptotically to a canonical integral which is discussed in detail. Beyong the transition region, the previously trapped mode pole becomes a leaky mode pole. The resulting formulation is compared with recent results obtained by other techniques. It is also shown how ray, ray-mode, and other relevant field representations can be obtained from the original integral.

B7-4
0945

LOCAL MODES IN A TAPERED DIELECTRIC WAVEGUIDE

J.M. Arnold, Department of Electrical and Electronic Engineering, University of Nottingham, England, and L.B.Felsen, Department of Electrical Engineering and Computer Science, Polytechnic Institute of New York, Route 110, Farmingdale, New York, 11735

An asymptotic procedure of inherent general validity for weakly tapered dielectric waveguides is presented, whereby an initial ray-optical field undergoing multiple reflection is converted into uncoupled local mode fields by Poisson summation. Independent numerical calculations performed elsewhere have shown that neglecting intermode coupling is justified for this class of guiding regions. Before the ray-to-mode conversion, a plane wave spectrum is fitted to the ray family, and the resulting Poisson-transformed spectral integrals, after asymptotic evaluation by the stationary phase method, are found to produce trapped modes in regions far from their cutoff points. As mode cutoff is approached in the narrowing portion of the waveguide, the simple stationary phase procedure must be modified, and the transformed spectral integrals become "canonical integrals" that trace the transition of each mode uniformly from the trapped to the radiating (leaky) regime. For small-angle linear tapers, results are shown for the transition function and its connection to the trapped and leaky mode fields below and above the cutoff region.

B7-5
1030 THEORY, DESIGN AND MEASUREMENT OF A 3 dB DIELECTRIC DIRECTIONAL COUPLER:

L. Lewin and M. Abouzahra, Electromagnetics Laboratory, Dept. of Electrical Engineering, University of Colorado, Boulder, CO 80309

Transmission line equations are used to derive expressions for the coupling of degenerate modes on two curved rectangular dielectric waveguides sandwiched between two parallel conducting plates. The coupling region avoids using a linear section in order to achieve a good bandwidth. This comes about through the achievement of a tight coupling region at the closest approach of the curved sections. Expressions for the directivity and reflection are derived and found to be very small. In order to test the accuracy of the theoretical results a 3 dB dielectric directional coupler was designed. The accuracy of the 3 dB design is confirmed by the experiments though there is substantial insertion loss in the experimental model at 95 GHz due to dielectric losses. Comparison between theoretical and experimental results is presented.

B7-6
1055

A TM MODAL SHUT-OFF PHENOMENON IN A LOSSY SLAB; S.K. Chang, Schlumberger-Doll Research, P.O. Box 307, Ridgefield, CT 06877

The TM modal characteristics of a lossy material slab surrounded by a lossy environment were studied. The pole trajectories of the TM modes for various frequencies were traced on the complex wavenumber plane. Only the condition when the slab was electrically denser than the environment was considered. Under such a condition the TM_o mode always exists at very low frequencies. In most cases the TM_o pole would move from near the wavenumber of the surrounding medium to near that of the slab when the frequency was increased. Such a trajectory was distinct from those of the higher order modes, which always have apparent cut-off at low frequencies.

A parametric study varying the material constants had revealed an unusual phenomenon for the TM modes. When the material contrast was quite high and the attenuation of the surrounding medium was small (for example: $\varepsilon_{slab} = 75-j29.4$ and $\varepsilon_{environment} = 3.71$) the TM_o mode would depart from the branch point and disappear into the lower Riemann sheet of the Sommerfeld branch cut as the freqnency was increased. In the meantime the TM_1 mode would move down to near the wavenumber of the slab medium and would resemble the characteristic of the TM_o mode at high frequencies. The mode numbering notations should deserve further discussions since the lowest order modes at low and high frequencies could be apparently different on this situation.

B7-7
1120

NARROW SLOT COUPLED WAVEGUIDING SYSTEMS:

Perry F. Wilson and David C. Chang,
Electromagnetics Laboratory, Department of Electrical Engineering, University of Colorado, Boulder, CO 80309

The slot coupling between two waveguiding systems has various applications. Examples include the usage of one guide to launch modes in the other, and remote sensing schemes. The specific coupling configuration to be considered here is that of a narrow slot, running longitudinally in the direction of propagation, which connects the guides. The propagation constant associated with each system mode is an important quantity, either as a design consideration to insure maximum coupling, or, when measured, as part of remote sensing inversion algorithm. The analytical determination of system mode propagation constants will be one of the primary topics addressed.

The above problems may be approached by first considering the manner in which two parallel plate waveguides, coupled as above, are excited by TEM modes obliquely incident upon the slot. This canonical problem may be solved by formulating an integral equation for the unknown fields in the gap. The kernel, which is singular, may be simplified by assuming that the gap width 2g is electrically small, that is $(k_0 g) << 1$. This results in a simpled closed form solution. The dominant behavior of the gap fields is of the order $(g^2 - x^2)^{-\frac{1}{2}}$, where $x \in [-g,g]$, and may be attributed to an equivalent magnetic quadrupole located in the gap. The contributions from equivalent electric, and magnetic dipole sources are of the order $k_0 g(g^2 - x^2)^{-\frac{1}{2}}$ and therefore may be neglected, except for certain special symmetries. The solution to this problem may be used to formulate a scattering matrix which represents the slot effect in the plane transverse to the slot. The scattering matrix will not be unitary due to partial power flow in the longitudinal direction. The amount of this longitudinal power will be determined by the angle of incident TEM modes. More complicated structures may be modeled by introducing appropriate reflection matrices. For specific system modes, conditions on resonance will lead to a modal equation which must be satisfied by the propagation constant. Various examples will be discussed.

SIGNAL DESIGN AND SENSING
Friday morning, 15 Jan., CRO-30
Organizer: Martin Nesenbergs,
U.S. Department of Commerce, NTIA/ITS,
Boulder, CO 80303
Chairman: Robert F. Linfield,
U.S. Department of Commerce, NTIA/ITS,
Boulder, CO 80303

C5-1
0830

SIGNAL GENERATION USING MARKOV CHAINS:

A. Steinhardt and R.A. Roberts,
Department of Electrical Engineering
University of Colorado
Boulder, CO 80309

The generation of colored noise is typically achieved by exciting a linear system with white noise. An appealing alternative scheme is to employ Circulant Markov Chain Random Processes (CMCRP). CMCRP have been studied as a means of generating colored noise by several authors. The appeal of this approach is that the implementaion is fast and simple. This is because a CMCRP basically consists of a random number generator that accesses a RAM. The utility of this approach has been limited by the fact that only a restricted class of spectra could be matched. In this paper a procedure is presented which will design a CMCRP having any specified rational power spectra. This new result is achieved by having the output map depend on the previous as well as the present state that the chain is in. This results in a modest increase in the system memory. The lack of multiplies and adds in these structures permits them to operate very fast at reasonable expense. Potential applications include spread spectrum modulation, as well as new models for spectral estimation. Existence and uniqueness issues of the design procedure are discussed and examples are given based on direct simulation.

C5-2 RAPID SCAN RADAR--A PRELIMINARY DESIGN
0900

R.J. Keeler and C.L. Frush
National Center for Atmospheric Research
Field Observing Facility
P.O. Box 3000
Boulder, CO 80307

Multiple Doppler radar systems used in present meteorological studies are severely limited by the excessive time required to scan a storm volume. When a large storm is directly overhead, nearly a full hemispheric scan is required and present systems require many minutes to measure reflectivity and Doppler velocity for this important case. Multiple Doppler analysts have found that advection and temporal evolution of the storm during the volume scan require data filtering that obscures the smaller scales of storm motion which are necessary in understanding the kinematics of the storm. Thus, the storm "snapshot" is smeared and contaminated by bias errors.

A rapid scan radar, which accurately measures reflectivity and velocity from only a few pulses, has the capability of scanning a hemispheric volume in tens of seconds and gives a measurement which more accurately characterizes the instantaneous properties of the storm. Krehbiel and Brook (1979, IEEE Trans. on Geoscience Electronics, GE-17: 196-204) have utilized a 30 MHz bandwidth random signal radar that can accurately estimate storm reflectivity in a single pulse and can scan a full hemisphere in about 20 seconds. The large bandwidth pulse combined with a radiometer-type detector simultaneously gives several independent estimates of reflectivity which obviates the long dwell time requirement. However, the random signal radars that are described in the literature require an unacceptably long time to estimate the velocity.

We intend to develop a Doppler rapid scan radar by using a suitable combination of frequency, time, scattering angle and space diversity techniques which will allow a dwell time of only a few pulses. Rayleigh fluctuations must be averaged over to obtain accurate mean reflectivity estimates and random noise components must be averaged over to obtain accurate Doppler velocity estimates. We will propose a preliminary rapid scan Doppler radar design that will measure reflectivity and velocity over a full hemispheric scan in approximately 20 seconds and present a schedule that will allow NCAR to field a triple Doppler rapid scan system by the mid-1980's. By combining large time-bandwidth pulses, real-time Doppler processing and efficient electronic antenna scans, we will measure scales of thunderstorm air motion that heretofore have not been observed.

C5-3
0930

MICROWAVE HOLOGRAPHY AND THE RADIO CAMERA

Bernard D. Steinberg
Valley Forge Research Center
The Moore School of Electrical Engineering
University of Pennsylvania
Philadelphia, Pennsylvania. 19104

The microwave holographer has certain tools available to him that generally are denied the optical holographer. Three such advantages are: (1) reference field may be eliminated and replaced by a correctly phased local oscillator within the microwave receiver; (2) reference field need not coexist in time with the object field; (3) object field need not be measured simultaneously across the array, e.g., synthetic aperture radar. These differences are due to differences in components (#1), the pulsed nature of radar wave forms (#2), and phase coherent local oscillators and coherent signal processors (#3).

A major advantage of optical holography is the small optical wavelength, which permits exceedingly fine resolution imaging with small optical apertures. To achieve equally fine resolution with microwaves requires apertures so large that they would be mechanically unstable. A fourth tool available to the microwave holographer, however, can compensate for this disadvantage. By introducing self-cohering or adaptive beamforming techniques, it is possible to design large-aperture microwave imaging systems in which (4) the coordinates of the antenna elements need not be known accurately. Such an instrument is called a radio camera.

The paper first discusses the relation of microwave to optical holography, and then reports on a two-dimensional microwave radio camera imaging experiment with a 40-meter random, distorted and time-varying aperture operated at 3 cm wavelength which incorporated features (2), (3), and (4).

C5-4
1030

VHF RADAR OBSERVATIONS OF THE ANGULAR PROPERTIES OF SCATTERING FROM TURBULENT AND STABLE ATMOSPHERIC LAYERS

J.L. Green, J.M. Warnock, W.L. Clark, and K.J. Ruth, Aeronomy Laboratory, National Oceanic and Atmospheric Admin., Boulder, CO 80303

The Sunset Radar, located near Boulder, Colorado, has been recently modified so that its antenna beam can be steered ± 45° in either the north-south or east-west vertical plane. This new capability has been used to investigate the angular properties of scattering and reflection from the troposphere and lower stratosphere at a wavelength of 7.4 m.

It has been found that during an observation period the scattering from most altitudes is not strongly sensitive to the observing angle when the data is averaged for an hour. Individual angular scans, which can also be interpreted as horizontal spatial sweeps, show instantaneous changes in intensity with angle or position. The behavior of these echoes is in agreement with current theories of scattering from turbulence.

On the other hand, the echoes from stable layers of the atmosphere have a sharp peak in intensity near the zenith with a half power width of only a few degrees. The angular characteristics of this latter class of echoes is consistent with the theories of Fresnel scattering.

C5-5
1100 AN OPTICAL PATH-AVERAGED RAIN GAUGE BASED ON NEAR FIELD MEASUREMENT: C.H. Chen and D.J. Fang, COMSAT Labs., Clarksburg, MC 20871

In modern satellite communications systems utilizing automatic power control and/or polarization compensation networks, a knowledge of instantaneous area rainfall information is essential. The conventional tipping bucket rain gauge, which has a slow response and a low saturation level is not adequate. The present paper examines laser sensing techniques for developing a high precision/fast resolution rain gauge. It is intended to show contrary to earlier theoretical studies that such an optical system samples precipitation accurately only in the far field region, the system can be used for near field applications as well, provided that a proper calibration procedure is established.*

*In the course of this work, the authors are indebted to Dr. Ting I. Wang of NOAA.

EARTH-SATELLITE COMMUNICATIONS
Friday morning, 15 Jan., CR2-26
Chairman: Donald Cox, Bell Laboratories,
Crawford Hill Laboratory, Holmdel, NY 07733

F6-1
0900

19 GHz SPACE-EARTH DEPOLARIZATION MEASUREMENTS AT 4° POLARIZATION

H. W. Arnold, D. C. Cox, M. F. Wazowicz and
H. H. Hoffman, Bell Laboratories, Crawford
Hill Laboratory, Holmdel, New Jersey 07733

Polarization transformation of rain and ice depolarization measured on an earth-space propagation path at Crawford Hill, New Jersey indicated very low depolarization values most of the time for linear polarizations near vertical and horizontal. The importance of the low-depolarization results in the design of satellite communication systems made their confirmation desireable.

This paper compares depolarization transformed to a polarization angle of 4° from vertical with depolarization measured at 4° along another path and scaled to the path elevation angle of the transformed measurements. Over the ranges of attenuation and depolarization for which both measurements are meaningful, the agreement between them is good. The results further reinforce our high confidence in the important results and conclusions obtained earlier using the polarization transformation technique.

F6-2
0925

PRELIMINARY RESULTS FROM THE FIRST YEARS WORK WITH AN 11.6 GHz DUAL POLARIZED SITE DIVERSITY EXPERIMENT EMPLOYING THE SIRIO SATELLITE: R.E. Marshall, E.A. Manus, G.C. Towner, and R.L. Lyall, Department of Electrical Engineering, Virginia Polytechnic Institute and State University, Blacksburg, VA 24061

The degradation of earth-space radio links above 10 GHz by hydrometers is significant enough to warrant the use of site diversity introduced as an answer to excess attenuation by D. C. Hogg. (SCIENCE, January 1968, Vol. 59, No. 3810, pp. 39-46) Site diversity for dual polarized paths is a relatively unexplored topic.

This paper describes an 11.6 GHz dual polarized site diversity experiment with a 7.3 km baseline and an 11 degree elevation angle. A tipping bucket rain gauge is located at each antenna, and an S band range gated meteorological radar observes the main site earth-space path during propagation events.

Data will be presented which include single site and joint rainrate, attenuation, and isolation statistics for the period July 1980 through June 1981. Attenuation diversity gain, isolation diversity gain, and faderate statistics for the same period will also be presented. Three dimensional plots of dBz vs range vs time and simultaneous attenuation and isolation plots of selected events will be presented.

F6-3
1010

AN EARTH/SPACE RAIN ATTENUATION DISTRIBUTION PREDICTION MODEL FOR THE '80's: E.J. Dutton, U.S. Department of Commerce, National Telecommunications and Information Administration, Institute for Telecommunication Sciences, Boulder, CO 80303

An attenuation distribution prediction model for earth/space telecommunications links has been developed over the decade of the 1970's at the Institute for Telecommunication Sciences (ITS), of the National Telecommunications and Information Administration (NTIA). This model, generically titled the "Dutton-Dougherty (DD) model", was primarily intended for microwave (3 to 30 GHz) satellite/earth-station application. In the 1980's, certain refinements of this model have become necessary to tailor the model for prospective future users.

Some of this refinement has been recently accomplished, with specific orientation toward the NASA Communications and Information Systems Program. These refinements include an extension of the range of the distribution predictions from 0.01% (99.99% system availability) to 0.001% (99.999% system availability). This refinement, however, revised the distribution prediction above 0.01%, as well as below. Another new feature in the DD model is a wider choice of raindrop size distributions and models of specific attenuation due to rain from which to select and compare distribution predictions at a given location and carrier frequency.

The development of cost-effective hardware and lack of spectrum crowding make the millimeter-wave (30 to 300 GHz) region of the radio spectrum extremely attractive for telecommunication-market expansion augmented for expansion into the 30 to 300 GHz region. This, of course, presents additional atmospheric problems to be analyzed. Among these are different gaseous absorption behavior, increased attenuation by cloud cover, tail considerations for small dropsizes of rainfall drop size distributions, and enhanced rainfall attenuation at these higher frequencies.

F6-4
1045 DETERMINATION OF EARTH-SATELLITE SPACE DIVERSITY PERFORMANCE CRITERIA USING RADAR TECHNIQUES, Julius Goldhirsh, Applied Physics Laboratory, Johns Hopkins Road, Laurel, Maryland 20707

Employing a radar data base of the rain reflectivity environment recorded on magnetic tape at Wallops Island, Virginia, a modeling program was pursued enabling space diversity criteria to be established for earth-space path configurations. A large number of paths through rain are modeled and the path attenuations and ground rain rates are determined using measurements of the radar derived rain reflectivity factor profiles $Z(mm^6/m^3)$ along the paths.

The technique uses an ergodic type of hypothesis, where pairs of modeled paths separated a distance, d, are sampled for attenuation and ground rain rate; as opposed to sampling in time. Specifically, an expression is derived given by,

$$P_d\{A_1, A_2 > A_q\} = \frac{N_d\{A_1, A_2 > A_q\}}{N\{R_1 > R_p\}} P\{R_1 > R_p\}$$

where $P_d\{A_1, A_2 > A_q\}$ is the desired absolute joint probability that the attenuation along two paths separated a given distance, d, have attenuations which jointly exceed, A_q. On the right hand side, $N_d\{A_1, A_2 > A_q\}$ represent the number of pairs of paths with separations, d, that jointly have attenuations greater than A_q, and $N\{R > R_p\}$ represents the number of paths sampled which have rain rates greater than the level R_p (mm/hr). The factor $P\{R_1 > R_p\}$ is the probability that the rain rate at the base of single path exceeds R_p. This latter term represents the absolute rain rate distribution and is arrived at from long time raingage data at Wallops Island, Virginia. The N values in the numerator and demoninator of the above fraction are arrived at through sampling of the paths from which the attenuations and base rain rates have been derived using radar methods.

Employing a data base consisting of 81 radar vertical scans (RHIs) corresponding to 16 rain days and the sampling of 15000 paths, joint fade distributions for a family of path separations are presented for the COMSTAR frequencies, f=28.56 and 19.04 GHz. Using these results, the corresponding "diversity gains" and "diversity advantages" are characterized.

F6-5
1110

SIMULTANEOUS 19/29-GHz SIGNAL ATTENUATION MEASUREMENTS FROM COMSTAR SATELLITES

Prabha N. Kumar, COMSAT Laboratories
Clarksburg, Maryland 20871

Measurements of precipitation attenuation for 19/29-GHz signals from COMSTAR D-1 (128°W long.), D-2 (95°W long.), and D-3 (87°W long.) satellites along the earth-space paths, were carried out at COMSAT Laboratories during a four-year period from 1976 through 1980. Auxiliary measurements included 12-GHz radiometric sky-noise temperature and tipping bucket precipitation. In this paper, simultaneous fades at 19 and 29 GHz are assessed for the four-year measurement period together with the auxiliary data. Results include the variations of measured fade ratios of 29- and 19-GHz fades with 19-GHz fades, and comparison with the available theoretical models based on the frequency scaling of attenuation. Year-to-year variation and elevation angle dependence are also provided, which give a useful indication of the margin of errors should one have only one-year data for a specific elevation angle for establishing the so-called long-term statistics.

F6-6
1135

A TERRESTRIAL POLARIZATION ADAPTION EXPERIMENT AT 11.7 GHz

W. J. Vogel, Electrical Engineering Research Lab
The University of Texas
10100 Burnet Rd., Austin, TX 78758

Depolarization caused by rain at 11.7 GHz is due to both differential phase shift and attenuation. In dual polarized communication systems it gives rise to crosstalk which may be severe enough to cause an outage even though the fade margin has not been exceeded. Since differential attenuation causes loss of orthogonality, any compensation method will have to achieve rejection of the unwanted signal by also rejecting some of the wanted signal.

This paper describes results obtained in an experiment over a 10 km path with circular polarization at 11.7 GHz. Three receivers are used on two antennas mounted side by side. Two receivers have fixed polarization and measure co-pol attenuation and cross-polarization of the transmitted wave. The third receiver, under control of a computer, can be adjusted to match any two orthogonal polarizations; one output is terminated, however. Moving in the polarization plane requires two variables. In this experiment in order to cause no system noise degradation, they are implemented with the use of a turnstile junction feed system, where one adjustment is the position of waveguide shorts in the junction and the other adjustment consists of rotating the whole receiver about the antenna axis.

A step tracking algorithm, using only the amplitude of the signal, continually attempts to keep this signal 35 dB below the level of the copolarized signal. The data presented demonstrate the stable performance of this scheme during several rain events. At fades below about 15 dB significant isolation improvements are achieved, compared to the fixed cross-polarization channel.

Commission G Session 3
Commission H Session 2

IONOSPHERIC MODIFICATION
Friday morning, 15 Jan., CR1-46
Chairman: W.E. Gordon, Rice University,
Houston, TX 77001

G3/H2-1
0900 THE RISE AND FALL TIMES OF HF-INDUCED FIELD-ALIGNED STRIATIONS: A.J. Coster and W.E. Gordon, Department of Space Physics, Rice University, Houston, TX 77001; F.T. Djuth, The Aerospace Corporation, P.O. Box 92957, Los Angeles, CA 90009; and J. Jost, N.A.S.A., Lyndon Johnson Space Center, Houston, TX 77058

In June, July, and September of 1981, heating experiments were performed to study 3 meter artifically induced field aligned striations in the E and F regions of the ionosphere. These experiments combined the use of the new and more powerful heating facility at the Arecibo Observatory with a portable 50 Mhz field radar. The 50 Mhz radar, situated either on the island of Guadeloupe or St. Croix, had a line of sight that was perpendicular to the magnetic field lines in the heated region and was used to detect the 3 meter irregularities. In addition, background ionospheric conditions were monitored with the 430 Mhz radar at Arecibo. For the first time during the Arecibo campaigns, the rise and fall times of the 3 meter striations were measured to millisecond accuracy. These rise time measurements were also coordinated with the simultaneous rise time measurements of the enhanced plasma line at Arecibo. A summary of our preliminary results will be presented.

G3/H2-2 0925 MULTITECHNIQUE PROBING OF THE ARTIFICIALLY MODIFIED IONOSPHERE OVER ARECIBO:

Santimay Basu and Sunanda Basu, Emmanuel College, Boston, MA 02115; E.J. Weber, J.G. Moore and J. Buchau, AFGL, Hanscom AFB, MA 01731; S. Ganguly and W.E. Gordon, Department of Space Physics, Rice University, Houston, TX 77001; M.C. Lee, Regis College Research Center, Weston, MA 02193; R.C. Livingston, SRI International, Menlo Park, CA 94025; B.W. Reinisch, University of Lowell, Center for Atmospheric Research, Lowell, MA 01854; R.A. Behnke, National Astronomy and Ionosphere Center, Arecibo, Puerto Rico 00613

A variety of experiments have been planned to probe the F-region ionosphere over Arecibo when it is modified by the new high-power high-frequency heating facility during September, 1981. The equipment to be used include an all-sky imaging photometer to determine airglow emissions at 5577 Å and 6300 Å, a vertical spectrometer, digital ionosonde and phase and amplitude scintillation receivers at 250 MHz on board the AFGL Airborne Ionospheric Observatory. The moving platform will help in defining the artificially modified volume both in horizontal and vertical extents. The airborne observations will be supported by a variety of ground-based measurements using the 1000-ft dish which may include radio-star scintillation observations, measurements of ionospheric density Ne and temperatures Te, Ti and ion drifts to help in analyzing the airglow and scintillation measurements, as well as, the HF induced plasma line enhancements. A 50 MHz portable radar will be operated from Guadaloupe to probe the heated volume over Arecibo at 250 km altitude to determine the generation and decay of 3-m scale-length irregularities in conjunction with the larger scales ($\sim$ km to a few hundred m) probed by the scintillation technique.

Initial results from this large experiment set will be reported.

G3/H2-3 1000 GENERATION OF EXTRATHERMAL ELECTRON FLUXES IN IONOSPHERIC HEATING EXPERIMENTS

M.C. Lee, Regis College Research Center, Weston, Massachusetts 02193

Enhancement of 6300 Å airglow in ionospheric heating experiments indicates the acceleration of electrons up to at least 1.98 ev. It is generally believed that Langmuir waves excited by O-mode pump waves via parametric instabilities are responsible for the generation of energetic electrons causing the 6300 Å airglow enhancement. Very recently, Carlson and Mantas (XXth URSI, Washington D.C., 1981) analyzed the height distribution of enhanced plasma lines and deduced that fluxes of energetic electrons with energies even greater than 20 ev could be generated via the O-mode heating. Broad energy spectra of extrathermal electrons were found in Carlson and Mantas' analyses. Simple wave-Particle interaction via Landau's mechanism obviously cannot explain the generation of these extrathermal electrons since the parametrically excited waves have a narrow range of phase velocities. Possible mechanisms of accelerating electrons in ionospheric heating experiments will be discussed. Theoretical calculations will be compared with the experimental results.

G3/H2-4
1045

UHF-RADIOSTAR SCINTILLATIONS DURING HF-MODIFICATION OF THE IONOSPHERE: A. Frey, Department of Space Physics and Astronomy, Rice University, Houston, TX 77001

HF-waves incident on an overdense ionosphere produce large scale (several hundred meters) electron density irregularities. These irregularities are intense enough to affect UHF-waves propagating through the modified volume. Celestial radio sources which had a line of sight slicing through the HF-modified volume within 15 to 30 minutes were observed at UHF with the 300m-dish of the Arecibo-Observatory. The measured effects of the electron density irregularities on these UHF-waves will be discussed.

G3/H2-5 1110 THE IONOSPHERIC RESPONSE TO EXPLOSIVE CHEMICAL RELEASES

P.M. Kintner, School of Electrical Engineering, Cornell University, Ithaca, NY 14853

Warm expanding plasmas have been produced in the ionosphere by explosive chemical releases. The plasmas are produced by using either a cesium doped high explosive or a barium shaped charge. In situ diagnostic measurements on the same magnetic flux tube as the plasma release indicate that the expanding plasmas produce a large electric field pulse followed by the precipitation of hot electrons ($\sim$ 200 eV). At higher frequencies the expanding plasma immediately produces broadband VLF fields followed by a narrow band emission which appears to be an acoustic mode associated with the plasma cloud boundary. Results from the Trigger and Ba-GEOS are described along with future plans to exploit these methods for the study of geophysical plasmas.

G3/H2-6 1135 MAKING THE SPACE PLASMA RING LIKE A BELL

Morris B. Pongratz, Space Plasma Physics Group, Mail Stop 438, Los Alamos National Laboratory, Los Alamos, NM 87545

High altitude shaped-change barium plasma injections have a wide potential for providing free energy to the space plasma. The Buaro experiment (June, 1976) injected about 50 megajoules of barium ion kinetic energy perpendicular to the local geomagnetic field. Free energy appeared in the form of streaming ions, temperature anisotropies, non-Maxwellian ring-shaped ion velocity distributions, and plasma density gradients. The dominant form of the free energy is a function of time after injection and distance from the injection.

In the highest free energy density regions of the resultant plasma the space plasma will try to radiate in every mode available. And the barium plasma injection can be sufficiently homogeneous to allow modes not available to particle-beam type injections to grow.

We will review the forms of free energy available using in situ active experimental techniques and discuss some plasma instabilities and wave modes that may be excited by these experiments.

BOLOMETERS FOR RADIOASTRONOMY
Friday morning, 15 Jan., CR2-6
Chairman: J.M. Payne, National Radio Astronomy Observatory, Tucson, AZ 85745

J6-1
0900

He-3 BOLOMETER CRYOSTAT DESIGN FOR TELESCOPES

I. Nolt[1], P. Ade[2], J. Davis[3], J. Payne[3], S. Prdeko[1], and J. Radostitz[1]
[1]Physics Dep't, Univ. of Oregon, Eugene, Or.
[2]Physics Dep't, Queen Mary College, London, U.K.
[3]NRAO, Tucson, Az.

The advantages of bolometer operation at pumped He-3 temperatures of ~ 0.4 kelvin were recognized in the original description of germanium bolometers by Low (J. Opt. Soc., 51, 1300-1304, 1961). The first He-3 cooled bolometer was built in 1966 by Drew and Sievers (Appl. Opt., 8, 2067-2071, 1969), but its size and use of diffusion pumps precluded application to astronomy. In 1969 absorption cryo-pumping of the He-3 was demonstrated to be a practical solution for telescope applications (Nolt and Martin, Rev of Sci Instr. 42, 1031-1033, 1971).

In recent years this basic cryogenic technology has been refined and adapted to various operational situations. The University of Oregon group has constructed He-3 cryostats for the f/14 NRAO 36-ft millimeter telescope and for the f/35 cassegrain 158-inch UKIRT telescope at Mauna Kea. The Cornell/Caltech group has operated a He-3 system at the f/3.3 prime focus of the 200-inch. The design of these instruments illustrates current He-3 cryogenic practice as applied to bolometers for near-millimeter ground-based astronomy.

J6-2
0930

A ONE MILLIMETER ^{3}He BOLOMETER SYSTEM FOR THE 5m HALE TELESCOPE

Thomas P. L. Roellig
NASA/Ames Research Center
Moffett Field, CA 94035
James R. Houck
Department of Astronomy
Cornell University
Ithaca, NY 14853

A 1mm ^{3}He bolometer system has been developed to work at the prime focus of the 5m Hale telescope. The system is used in conjunction with the reimaging photometer described in Elias et al, (AP. J., 220, 25-41, 1978), to give a beam size of 55" FWHM on the sky. The system employs an internal adsorption pump so that no pumping lines are needed in the prime focus cage. Typically, the ^{3}He maintains the bolometer at a temperature of 0.37°K for 14 hours before recycling becomes necessary. This recycling process takes less than one hour. The bolometer is of a composite design with a sapphire nichrome substrate and a Ge:In:Sb thermistor. The electral NEP of the bolometer is 1×10^{-15} W/$\sqrt{\text{Hz}}$. Filters and internal diffraction, respectively, give spectral half power points of 750 μm and 1200μm. The system NEFD on the telescope in good weather is 5.8 Jy/$\sqrt{\text{Hz}}$.

J6-3
1000

NEAR-MILLIMETER OBSERVATIONS USING THE 3.8 m UKIRT FLUX COLLECTOR

P. Ade[1], C. Cunningham[1], I. Nolt[2], E.I. Robson[3], and J. Radostitz[2]
[1]Physics Dep't, Queen Mary College, London, U.K.
[2]Physics Dep't, Univ. of Oregon, Eugene, Or.
[3]Preston Polytechnic, Preston, U.K.

In 1979 the University of Oregon and Queen Mary college infrared groups conducted a joint study of our available bolometer materials and the performance limits of He-3 cooled bolometers for near-millimeter detection. The results of this study (S. El-atawy, P. Ade, J. Radostitz, and I. Nolt, Int. J. IR and Mm Waves, 1, 459-467, 1980) prompted a systematic effort since then to develop and test a He-3 bolometer system for near-millimeter observations using the UKIRT 3.8 m Flux Collector at Mauna Kea Observatory. Considerable instrument evolution has occurred over the past two years. The current instrument features f/35 optics, self-resonant bendpass filters(J. Davis, Infr. Phys., 20, 287-290, 1980), and nodding secondary chopping at 15 Hz. Observations in Sept. 1981 demonstrated a noise equivalent flux density (NEFD) of less than 5 Jy/$\sqrt{\text{Hz}}$ with an 86 GHz FWHM wide filter at 270 GHz(1.1 mm). With good weather conditions and some further system improvements we think an ultimate sensitivity of about 1 Jy/$\sqrt{\text{Hz}}$ is possible in the 1 mm. band.

J6-4
1030

THE NRAO 0.4 K BOLOMETER RECEIVER SYSTEM FOR MILLIMETER CONTINUUM OBSERVATIONS

J. Payne[1], J. Radostitz[2], S. Predko[2], I. Nolt[2], R. Howard[1], J. Davis[1] and P. Ade[3]
[1]NRAO, Tucson, Az.
[2]Physics Dep't, Univ. of Oregon, Eugene, Or.
[3]Physics Dep't, Queen Mary College, London, U.K.

An evaluation of 0.4 K bolometer technology (S. Elatawy, P. Ade, J. Radostitz, and I. Nolt, Int'l J. IR and Mm Waves 1, 459-467, 1980) indicated sensitivities could be achieved which are competitive with those of cooled mixer receivers for continuum source observations at near-millimeter wavelengths. A custom He-3 bolometer system has been built for NRAO by the U of O/QMC infrared group. This instrument, for use on the 36-ft telescope, incorporates the following unique features: (1) bandpass filters for the 1,2, and 3 mm bands of 7.5 cm aperture cooled to ~20K by helium gas (J. Davis, Infr. Phys. 20, 287-290, 1980); (2) a He-3 cooled detector stage which will operate at 0.37 K for more than 40 hr with the full system charge of 10 l STP; (3) remotely controllable recycling; and (4) a cryogenics design adaptable, if desired, to closed cycle 4.2 K cooling for continuous operation.

Limited engineering tests were conducted in the 1980/81 observing season. In the March tests we acheived about an 8 mK rms brightness temperature sensitivity at 270 GHz with an 86 GHz FWHM band width. The input optics are matched to the f/14, 4.1 cm aperture of the telescope. The same tests showed that the background radiation levels through the cold filters permit some additional improvement in the bolometer performance. These results can be compared to current cooled mixer recievers which achieve typical sensitivities of 25 mK for a double sideband system temperature of 400 K and an instantaneous bandwidth of 1 GHz.

RADIO ASTRONOMY INSTRUMENTATION
Friday morning, 15 Jan., CR2-6
Chairman: T.A. Clark, Goddard Space Flight Center, Greenbelt, MD 20771

J7-1 1100 UPGRADING THE NRAO 11-METER ANTENNA--A PROGRESS REPORT: John W. Findlay and J.M. Payne of the National Radio Astronomy Observatory, and Gene Rhoades and M.J. Brenner of ESSCO, Concord, MA 01742

The 11-meter mm-wave antenna on Kitt Peak is being provided with a new surface, supported by a new structure down to the elevation axis. The telescope in its upgraded form will have a 12-meter diameter reflector, with an f/D of 0.42 and a surface RMS of 70 μm.

Progress on this work will be reported in three areas:

(a) The surface panel manufacture and measurement at ESSCO. It is expected that panel fabrication will be nearing completion so that the results of the measurements of the panels will be reported.

(b) Measuring and setting the surface at NRAO. A template measuring and setting system will be used, and results of first tests of this will be available.

(c) The radiometer system. The layout of radiometer front-ends and the radio-optical systems associated with them will be described.

The present telescope will cease observing in early June 1982 and resume, in its new form, before the end of the year.

* National Radio Astronomy Observatory is operated by Associated Universities, Inc., under contract with the National Science Foundation.
† Electronic Space Systems Corporation, Concord, MA 01742

J7-2 1130 THE CLARK LAKE TEEPEE-TEE TELESCOPE: W.C. Erickson, M.J. Mahoney, and K. Erb, CLRO, Astronomy Program, University of Maryland, College Park, MD 20742

A new, fully steerable, decametric array for radio astronomy has been built at the Clark Lake Radio Observatory near Borrego Springs, California. This array is a "T" of 720 conical spiral antennas, 3.0 km by 1.8 km. It is capable of operating between 15 and 125 MHz, but has best sensitivity in the 25 to 75 MHz range. Both its operating frequency and beam position are adjustable in about one millisecond.

A 1024-channel digital correlator has been built and attached to the array. This permits the simultaneous measurement of the complex visibility function on 512 interferometer baselines between various portions of the array. After Fourier transformation these visibility data yield a 32 x 32 resolution element picture of the area of sky under observation with angular resolution ranging from 15 to 3 arc-minutes. The system is described and some initial observations are presented.

NUMERICAL METHODS

Commission B, Session 8, CR2-28
Chairman: Allen W. Glisson,
Department of Electrical Engineering,
University of Mississippi, University, MS 38677

B8-1
1330

WIRE RADIATORS ON ASYMMETRIC BODIES:

L.N. Medgyesi-Mitschang, McDonnell Douglas Research Laboratories, St. Louis, MO 63166

A formulation is developed for the analysis of off-surface wire radiators on asymmetric bodies, such as formed by surfaces of translation. An electric field integral equation representation, solved by the method of moments, is used for both the body and the antennas. Specific antennas considered are loops and monopoles. An analytical representation for the junction region at the antenna attachment points is obtained. Trapezoidal patch modeling is used to describe the ends of the body. A subcase of the analysis treats the near fields in the vicinity of the radiators. Gain pattern predictions using this formulation are compared with experimental data and published results for wire antennas on cylindrical surfaces. Extensions of the method, incorporating optic derived techniques to treat radiators on electrically extended surfaces, are discussed.

B8-2
1400 TETRAHEDRAL CELL MODELING OF ARBITRARILY-SHAPED INHOMOGENEOUS DIELECTRIC BODIES:

D. R. Wilton, Department of Electrical Engineering, University of Mississippi, University, MS 38677; D. H. Schaubert, Division of Electronic Products, Bureau of Radiological Health, 12721 Twinbrook Parkway, Rockville, MD 20857; A. W. Glisson, Department of Electrical Engineering, University of Mississippi, University, MS 38677.

Several numerical approaches have been developed for treating the problem of scattering and absorption by inhomogeneous lossy dielectric bodies. Most of the approaches developed to date, however, either restrict the body to have rotational symmetry, or model the body by means of cubic cells which may not conform well to surface boundaries nor to the interface surfaces between regions of differing material parameters.

This paper describes a recently-developed numerical approach for modeling an arbitrary inhomogeneous body by means of tetrahedral cells. The formulation employs an integro-differential equation for the volume polarization current from which the desired internal fields, absorption, scattered fields, and other quantities of interest can be determined. Special basis functions defined on the tetrahedral domains ensure continuity of conduction-plus-displacement current normal to the interfaces between tetrahedral cells containing different media, and has constant divergence (charge density) in each cell. The integro-differential equation is formulated in terms of both vector and scalar potentials, and a testing procedure is used which obviates the need for integration over the potentials yet which properly handles the derivatives in the equation. Preliminary calculations using the method show good agreement with existing data.

B8-3
1430

ON THE CONDITION NUMBER OF BOUNDARY INTEGRAL OPERATORS FOR THE EXTERIOR DIRICHLET PROBLEM OF THE HELMHOLTZ EQUATION

R. Kress, Department of Mathematics
University of Delaware, Newark, DE 19711

Brakhage and Werner, Leis and Panich suggested to reduce the exterior Dirichlet boundary value problems for the Helmholtz equation to an integral equation of the second kind which is uniquely solvable for all wave numbers by seeking the solution in the form of a combined double- and single-layer acoustic potential. We present an analysis of the appropriate choice of the parameter coupling the double- and single-layer potential in order to minimize the condition number of the integral operator.

B8-4
1500

PLANE WAVE REFLECTION FROM A PERIODIC ARRAY OF APERTURES IN A THIN SCREEN OF FINITE CONDUCTIVITY: B. Rubin* and H.L. Bertoni, Department of Electrical Engineering and Computer Science, Polytechnic Institute of New York, Brooklyn, N.Y. 11201

A moment method is developed for computing the induced currents and reflected fields generated by a plane wave incident at an angle on a thin screen that is perforated by a two-dimensional periodic array of apertures. The screen may be perfectly conducting or have finite surface resistivity $R_s\Omega$/square, and the apertures need not be rectangular. Using a double Fourier series expansion, the scattered fields are expressed in terms of the Fourier coefficients of the surface current $\underline{J}_s$. Within each unit cell, $\underline{J}_s$ is approximated by a set of currents, each of which has "rooftop" dependence over different subsections of the cell (A.W. Glisson and D.R. Wilton, IEEE Trans., AP-28, 593-603, 1980). With this approximation, the doubly infinite set of unknown Fourier coefficients can be expressed in terms of the finite number of unknown subsectional current amplitudes.

The unknown current amplitudes are found from an equal number of tests of the boundary conditions for the electric field $\underline{E}$ on the screen. These tests result in a finite dimension matrix equation relating current amplitudes to incident fields, where the matrix elements are double Fourier sums. If point testing is used, the Fourier sums are conditionally convergent, and the matrix equation is not practical for numerical evaluation. To improve convergence, and thus allow efficient numerical evaluation, a weighted average of $\underline{E}$ is tested over subsectional regions of the screen. Such testing of $\underline{E}$ introduces complications since its line integral in the screen is not necessarily equal to the line integral of $R_s\underline{J}_s$ (which must vanish for a perfect conductor). To overcome this difficulty, some tests for $\underline{E}$ are replaced by tests for the weighted average of the normal component of magnetic field $\underline{H}$ over subsectional regions. A simple scheme has been devised to relate the various test regions to the subsectional regions use to approximate the current.

The current distribution and reflection coefficient has been computed for apertures in the forms of squares and crosses. Computations have been made for $R_s = 0$ and 377Ω. Results display the behavior expected for low frequencies.

* On leave from IBM, East Fishkill, N.Y. 12533, under their Resident Work-Study Program.

Commission F Session 7
SPECIAL TOPICS
Friday afternoon, 15 Jan., CR2-26
Chairman: Dusan S. Zrnic,
National Severe Storms Laboratory, NOAA,
Norman, OK 73069

F7-1
1340

DETECTION OF AIRCRAFT WAKES BY RADAR.

R. B. Chadwick
NOAA/ERL/WPL, R45x6
325 Broadway
Boulder, CO 80303

A valid approach to increasing the efficiency of commercial air travel is to decrease the spacing between aircraft on take-offs and landings. This reduces the amount of time and fuel spent in holding patterns. One of the obstacles to reducing spacing between aircraft is the presence of the trailing wingtip vortices behind a heavy jet. These vortices are hazardous to smaller aircraft. Several methods for detecting these vortex systems involving optics, acoustics, anemometers and pressure sensing devices, have been under investigation for the past decade, but none have proved to be operationally promising.

It is known that radar can detect returns from aircraft wakes, but little is known about the details of the interactions between aircraft wakes and electromagnetic waves. Since all of the experimental work has been done at 10 cm, nothing is known of the frequency dependence of the scattering or the polarization dependency. Before radar can be considered a viable candidate for hazardous wake detection, more knowledge of this scattering phenomena is needed.

Data from four different wake detection experiments will be presented and puzzling inconsistencies with present vortex models will be pointed out. The region causing the return appears to narrow in range and narrow in velocity even though an aircraft wake is distributed in range and velocity.

F7-2
1400 EVALUATION OF TECHNIQUES FOR RECORDING AND REDUCTION OF ENTOMOLOGICAL RADAR DATA:

C. R. Vaughn, National Aeronautics and Space Administration, Wallops Island, VA 23337
J. R. Rowland, Applied Physics Laboratory, Johns Hopkins University, Laurel, MD 21227
W. W. Wolf, USDA-ARS, Southern Grain Insects Research Laboratory, Tifton, GA 31793

Radar is a proven tool for entomological research. Primary data is presently obtained from visual observations of intensity modulated displays and from small numbers of gated range cells recorded on analog tape. A computer controlled data collection system has been constructed to collect entomological data with radar. A field experiment was conducted in the fall of 1981 with this prototype system connected to a short pulse width 9.4 GHZ mobile radar. Data gathered with the computer system were compared to data obtained from a conventional intensity modulated display. A case study comparison of the two forms of data is presented.

F7-3 1420 THE ATTENUATION OF MICROWAVE PROPAGATION THROUGH VEGETATION AND OVER HILLS: Per Krogh Hansen, Hinsburg, VT

A theoretical propagation model is developed and implemented on the computer. The vegetation is set equivalent with a knife-edge, which is semitransparent above the earth with the attenuation of the vegetation. The hill is also set equivalent with a knifeedge, with attenuation ∞, and corrections are made after an empiric model for rounded hills. The model separates the fields into transmitted, reflected, and diffracted fields.

A transmitter/receiver measurement system is developed to test the theoretical model. The system operates at five different frequencies in the UHF, L, S, C, and X-band and is able to operate over more than 500 m.A short-back-fire antenna is used at UHF and horn antennas are used at the higher frequencies. The transmitted signals are modulated with a 5 kHz square wave. A heterodyn receiver is used at UHF with a sensitivity of -120 dBm. The square wave is detected in this receiver and used for syncronization of the crystal-diode detectors in the other receivers, resulting in a sensitivity better than -80dBm. The system also includes a position measurement system and a control unit, which stored the measurements on paper tape.

Measurements were made over one year at selected sites. The measurements were made with the transmitter at a fixed position at one side of the vegetation and the receivers at a fixed distance from the transmitters as a function of the receiver height up to 12 m above the ground.

The comparison of measurements and calculations show good agreement, when the different fields are added in phase. Some disagreements exist when the receivers are close to the ground. Some small displacement errors do occur in the line-of-sight area. There is almost no attenuation in the UHF and L-band, whereas the approximately 1 dB/m attenuation at S, C, and X-band. No practical difference (<0.05dB) was measured in the attenuation between horizontal and vertical polarization. A very small variation ($< \pm 0.05$ dB/m) occured over the year at the higher frequencies.

F7-4
1440

PREDICTION OF SAND AND DUST STORM ATTENUATION OF MICROWAVE SIGNAL: S.C. Gupta and A. Srinivasan, Department of Electronics and Communication Engineering, U.O.R., Roorkee, India

Sand and dust storms are frequent in desert areas. During sand and dust storms, the sand particles rise up to the height of 100 meters or more for short duration, the optical visibility reduces to twenty meters or less, under severe conditions. The sand particles like rain, snow, hail, fog are expected to absorb and/or scatter electromagnetic waves at higher-frequencies and also modifies the refractive index of the atmosphere. It is the order of the day to go for higher and higher frequencies, for the obvious reason of increased band width and increased traffic handling capability. Thus it is very important to evaluate the various effects of sand-particles on the microwave radio links, satellite earth stations and radar, operating under adverse sand and dust storms.

Very few literatures are available in the study of the effects of sand and dust storms. On microwave propagation compare to literatures on similar line such as rain, snow and fog, etc.

Ghobrail et al (1) have used Maxwell-Garnet equation for calculating the attenuation. Chu (2) has derived an empirical formula for calculation of attenuation and has compared his calculated result at 10 GHz given by Ahmed et al. Gupta et al (3) have developed an empirical formula for the estimation of attenuation of microwave signal using the concept of Form-factor, and they have compared their results with the Mic-Ryde, Maxwell-Garnet and Chu, expressions.

Ahmed et al (4), Gupta et al (3) have measured attenuation in the Laboratory under the simulated dust and storm conditions using Fabry-perot resonator.

The above theories developed have assumed spherical shape of the particle with single-layer. A theoretical model is proposed to study the effects of sand and dust particles on microwave propagation, which deals with the non-spherical and multilayered dielectric. The Extended Integral equation method can be easily applied to non-spherical objects (5) (6). The Extended integral equation provides a mathematical tool in the estimation of attenuation of microwave signals due to sand and dust storms.

F7-5
1520 ELECTROMAGNETIC SCATTERING FROM RANDOM CONDUCTIVITY FLUCTUATIONS:

J. W. Sari, R. I. Joseph, and M. E. Thomas, all at:
The Johns Hopkins University/Applied Physics Laboratory, Laurel, Maryland 20707

Scattered electromagnetic fields are considered for a source and receiver located in a conductive medium which contains small perturbations in conductivity. The conductivity perturbations are assumed to be random and describable by a spatial correlation function. The scattered fields in the near field are computed for a finite-sized source/receiver system located in-situ with the perturbations. Properties of the scattered fields are examined as a function of source frequency and system dimension size. Cases of a spherical system in a region of isotropic perturbations are considered for exponential and gaussian correlation functions. The normalized root-mean-square scattered fields can be generalized in terms of ratios of the electromagnetic skin depth of the medium, system radius and the correlation length of the random conductivity perturbations.

F7-6
1540

SUPERRESOLUTION TECHNIQUES WITH PERFORMANCE BETTER THAN MAXIMUM ENTROPY METHOD (MEM): Ajay K. Luthra, Valley Forge Research Center, The Moore School of Electrical Engineering, University of Pennsylvania, Philadelphia, PA 19104; and Interspec Inc. 3508 Market Street, Philadelphia, PA 19104

Two of the major problems associated with maximum entropy method (MEM) are: (i) in the presence of coherent sources its performance--the resolving power and accuracy in finding the directions of the sources--is very poor and (ii) although its performance is very good in the presence of incoherent targets it needs very high signal-to-noise ratio to resolve very closely placed targets. In this paper it is shown that if the estimate of the noise power is available the restriction on the maximum noise power for the desired resolving power can at least be released by 7 to 15dB, depending upon the desired resolution.

In addition, a new technique is developed which performs much better in the presence of coherent sources and is very much less sensitive to noise than MEM. The relationships among this technique, MEM and Prony's method are also pointed out. In the presence of incoherent targets the concept presented can be extended to aperiodic arrays.

F7-7
1600 PRELIMINARY RESULTS OF FM RADAR PROBING OF CONCRETE BLOCK WALLS AND THE GROUND

C. Nasseri, R. Onstott, R.K. Moore
Remote Sensing Laboratory
University of Kansas Center for Research, Inc.
Lawrence, Kansas 66045

FM radars with very broad sweep bandwidths can be used to probe volumes such as concrete and soil. An FM radar with sweep from 8 to 12 GHz and another with sweep from 1.1 to 1.9 GHz have been tested in penetrating the soil and a block wall with and without voids. Design problems for such a short-range FM radar are discussed, and results of the experiments presented.

INDUCED PLASMA WAVE EMISSIONS
Friday afternoon, 15 Jan., CR1-46
Chairman: R.F. Benson, GFSC, NASA, Greenbelt, MD

H3-1
1330 WIDEBAND INVESTIGATIONS OF THE WAVES SIMULATED IN PLASMA IN ACTIVE EXPERIMENTS - A REVIEW:

Yu. V. Kushnerevsky, S. A. Pulinets, V. V. Selegey, Institute of Terrestrial Magnetism, Ionosphere and Radio Wave Propagation, USSR Academy of Sciences, 142092, Troitsk, Moscow Region, USSR

The wideband receiver employment in plasma wave experiments is especially effective in active experiments where several plasma modes are stimulated simultaneously (in the case of particle beam injection) or in the case of multifrequency nonlinear processes under the influence of powerful radio pulses emitted into a plasma. In geophysical research this method was used for the first time in 1975 during the French-Soviet experiment Araks. Several types of waves stimulated by the electron beam were registered onboard the separable nose cone in the course of two launches of Eridan rockets with onboard electron guns. Two modes were observed continuously during the whole flight: in the frequency band $\omega_p \leq \omega \leq \omega_H$ - plasma mode and $\omega \leq \omega_H$ - the whistler mode. The analysis of the results obtained permits us to determine the coherent Cherenkov emission of the leading edge of the electron beam as responsible for emission in the frequency band of the plasma mode. According to the whistler mode emission mechanism, there are several hypotheses. In particluar for the first launch, where the influence of the plasma source for the rocket charge neutralization was noticed, the Diocotron instability mechanism was suggested. A series of effects observed in the Araks experiments forces us to the conclusion that the near rocket environment region is a very important factor in the physical processes of the plasma wave stimulation. During the second launch of the Araks experiment, the electron precipitation stimulated by the whistler mode emission of the electron beam was detected as well as the whistler decay in the interaction region. The results obtained in the Araks experiment inspired us to include the similar wideband receiver to the wave measurement complex of the Intercosmos-19 satellite which participated in the IMS program. Several new experimental results, related to interaction of powerful pulse radio-emissions of the topside ionosonde with the ambient plasma, will be reported.

H3-2 1400 CHARACTERISTICS OF THE WAVES PRODUCED IN THE BEAM PLASMA DISCHARGE

X. Llobet*, W. Bernstein*, Rice University, Houston, TX 77001
P. J. Kellogg, University of Minnesota, Minneapolis, MN 55455
R. J. Jost, Johnson Space Center, Houston, TX 77058

A moderately high perveance ($K > 1 \times 10^{-7}$ Amp Volts$^{-3/2}$) non-relativistic, electron beam injected into the lower ionosphere ($h < 200$ km) from a rocket borne accelerator can produce the beam-plasma-discharge (BPD) at the injection point. We have reproduced the ignition of the BPD in a series of experiments performed in the very large (17.5 m diam x 26 m high) vacuum chamber at the Johnson Space Center. Because of the large chamber size, the important experiment parameters ($B \approx 0.5$-2.0 G and neutral density 5×10^{10}-10^{12} cm^{-3}) were very similar to those encountered in flight.

Ignition of the BPD is identified by 1) a characteristic wave spectrum, 2) enhanced ionization of the neutral gas and consequent elevated plasma density, 3) heating of the monoenergetic injected beam, and 4) modification in the beam spatial profile. BPD waves have been studied in the VLF (10 Hz-16 KHz), LF (16 KHz-f_{ce}) and HF ($> f_{ce}$, $\approx f_{pe}$ of the enhanced plasma density) ranges. The HF band shows large amplitude peaks at $\sim (n + 1/2) f_{ce}$ with $5 \leq n \leq 10$. The remarkable similarity between flight and laboratory data will be shown. Preliminary results of theoretical analysis of possible wave generation mechanisms will be given.

* Supported by NASA Grant NAGW-9 and NSF Grant ATM 80-22550.

H3-3
1430 WAVE MODES AND PARTICLE HEATING BY A keV ELECTRON BEAM IN CHAMBER A, JOHNSON SPACE CENTER

P.J. Kellogg and S.J. Monson,
School of Physics and Astronomy,
University of Minnesota,
Minneapolis, MN 55455

We have continued our analysis of data on identification of the wave modes responsible for particle heating and production of beam-plasma-discharge in the large vacuum chamber, Chamber A, at Johnson Space Center.

We tentatively propose that there are three frequency ranges which are important in energy transfer and diffusion, i.e., (1) a usually featureless band near the ion cyclotron frequency, of order 100 Hz; (2) a higher frequency band, from a few to 10 kHz; (3) the "plasma line", usually 10-30 MHz. Indirect evidence that the ion modes (1) heat ions significantly, even at beam currents well below BPD threshold. These hot ions drive an instability (mode (2)), which energizes electrons. Evidence for and against significant particle heating by each of these modes will be presented.

At present, it seems on theoretical grounds that the Whistler mode, although it is an accurate diagnostic for the transition to BPD (Kellogg and Monson, Adv. Space Res. 1, 61-68 (1981)), is not a major energizer of particles, but is rather a result of particle energization.

H3-4
1530 THE DYNAMIC BEHAVIOR OF WAVES STIMULATED BY A FAST PULSE ELECTRON GUN IN A SPACE SIMULATION CHAMBER:

W.F. Denig and W.J. Raitt, Center for Atmospheric and Space Sciences, Utah State University, Logan, UT 84322; and P.M. Banks, Radioscience Laboratory, Department of Electrical Engineering, Stanford University, Stanford, CA 94305

The results from a series of experiments that deal with the onset and dynamic behavior of HF and VLF waves due to electron beam emission inside a large space simulation chamber are presented. The electron gun had an adjustable beam current from 1 ma to 100 ma at a fixed accelerating potential of 1 KeV and a switch-on time of about 100 ns. Chamber A at JSC is a 27 meter high cylindrical vessel with an 8 meter radius that can be evacuated to a gas pressure of about 5×10^{-6} torr. A set of coils can induce an artificial magnetic field up to about 1.5G and a plasma source can be used to generate a background plasma. Experiments were performed using a variety of pitch angles, beam currents and magnetic field strengths in either an initially neutral or partially ionized background gas. The work was undertaken to better understand the plasma instability commonly known as the Beam Plasma Discharge (BPD).

Temporal variations in the HF electric spectrum were monitored by making video recordings of a spectrum analyzer yielding 40 msec resolution. Flickering at low frequencies ($\sim$10 Hz) of discreet emissions at the cyclotron fundamental and harmonics attest to the unstable nature of the beam induced plasma column. The rise in the local plasma density during the first few milliseconds after beam commencement can be determined by measuring the plasma frequency as a function of time. This information may provide clues into the nature of the instability through its associated growth rate. The VLF electric spectrum was examined in detail by producing a series of frequency versus time sonagrams. Flickering at near 10 Hz is also a feature in the VLF regime as it was in the HF measurements. Coherent emissions were observed in the VLF spectrum produced by analyzing current variations measured by a spherical Langmuir probe.

Some of the apparatus used in these experiments will be flown aboard STS-3 to investigate the effects of an electron gun on the charging of the Space Shuttle and on the local ionosphere. The Shuttle measurements will be complemented by a NASA sounding rocket with the objective of investigating the transient behavior of electron injection on the rocket and its surroundings. The chamber tests will help to determine if there are differences between the BPD in large vacuum chambers and in space.

H3-5 1600 COMPREHENSIVE MEASUREMENTS OF A SELF-CONTAINED PLASMA COLUMN BY THE UNIVERSITY OF IOWA PLASMA DIAGNOSTIC PACKAGE (PDP):

Stanley D. Shawhan and Gerald B. Murphy,
Department of Physics and Astronomy,
University of Iowa, Iowa City, Iowa 52242

The interaction between an energetic electron beam and its self-produced plasma which results in a range of wave emissions and an enhancement of the thermal plasma density in the vicinity of the beam was first given the name Beam Plasma Discharge (BPD) during the experiments of Getty and Smullin (J. Appl. Phys. 34:3421, 1963). Controversy still exists over whether the BPD phenomenon is an intrinsic property of a beam excited plasma or a containment effect and over the role of electrostatic waves.

In March 1981 an experiment was conducted in the large vacuum chamber A at Johnson Space Center. The experiment made use of two instruments which will fly together on the OSS-1 pallet on Shuttle Mission 3. The Utah State University Fast Pulsed Electron Generator was the source of a variable current, variable pulse rate 1 Kev electron beam. The University of Iowa Plasma Diagnostic Package (PDP), a spacecraft with multiple instruments, was the beam probe. The PDP was designed to provide a comprehensive set of data on the near earth plasma by measuring electron and ion density, energy, and distribution functions; and measuring magnetic fields, electric fields, and electromagnetic waves over a broad frequency range. Thus the PDP serves as the most comprehensive plasma beam probe yet designed and the chamber A provided the appropriate size vacuum tube for the measurements. Comprehensive measurements were made at various generator currents, pulse widths and injection pitch angles. The PDP probed in and around the beam under all these conditions plus varying magnetic field strengths.

Results of electron and ion energy distribution functions indicate an enhancement of 10 ev - 100 ev ions following the onset of BPD as well as a depletion of 2.5 to 20 ev electrons. Angular distributions indicate significant return current outside the visible column. Significant parallel electric fields inside the beam acting in a direction to decelerate primary beam electrons and perpendicular electric fields outside the beam directed inward were noted. Several wave modes have been identified with the onset of BPD including an enhanced lower hybrid resonance and plasma frequency. Other wave measurements and wideband receiver studies of a flicker phenomenon marking BPD onset will also be discussed.

H3-6
1630 REVIEW OF PLASMA WAVE EMISSIONS STIMULATED IN SPACE BY IN SITU TRANSMITTERS AND A LOOK TOWARD THE SHUTTLE ERA: Robert F. Benson, Laboratory for Planetary Atmospheres, NASA/Goddard Space Flight Center, Greenbelt, MD 20771

A number of observational and theoretical studies over the last two decades have indicated the importance of nonlinear wave-particle interactions to the energetics of the ionosphere and the magnetosphere. In most cases, however, it has been difficult to specify the relevant physical process because of restricted diagnostic capabilities in space combined with the uncertainties in the initial and boundary conditions in the ambient medium. In an attempt to overcome these limitations, active experiments have been carried out involving the injection of particles, waves and chemicals into space. Wave injection experiments have been performed using both ground-based and spacecraft-borne transmitters. The ground-based experiments have mainly been directed toward the goal of ionospheric modification or the investigation of wave-particle interactions in the equatorial magnetosphere. Experiments using space-borne transmitters have been directed toward the investigation of plasma waves and wave-particle interactions in the ambient medium surrounding the spacecraft. A review of the latter indicates that considerable progress has been made in understanding the stimulated processes while a number of fundamental questions remain to be addressed. For example, the stimulated emissions at the half harmonics of the electron cyclotron frequency f_H (which may be related to the similar emissions observed naturally in the magnetosphere) are caused by a plasma wave instability which is driven by an electron temperature anisotropy induced by the transmitted pulse. The long time-durations of these waves requires a nonlinear mechanism. Two competing mechanisms have been proposed, one based on a 3-wave decay process and one on the process of nonlinear Landau damping. Some of the future WISP (Waves in Space Plasmas) Spacelab/Shuttle experiments are being planned to uniquely specify the dominant mechanisms pertinent to space plasmas in such cases.

Recent observations, which combine the benefits of the high frequency-resolution available from existing topside-sounder analog data and modern digital graphics techniques, have revealed and classified a number of new stimulted emissions. Among these are waves between the plasma and upper hybrid frequencies which show a remarkable change in character when the plasma to electron cyclotron frequency ratio is near unity.

INDEX

E-2	Non-Gaussian Noise: Measurement and Theory	CR1-40
F-3	Surface Sensing From Airborne and Space Platforms	CR2-26
G-1	Ionospheric Phenomena and Propagation	CR1-46
J-3	Data Processing in Radio Astronomy With Emphasis on the Use of Array Processors	CR2-6
J-4	Remote Observing and Data Transfer Problems in Radio Astronomy	CR2-6

1330-1700

A-4	Near Field Measurements-I	CR1-42
B-6	Singularity Expansion Method	CR2-28
C-4	Communication Satellite Systems Incorporating Multiple Beam Antennas	CR0-30
F-4	Radar Oceanography	CR2-26
F-5	Tropospheric Propagation	CR1-40
G-2	Transionospheric Radio	CR1-46
J-5	Radio Astronomy and Instrumentation	CR2-6

1530

Commission J Business Meeting CR2-6

1630

Presentation of Harry Diamond Memorial Award to Jules Aarons CR1-46

1700

Commission B Business Meeting CR2-28

Commission G Business Meeting CR1-46

2000

Executive Council Meeting OT8-6

FRIDAY, 15 JANUARY

0830-1200

A-5	Near Field Measurements-II	CR1-42
B-7	Guided Waves	CR2-28
C-5	Signal Design and Sensing	CR0-30
F-6	Earth-Satellite Communications	CR2-26
G3/H2	Ionospheric Modification	CR1-46
J-6	Bolometers for Radio Astronomy	CR2-6
J-7	Radio Astronomy Instrumentation	CR2-6

1330-1700

B-8	Numerical Methods	CR2-28
F-7	Special Topics	CR2-26
H-3	Induced Plasma Wave Emissions	CR1-46

Prof,
Res. Photo

Applied Physics